Dany Pascal Moualeu-Ngangue

A Mathematical Tuberculosis Model in Cameroon

Dissertation
am Fachbereich Mathematik und Informatik
der Freien Universität Berlin
zur Erlangung des akademischen Grades
eines Doktors der Naturwissenschaften

vorgelegt von

Dany Pascal Moualeu-Ngangue, M.Sc.

Berlin, May 2013

Betreuer/Gutachter:	Prof. Dr. Dr. h.c. Peter Deuflhard Fachbereich für Mathematik und Informatik, FU Berlin, Arnimallee 2-6, 14195 Berlin
Zweitgutachtervorschlag:	PD Dr. Samuel Bowong Senior Lecturer, Faculty of Sciences, University of Douala, PO Box 24157, Douala, Cameroon
Tag der Disputation:	12. September 2013

To everyone who supports or intended to support me

Contents

List of Figures

List of Tables

List of abbreviations

AIDS	Acquired Immune Deficiency Syndrome
BCG	Bacillus Calmette-Guérin
CDC	Center for Disease Control
CSF	Cerebro-Spinal Fluid
DOTS	Directly observed treatment strategy
FBSM	Forward Backward Sweep method
HIV	Human Immunodeficiency Virus
INH	Isoniazid
MTB	*Mycobacterium tuberculosis*
NCFT	Cameroonian National Committee of fight against TB
NGM	Next-Generation Matrix
NIS	Cameroonian national institute of statistics
SEIR	Susceptible, Latently infected, Infectious and Recovered or Removed
SVD	Singular values decomposition
PCR	Polymerase Chain Reaction
POEM	Parameter Optimization and Estimation Methods
TB	Tuberculosis or Tubercle Bacillus
UN	United Nations
WHO	Word Health Organization

Notations

- $\rho(M)$, the spectral radius of a square matrix M is the largest eigenvalue of M.
- $\mathbb{R}_+$ or $\mathbb{R}_{\geq 0}$ denotes the set of non-negative real numbers.
- $\mathbb{R}_{>0}$ denotes the set of positive real numbers.
- $\mathbb{R}_{<0}$ denotes the set of negative real numbers.
- $\mathbb{R}_{\leq 0}$ or $\mathbb{R}_-$ denotes the set of non-positive real numbers;
- $\mathcal{M}_{mn}(\mathbb{R})$ is the set of matrices with m lines and n columns, when m, n are non-negative integers.
- $\mathcal{M}_n(\mathbb{R})$ is the set of square matrices of order n.
- $Sp(M)$ the spectrum of matrix M.
- $\alpha(M) = \max_{\lambda \in Sp(M)} Re(\lambda)$ where $Re(\lambda)$ is the real part of the eigenvalue λ.

Let $x = (x_i)_{i \in \{1,\dots,n\}} \in \mathbb{R}^n$ be a vector:

- $x > 0$ if and only if $x_i \geq 0$ for all i;
- $x \gg 0$ if and only if $x_i > 0$ for all i.
- Equivalently, we use $<$ and $\ll$

Equivalently, we define the same inequalities for matrices $A \in \mathcal{M}_{mn}(\mathbb{R})$.

$\langle \cdot | \cdot \rangle$ denotes the scalar product in $\mathbb{R}^n$.

Introduction

Tuberculosis (TB) is a preventable and curable disease caused by *Mycobacterium tuberculosis* (MTB) that most often affects the lungs. To date, TB claims the second largest number of victims due to a single infectious agent right after Human Immunodeficiency Virus and Acquired Immune Deficiency Syndrome (HIV/AIDS) [132]. In 2009, there were about 9.7 million orphan children as a result of TB deaths among parents. In 2010, 8.8 million people were infected including 1.1 million cases among people with HIV and 1.4 million died from it, including 350,000 people with HIV, equal to 3,800 deaths a day. Over 95% of TB deaths occur in 22 low- and middle-income countries mostly located in Sub-Saharan Africa and in South-east Asia [132], and it is among the top three causes of death for women aged 15 to 44 (320,000 women died from TB in 2010). Young adults are mostly affected by tuberculosis, in their most productive years. The estimated global incidence rate dropped to 128 cases per 100,000 population in 2010, after peaking in 2002 at 141 cases per 100,000. An estimated half a million people emerge annually with multidrug-resistant(MDR) [132]. In 2011, the largest number of new TB cases occurred in Asia, accounting for 60% of new cases globally. However, Sub-Saharan Africa carried the greatest proportion of new cases per population with over 260 cases per 100 000 population in 2011 [132].

Despite a widespread implementation of control measures including Bacillus Calmette-Guérin (BCG) vaccination, the Directly Observed Treatment Strategy (DOTS) of the Stop TB department of the World Health Organization (WHO) which focuses on case finding and short-course chemotherapy, the global burden of TB has increased over the past two decades [130]. This rise has been attributed to the spread of HIV/AIDS, the collapse of public health programs and the emergence of drug-resistant strains of MTB.

As the world is experiencing the devastating effects of HIV/AIDS epidemic, it is now necessary to ask why we have failed so far to control TB and throw light on the limits of the global TB control programs [138]. Currently, according to WHO, nearly half of the people living with HIV are TB co-infected and three quarters of all dually infected people live in Sub-Saharan Africa.

A preventive therapy of TB in HIV infected individuals is highly recommended [130] and could dramatically reduce the impact of HIV on TB epidemiology, but its implementation is limited in developing countries because of complex logistical and practical difficulties [76]. The exogenous re-infection, where a latently-infected

individual acquires a new infection from another infected person [46, 70] is also essential to the TB epidemiology. Another important issue is the diagnosis and treatment of infectious who do not have access to hospitals and people who quit treatment before the end and thus develop drug resistances.

Tuberculosis is an ancient and complex infectious disease on which a large number of theoretical studies have been carried out. MTB's infection can remain latent, become active, or it can progress from latent TB to active TB either by endogenous re-activation and/or exogenous re-infection. Active TB is most of the time acquired through co-infection of MTB with other diseases (diabetes, HIV/AIDS) or some substance abuse such as alcohol and tobacco. The mathematical analysis of biomedical and disease transmission models can significantly contribute to the understanding of the mechanisms of those processes and to the design of potential therapies [3, 4, 37, 86, 155].

History of mathematical modelling of tuberculosis. The advent of new antibiotics changed the whole ethos of disease control. Just over 30 years ago, in 1978, the United Nations (UN) signed the 'health for all, 2000' accord which set the ambitious goal of the eradication of disease by the year 2000 [141]. However, the reality of bacterial mutation is dramatically seen in New York city with tuberculosis. Control of the TB w-strain (a highly drug-resistant strain of *Mycobacterium tuberculosis*), which first appeared in the city in 1990, resistant to every available drug killing over half of its victims, has already cost more than $1 billion [119]. 30 years ago, TB has been predicted to be eradicated in the world by 2000. Diseases (including heart disease and cancer) cause orders of magnitude more deaths in the world than anything else, even wars and famines [119, 141]. The appearance of new diseases, and resurgence of old ones, makes the interdisciplinary involvement even more pressing.

The earliest mathematical models describing the TB dynamics have been built by the statistician H. T. Waaler, chief of the Norwegian TB control services in 1960 [161]. The model focused on the prediction and control strategies using simulation approaches. Waaler and coworkers [166, 165, 164, 163, 162, 170], and later Revelle and coworkers [140, 139] and Ferebee [72] developed many other mathematical models with the same aim. Following them, modelers have made several different choices depending on their focus. Waaler considered an exponential population dynamics in the absence of TB [161]. However, this hypothesis for demography modelling was partially limited since it appears not realistic for long term dynamics of a real population. Waaler's first linear model did not describe the mechanics of TB transmission. He introduced a new model of 160 linear equations in [163], keeping the same structure, but including BCG vaccinated and different recovered classes for 20 different age classes. Using the model of Brogger and Waaler as a template, Revelle firstly introduced nonlinear systems of ODEs that model TB dynamics [140, 139]. Revelle explained why the infection rate depends linearly on the prevalence using the probabilistic approach that is common today (homogeneous mixing). He devel-

oped an optimization model and studied the minimal cost strategy against TB. It is worth mentioning that Waaler also developed a model in 1970 that would minimize the cost of alternative tuberculosis control measures.

Blower and colleagues discussed the persistence condition of tuberculosis inside the population and determined the basic reproduction ratio $\mathcal{R}_0$ (the average number of new infectious cases caused by a single infectious case in a fully susceptible population over the course of the entire infectious period) [24, 27, 160, 58, 157, 23]. A sensitivity analysis of $\mathcal{R}_0$ has been performed by several authors [24, 23, 27]. However, the sensitivity analysis of parameters on $\mathcal{R}_0$ does not really illustrate the impact of these parameters on the global trajectory of the system in the case of backward bifurcation. Blower and colleagues found in their model that one has $1 < \mathcal{R}_0 < 9$, and the most important parameters are the infection rate, the probability of fast progression, the re-activation rate, and the TB related death rate. Chavez and colleagues developed a mathematical analysis of a TB model without fast progression [40]. Thereafter, most publications include sophisticated mathematical theories such as center manifold theory and Lyapunov functions, to study the dynamics of tuberculosis [70, 41, 116, 5, 47, 115, 129, 64, 154].

Modelling TB latency and re-infection. Numerous TB models discuss the TB latency and re-infection. In some cases, the progression probability is modeled as a function of time since the first infection. This may be done either with explicit age of infection and maturation structure [162, 159, 7], or the explicit inclusion of variable latent periods in a delayed (delay ordinary differential equation) and/or integro-differential equation [71, 36]. Several authors have found that including re-infection or vaccination leads to backward bifurcation when there is coexistence between an endemic equilibrium and the disease free equilibrium [18, 19, 22, 31, 34, 39, 64]. The mathematical analysis of these models is still a difficult task. Bacaer et al. [10] and some other authors have shown that backward bifurcation appears only for unrealistic re-infection parameter values. Nevertheless, including exogenous re-infection is very common in epidemiological models since its impact is still fundamental. Observations show that individuals may be infected by many TB strains at different times of their life. Numerous models divided the latently infection class into a fast progression class and a slow progression class [173, 65] with different re-activation rates to infectious classes. Some others include differential infectivity stages (see [115] and reference therein).

TB infectious classes. Another discussion is on the number of infectious classes. Most authors included a single class of infectious [136], and sometimes, when taking into account extra-pulmonary tuberculosis, they considered a class of non-infective TB cases [27, 20, 19]. These hypotheses assumed that all infectious individuals were diagnosed, and were following the treatment until the end. It is true when everybody has access to treatment, but it is not always the case in many developing countries where WHO estimated a large number of undiagnosed infectious. A class of lost sight (people who quit the treatment before the end) has also therefore been included in some models [33, 115]. The aspect of disease relapse have been included

by Porco and Blower [136] into their model and they investigated the long term trends of the disease.

Approach in this thesis. The challenge of TB control in developing countries is due to the increase of TB incidence by a high level with undiagnosed infectious and lost sight with respect to diagnosed infectious. Comparing to existing results [41, 40, 17, 117, 116, 10, 5, 6, 27, 26, 47, 115, 129, 48, 70, 136, 24], our work differs from these studies in that our model in addition to undiagnosed infectious and lost sight, also considers the aspects of exogenous re-infections, disease relapse as well as primary active TB cases, natural recovery and traditional medicine (practiced in Sub-Saharan Africa). The purpose of the current study is to complement and extend the aforementioned studies. To the best of the author's knowledge, no model in the literature takes into account all these aspects by combining both frequency-dependent and density-dependent infection. We will design and qualitatively analyze a new and more comprehensive deterministic model for gaining insights into the transmission dynamics and control of TB in a population in developing countries. We will divide the infective class into three subgroups with different properties: i) diagnosed infectious, ii) undiagnosed infectious and iii) lost sight. According to the National Committee of Fight against TB of Cameroon (NCFT) [124], about 8% of diagnosed infectious that begun their therapy treatment never returned to the hospital for the rest of sputum examinations and treatment, and then become lost sight. The parameters of the model are identified using the error-oriented Gauss-Newton method [53] implemented in the software POEM 2.0 (Parameter Optimization and Estimation Methods). Furthermore, an optimal control strategy will be studied in order to eradicate TB using data of Cameroon. The optimal control schedule to fight against tuberculosis in 10 and 20 years through education, treatment of undiagnosed population and lost sight and chemoprophylaxis of latently infected population will be implemented. This class of TB epidemiological models can be extended to many classes of infective individuals and data for many other African countries.

We point out that according to the DOTS strategy, applied in most developing countries, a patient with a pulmonary tuberculosis must make three sputum examinations during the treatment and will be considered cured when the last result of the sputum examination is negative. The quite high rate (5 to 17 %) of lost sight individuals among the Cameroonian population raises a number of concerns. Indeed, what is happening with the undiagnosed cases of active TB and lost sight? How do these people affect the dynamics of TB in Sub-Saharan Africa? What are the conditions for the diagnosed rate (the proportion of the diagnosed cases treated under a DOTS program) that can ensure the eradication of TB, or at least minimize its incidence? Are the undiagnosed cases undermining the efforts of the DOTS strategy with respect to reducing the incidence of TB in Sub-Saharan Africa and effecting proper and efficient treatment policy for patients with active tuberculosis? What is the mathematical and the numerical consequence of adding such classes?

Outline. The thesis is organized as follows. Some theoretical background use-

ful for mathematical modelling of infectious diseases in general and tuberculosis in particular is introduced in Chapter 1. Several mathematical concepts and results that are used throughout the thesis to qualitatively analyze and numerically implement the model are presented: matrices, equilibria, Lyapunov stability, LaSalle invariance principle, bifurcation theory, maximum principle, optimal control theory and numerical implementation by the Forward Backward Sweep Method (FBSM).

In Chapter 2, the tuberculosis model is formulated and analyzed. The total human population is divided into several virtual compartments, each containing a number of people according to their epidemiological status (susceptible, latently infected, undiagnosed infectious, lost sight, diagnosed infectious and natural recovery). The model is shown to have positive trajectories, and to be in a compact positively invariant subset of $\mathbb{R}^6$. The parameter identification is performed using data of Cameroon. With the sensitivity analysis, most sensitive parameter values among the set of unknown ones are estimated. Using artificial data, the impact of some parameter change to reduce the burden of tuberculosis by 20% and 60 % is investigated.

The mathematical analysis of the model is presented in Chapter 3. The basic reproduction ratio is calculated and analyzed. The existence of bifurcations is discussed and the consequence on the stability of the endemic equilibrium (EE) and the disease free equilibrium (DFE) are discussed. Using the center manifold theorem, the stability of the endemic equilibrium will be explored.

Chapter 4 of this work deals with the optimal control by education of the population strategy and the chemoprophylaxis strategy of latently infected to reduce the burden of tuberculosis. The existence of the optimal control pair is discussed. Using an adapted numerical technique for solving optimal control problems from Forward Backward Sweep Method, an optimal control schedule of tuberculosis through education or/and chemoprophylaxis is solved. Chemoprophylaxis is a treatment prevention strategy for latently infected which is not applied in Cameroon. Education aims to reduce the number of undiagnosed infectious in the population. The FBSM technique is one of the indirect methods in which the differential equations from the Pontryagin Maximum Principle are solved numerically. Numerical simulation is conducted to find the optimal schedule depending on the quantity of money available.

Chapter 1

Mathematical Background

Mathematical models generally go through several versions before qualitative phenomena can be explained or predicted with any degree of confidence. Great care must be exercised before practical use is made of any epidemic model. However, even simple models do frequently pose important questions with regard to the underlying process and possible means of control of the disease or epidemic behavior. The practical use of mathematical models must rely heavily on the realism put into the models. Usually, inclusion of all possible effects is not possible, but rather the incorporation in the model mechanisms, in a way as simple as possible, of what appears to be the major components.

Childhood infections motivated the development of modern epidemiological theory, most notably measles which was public health importance in the 19th and early 20th century [141]. An important early mathematical model by Bernoulli (1760), involving a nonlinear ordinary differential equation, considered the effect of cowpox inoculation on the spread of smallpox (cf. [16]). This article includes some important data on child mortality at that time. It is probably the first time that a mathematical model was used to assess the practical advantages of a vaccination control programme. However, Thucydides mentions immunity in connection with the Athens plague and there is evidence of an even more ancient Chinese custom where children were made to inhale powders made from the crusts of skin lesions of people recovering from smallpox. In England during the 19th century, William Farr initiated a sophisticated system of vital statistics, and data series relating to several childhood infections became available that were both reliable enough and long enough to generate hypotheses about the mechanisms underlying epidemic spread. At this time, the notion that certain infections are caused by living organisms multiplying within the host and capable of being transmitted between hosts (theory of infection) became firmly established, due to the work of Pasteur and

others [141, 119]. The regular cyclic behavior of measles epidemics was noticed first by Arthur Ransome around 1880.

Epidemiological modelling led to the analysis of ordinary differential, discrete (stochastic) or partial differential systems. Throughout this thesis, we will mostly use non-linear ordinary differential systems. To raise this analysis, it is important to revise some mathematical concepts relating to the analysis of nonlinear differential systems. In this chapter we introduce some mathematical concepts, definitions and theories needed especially for model analysis and also for numerical study. Some of these results have already been given in [29, 99] and the most proofs can be found in [15, 108, 113, 29, 153, 99].

1.1 Introduction to mathematical modelling of tuberculosis

Originally, there are five basic hypotheses for TB models:

- tuberculosis is transmissible from human to human (for simplicity, we neglect the bovine tuberculosis);
- only few among the infected become a source of infection (and among them, for simplicity, only those who are coughing and have bacilli in sputum are considered);
- there is no vertical transmission (all new births are susceptible);
- all infected individuals remain infected throughout their lives; this is still a simplification, since it seems that in the absence of reinfection, the initial infection eventually fades after a number of years not yet well defined;
- the vaccination of susceptible does not prevent infection. It prevents a proportion (variable with time) of infected to become infectious and contagious.

Based on those hypotheses, TB models thrived but share important structural similarities, if sometimes subtle differences in the way that the natural history of the disease and the transmission process are represented. In the literature, one can group models by their structure: ordinary differential equations (ODE) and spatially structured models. ODE models include SEIR (Figure 1.2) and SEI (Figure 1.1), SEIS and SEIRS-type models (where S denotes susceptible population, E denotes latently infected, I denotes infectious and R stands for recovered or removed population), age-structured models, delayed models. Delay models are formed by

discrete time compartmental and/or integro-differential equations according to the means that delay is modeled. Age-structured models comprise partial differential equations, discrete-time compartment models and spatially structured models depending on whether the age of the population and the age of the infection is taken into account. TB model assumptions are made in order to answer questions and evaluate the impact of some specific phenomena. We will shortly describe within each type the contributions found in the literature. For more details, a summary of tuberculosis models may be found in [52, 133].

The disease transmission to susceptible population to the population is one of the discussion focus while modelling TB. The models built by Waaler and many others later are in the classical form

$$\begin{cases} \dot{S} = \Lambda - \lambda(I)S - \mu S, \\ \dot{E} = (1-p)\lambda(I)S - (\mu + k)E, \\ \dot{I} = p\lambda(I)S + kE - (\mu + d + r)I, \end{cases} \tag{1.1}$$

where Λ is the recruitment number in the population, $\lambda(I)$ the force of infection, μ the natural mortality rate, p the proportion of fast progression to TB (the proportion of new infections that move directly into the infectious class), r the recovery rate, k the reactivation rate and d the TB mortality rate. The transmission flowchart is presented in Figure 1.1.

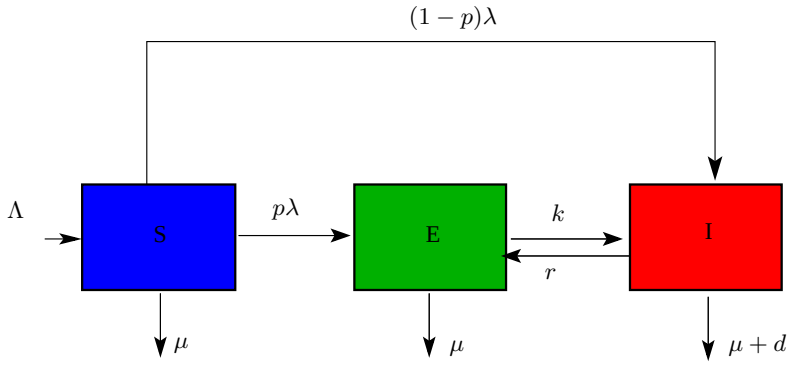

Figure 1.1: Flowchart for an SEI model of tuberculosis dynamics.

In [24, 28, 26, 51], using same hypotheses as in model(1.1), authors included a class of recovered population. The flowchart of an example developed is give in

Figure 1.2. Equations are defined by

$$\begin{cases} \dot{S} = \Lambda - \lambda(I)S - \mu S, \\ \dot{E} = (1-p)\lambda(I)S - (\mu + k)E, \\ \dot{I} = p\lambda(I)S + kE - (\mu + d + r)I, \\ \dot{R} = rI - \mu R \end{cases} \tag{1.2}$$

Some authors choose not to consider fast progression to tuberculosis ($p = 0$) for various reasons [168, 169, 167, 40] and others considered the impact of HIV/AIDS and immunodeficiency in general as a factor of fast progression to TB [24, 28, 26, 51, 67, 10]. Parameter $\lambda(I)$ can be linear ($\lambda(I) = \beta \in \mathbb{R}$) [161], density dependent ($\lambda(I) = \beta I$) [25, 28, 30, 33] or frequency dependent ($\lambda(I) = \beta\frac{I}{N}$) [29, 40, 70, 71].

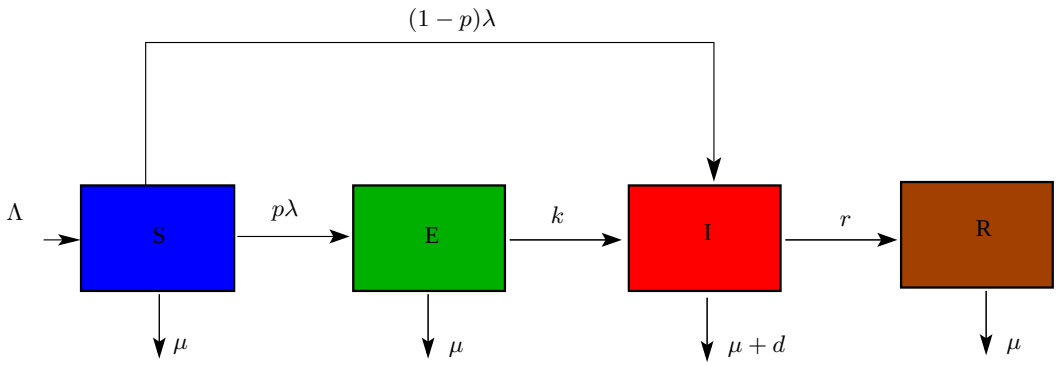

Figure 1.2: A classic mathematical model of tuberculosis dynamics.

The choice of the force of infection had its origin in chemical reaction kinetics, and remain fundamental to the modern theory of deterministic epidemic modelling (mass action). The popularity of mass action is explained by its mathematical convenience and the fact that at low population densities it is a reasonable approximation of a much more complex contact process. The contact rate is often a function of population density, reflecting the fact that contacts take time and saturation occurs. One can envisage situations where contacts could be approximately proportional to N (frequency-dependent or density-dependent mass action) and other situations where contacts may be approximately constant. Hence terms like $\lambda(I) = \beta SI$ and $\lambda(I) = \beta SI/N$ are frequently seen in the literature. In this case, β is the transmission coefficient per time units.

1.2 Non-negatives matrices

In dynamical systems, one finds matrices directly when the system is linear, or by calculating the Jacobian matrix at any point when the system is non-linear. In many epidemiology models, it is possible to separate the linear part of the system from the nonlinear part. Stability analysis of a system of ODEs usually calls-back the manipulation of matrices. In this section, we will recall some definition and properties related to matrices, useful for the stability of a TB deterministic model. We will also explore some link between dynamical systems and matrices. Following results and standard definitions can be found in [15, 108, 113, 29, 153, 99]). Let $M = [M_{ij}] \in \mathcal{M}_n(\mathbb{R})$ be a matrix.

Some definitions related to matrices

Definition 1.2.1. (*Diagonally dominant matrix*)

- M is *column* diagonally dominant if one has

$$\mid M_{ii} \mid \geq \sum_{j=1, j\neq i}^{n} \mid M_{ji} \mid \ \ \forall i \in \{1, \cdots, n\}.$$

- M is *row* diagonally dominant if one has

$$\mid M_{jj} \mid \geq \sum_{i=1, i\neq j}^{n} \mid M_{ij} \mid \ \ \forall j \in \{1, \cdots, n\}.$$

- M is *strictly column* (respectively *row*) diagonally dominant if the previous relative inequalities are strict.

Definition 1.2.2. (*Metzler matrix*)
The matrix $M \in \mathcal{M}_n(\mathbb{R})$ is called Metzler (or *quasi-positive* or *essentially non-negative*) if all of its elements are non-negative except for those on the main diagonal, which are unconstrained.

Definition 1.2.3. (*M-matrix*)
A matrix M is called an *M-matrix* if it can be written in the form $A = \mu * I_n - N$, where $N \geq 0$ and $\mu > \rho(N)$.

Definition 1.2.4. (*Compartmental matrix*)

A matrix M is *compartmental* if M is a Metzler matrix and is column diagonally dominant.

The compartmental matrix is associated to the notion of compartmental systems. A compartmental system is a system consisting of a finite number of subsystems, which are called compartments. Each compartment is kinetically homogeneous, i.e., any number of persons entering the compartment is instantaneously mixed with other persons of the compartment. Compartmental systems are dominated by the law of conservation of mass. They form also natural models for other areas of applications that are subject to conservation laws. Another property of compartmental systems is that the total flow out of a compartment over any time interval cannot be larger than the amount that was initially present plus the amount that flowed into the compartment during that interval.

Linearization

In this section, we will consider an autonomous system defined by

$$\dot{x} = f(x), \qquad x \in \mathbb{R}^n, \tag{1.3}$$

where the function f does not depend on the independent variable t. Here, the dot represents differentiation w.r.t. time t. The following results are standard definitions and theorems required to analyze the stability of an equilibrium point of an autonomous system (see [134, 82, 91]).

Definition 1.2.5. (*Equilibrium point*)
Let $x^* \in \mathbb{R}^n$ be a point such that $f(x^*) = 0$; x^* is an *equilibrium point* or *steady state* solution of (1.3). Further, an *equilibrium point* x^* is a *hyperbolic equilibrium point* of (1.3) if none of the eigenvalues of the matrix $Df(x^*)$ have zero real part where $Df(x^*)$ is the Jacobian matrix of f at x^*.

Let $x^* \in \mathbb{R}^n$ and consider the following equation

$$\dot{x} = Mx, \qquad x \in \mathbb{R}^n, \qquad M = Df(x^*) \tag{1.4}$$

with f defines in eqn. (1.3).

Definition 1.2.6. (Linearization)
The linear system (1.4) is the *linearization* of (1.3) at x^*.

Definition 1.2.7. (*Sink, source and saddle equilibrium*)
Let x^* be an equilibrium of system (1.3).

- x^* is a *sink* if all eigenvalues of the matrix $Df(x^*)$ have negative real part;
- x^* is a *source* if all eigenvalues of $Df(x^*)$ have positive real part;

- x^* is a *saddle* if it is a hyperbolic equilibrium point and $Df(x^*)$ has at least one eigenvalue with a positive real part and at least one with negative real part.

The following result is fundamental and used to prove the local stability of autonomous dynamical systems.

Theorem 1.2.1. *(Grobman and Hartman)*

If x^* is a hyperbolic equilibrium point of (1.3), then there is a neighborhood of x^* in which f is topologically equivalent to the linear system (1.4).

This result means that basic properties of system (1.3) are equivalent to basic properties of (1.4) in a neighborhood of x^*. Let us now recall some results about the notion of irreducible matrices.

Irreducible matrices. Let $M \in \mathcal{M}_n(\mathbb{R})$ be a square matrix.

Definition 1.2.8. (*Irreducible matrices*)
The matrix M is irreducible if any of the following equivalent properties holds.

i) M does not have non-trivial invariant subspaces. More explicitly, for any linear subspace spanned by basis vectors $e_{i1}, ..., e_{ik}$, $n > k > 0$, its image under the action of M is not contained in the same subspace.

ii) For every pair of indexes i and j, there exists a natural number m such that $(M^m)_{ij}$ is not equal to 0. M cannot be transformed into block upper triangular form by a permutation matrix P:

$$PMP^{-1} \neq \begin{pmatrix} E & F \\ 0 & G \end{pmatrix},$$

where E and G are non-trivial square matrices.

iv) If $M > 0$, then one can associate with a matrix M a certain directed graph G_M. It has exactly n vertices, where n is the size of M, and there is an edge from vertex i to vertex j precisely when $M_{ij} > 0$. Then the matrix M is irreducible if and only if its associated graph G_M is strongly connected.

It is evident that if $M \gg 0$, then M is irreducible. Now let us enunciate the theorem of Perron-Frobenius which is a finite dimensional version of the theorem of Krein-Rutman.

Theorem 1.2.2. *(Perron-Frobenius)*
Suppose $M \in M_n(\mathbb{R})$ is a non-negative matrix, then

- *The spectral radius $\rho(M)$ of M is an eigenvalue of M and there exists an associated eigenvector $v > 0$;*
- *If M is irreducible, the spectral radius is positive ($\rho(M) \geq 0$) and $v \gg 0$. Moreover, $\rho(M)$ is a simple eigenvalue and if u is another eigenvector of M for $\rho(M)$, then there exists $k \in \mathbb{R}_{>0}$ such that $u = kv$;*
- *If N is a matrix such that $N \gg M$ then, $\rho(N) > \rho(M)$ holds;*
- *If $M \gg 0$, then for all other eigenvalues λ of M, one has $|\lambda| < \rho(M)$.*

See [15] for the proof and more explanations.

Metzler matrices. Let x^* be an equilibrium of system (1.3), then if $M = Df(x^*)$ is irreducible, it is a Metzler matrix. We remark that the stability modulus defined by $\alpha(M) = \max\{Re(\lambda), \quad \lambda \in Sp(M)\}$ determines the stability of the equilibrium x^*. The following corollary is a consequence of theorem 1.2.2.

Corollary 1.2.1. *Let $M \in \mathcal{M}_n(\mathbb{R})$ be a Metzler matrix.*

- *The stability modulus $\alpha(M)$ is an eigenvalue of M and there exists $v > 0$ such that $Mv = \alpha(M)v$. Moreover, $Re(\lambda) < \alpha(M)$ for all $\lambda \in Sp(M) \setminus \{\alpha(M)\}$*
- *If M is irreducible, then*

  i- *$\alpha(M)$ is a simple eigenvalue;*

  ii- *$v \gg 0$ and all other eigenvectors of M are multiples of v;*

  iii- *If N is a matrix such that $N > M$ then, $\alpha(N) > \alpha(M)$;*

  iv- *If $\alpha(M) < 0$, then $-M^{-1} \gg 0$*

Proof : (see also [153]) Since $M = [M_{ij}]_{1 \leq i,j \leq n}$ is a Metzler matrix, there exists $\tau \geq 0$ such that $M + \tau I_n > 0$ (it is sufficient to take $\tau = max\{|M_{ii}|\}$). Then Theorem 1.2.2 of Perron-Frobenius can be applied to $M + \tau I_n$. Since $\rho(M + \tau I_n)$ is a positive eigenvalue of $M + \tau I_n$, there exists an associated eigenvector $v > 0$. Since $Sp(M + \tau I_n) = \tau + Sp(M)$, one has

$$\alpha(M + \tau I_n) = \rho(M + \tau I_n) = \alpha(M) + \tau.$$

Thus, $\alpha(M)$ is an eigenvalue of M.

If M is irreducible, then $M + \tau I_n$ is irreducible and non-negative. Applying Theorem 1.2.2, it follows that (i), (ii) and (iii) are satisfied. On the other hand, it follows from the equality $-M^{-1} = \int_0^\infty e^{Mt}dt \gg 0$ that (iv) is true. □

The following theorem gives some equivalent properties of the definition of Metzler stable matrices. Stability of matrix throughout this thesis refers to the stability of the associated linear ODE.

Theorem 1.2.3. *(Metzler stable matrices)*
Let $M \in \mathcal{M}_n(\mathbb{R})$ be a Metzler stable matrix. Then, the following properties are equivalent

1. *M is asymptotically stable*
2. *$-M^{-1}$ exists and is non-negative.*
3. *If P is a positive matrix, then the equation $Mx+P = 0$ has a positive solution $x \in \mathbb{R}^n_{>0}$.*
4. *There exists a positive vector $q \gg 0$ such that $Mq \ll 0$ is negative.*
5. *There is a diagonal matrix $R \in \mathbb{R}^n_{>0}$ such that MR is row diagonally strictly dominant (RM is column diagonally strictly dominant respectively).*
6. *There is a diagonal positive matrix N such that $-(MN^T+NM)$ is symmetric and Metzler stable.*

The proof can be found in [153].

M-matrices. The following result on M-matrices will be useful for the next section.

Theorem 1.2.4. *[73, 15] Let $M \in \mathcal{M}_n(\mathbb{R})$, each of the following conditions (among others) is equivalent to the statement "M is an M-matrix"*

- *All principal minors of M are nonnegative.*
- *Every real eigenvalue of M is nonnegative.*
- *The real part of each nonzero eigenvalue of M is positive, i.e., $s(M) > 0$.*

Lemma 1.2.1. *Let M be a non-singular M-matrix and suppose $-N$ and $-NM^{-1}$ are Metzler matrices. Then N is a non-singular M-matrix if and only if NM^{-1} is a non-singular M-matrix.*

The proof of this Lemma can be found in [15], for the reverse implication this is an exercise given in [88]. In general, this lemma does not hold if N a singular M-matrix. It can be shown to hold if N is singular and irreducible. However, this is not sufficient for our needs.

Lemma 1.2.2. *Let M be a non-singular M-matrix and suppose $P > 0$. Then,*

- *$M-P$ is a non-singular M-matrix if and only if $(M-P)M^{-1}$ is a non-singular M-matrix.*
- *$M - P$ is a singular M-matrix if and only if $(M - P)M^{-1}$ is a singular M-matrix.*

Proof :
Let M be a non-singular M matrix. Let $N = M - P$. Since $P > 0$, both N and $NH^{-1} = I - MH^{-1}$ are Metzler matrices. In fact, M is an M-matrix implies that $-M$ is a Metzler matrix; recall Theorem 1.2.3, one has $-M^{-1} < 0$. Hence, Lemma 1.2.2 implies the statement of the first proposition. A similar continuity argument can be constructed for each implication in the singular case. □

Stability of an equilibrium

The notion of stability of an equilibrium point is of considerable theoretical and practical importance, and it has been widely discussed in the literature. Some books developed the theory of dynamical systems [80, 106, 109] and many others focused on the applications [119, 120, 4, 35]. We have the following definition of the stability.

Definition 1.2.9. (*Stable equilibrium*)
Let $x^* \in \Omega$ be an equilibrium point of system (1.7)

- x^* is said to be *Lyapunov stable* if for a given $\varepsilon > 0$, there exists $\delta(\varepsilon) > 0$, such that, for any $x_0 \in \Omega$ for which $||x^* - x_0|| < \delta(\varepsilon)$, the solution $x(t, x_0)$ of (1.7) through x_0 at 0 satisfies $||x(t, x_0) - x^*|| < \varepsilon$ for all $t \geq 0$.
- $x^* \in \Omega$ is said to be *unstable* if it is not stable.
- $x^* \in \Omega$ is said to be *asymptotically stable* if it is Lyapunov stable and, in addition, there exists a constant $c > 0$ such that if $||x^* - x_0|| < c$ then $||x(t, x_0) - x^*|| \longrightarrow 0$ as $t \longrightarrow \infty$.
- $x^* \in \Omega$ is said to be *globally asymptotically stable* if it is asymptotically stable for all $x_0 \in \Omega$ and every solution $x(t, x_0)$, $x_0 \in \Omega$ of (1.7) possesses the property $||x(t, x_0) - x^*|| \longrightarrow 0$ as $t \longrightarrow \infty$.

Lyapunov functions are scalar functions that may be used to prove the stability of an equilibrium for a giving ODE. Their existence is a necessary and sufficient condition for stability. Whereas there is no general techniques for the construction of Lyapunov functions for ODEs, in many specific cases they are known.

Definition 1.2.10. (*Positive definite function*)
Let Ω be a neighborhood of x^*. A function $V : \mathbb{R} \times \Omega \longrightarrow \mathbb{R}$ is said to be *positive definite* if the following three propositions are true.

i) $V(t, x) > 0$ for all $x \neq x^*$;

ii) $V(t, x^*) = 0$;

iii) $V(t, x) \longrightarrow \infty$ when $x \longrightarrow \infty$

Informally, a Lyapunov function takes positive values everywhere except at the given equilibrium, and decreases along every trajectory of the ODE. The principal advantage of Lyapunov function-based stability analysis of ODEs is that the solution of the ODE is not required. The quantity

$$\dot{V}(t, x) = \frac{\partial V}{\partial t} + \langle \bigtriangledown_x V, f \rangle,$$

where f is defined as in (1.7) is the Lie derivative along the flow of system (1.7). Function V can be interpreted as the energy function of the system.

Theorem 1.2.5. *If there exists a positive definite function V such that $\dot{V} < 0$ outside Ω and $V = 0$ on Ω, where Ω is a set which contains no entire trajectories apart from the point 0, then the equilibrium point 0 is asymptotically stable.*

1.3 The basic reproduction number

In epidemiology, the basic reproduction number sometimes called *basic reproductive rate*, *basic reproductive ratio* and denoted $\mathcal{R}_0$ of an infection is the expected number of cases generates over the course of its infectious period by an infectious. In this section, we will recall history of $\mathcal{R}_0$, we will give the biological interpretation and the computation.

An introduction of the historical concept

The concept of the basic reproductive number denoted $\mathcal{R}_0$ is now unanimously recognized as a key concept in mathematical modelling of infectious diseases. It is

defined as the expected number of new cases caused by a typical infected person in a population consisting entirely of susceptible subjects during its infectivity period. Since more than twenty years, this concept has been discussed in most research articles about mathematical modelling of infectious disease. The concept originates from research in demography and ecology where $\mathcal{R}_0$ is the expected number of offspring girls (or females) born to a woman (or a female) during her entire life. The first person who has introduced the concept in 1886, is probably the director of the statistics office of Berlin, Richard Böckh. Using a life table for women in 1879, he summed up the products of probability of survival by the birth rate of girls. He concluded using the sex ratio, that on average 1.06 girls were born of a woman. This would be defined as $\mathcal{R}_0$. In the demographic context, Dublin and Lotka (1925) [112] and Kuczynski (1928) introduced, the concept and calculation of $\mathcal{R}_0$. In an abstract in 1939, Lotka wrote "Net reproductivity $\mathcal{R}_0$, introduced by Böckh, has more merit, because it gives in a essentially independent way a measure of population distribution by age". In fact, if $\mathcal{P}(a)$ is the probability for a women to be alive at age a, and if $\mathcal{F}(a)$ is the probability to have a girl at age a, then

$$\mathcal{R}_0 = \int_0^{+\infty} \mathcal{P}(a)\mathcal{F}(a)da. \tag{1.5}$$

This approximation of the average number of girls that a woman will give birth throughout her life was found by Böckh. We can also define moments of higher order n by

$$\mathcal{R}_n = \int_0^{+\infty} a^n\mathcal{P}(a)\mathcal{F}(a)da. \tag{1.6}$$

Obviously, $\mathcal{R}_0$ is the moment of order $n = 0$.

According to its definition, $\mathcal{R}_0$ is a multiplicative coefficient. The most intuitive example is that for a population of n infected, after one time step, one will have $\mathcal{R}_0 n$ infected, and after k time steps, one will have $\mathcal{R}_0^k n$ infected. This suggests that for $\mathcal{R}_0 > 1$, there will be an increase in cases leading to an epidemic, and the disease will disappear if $\mathcal{R}_0 < 1$.

Ross (Nobel prize of medicine 1902), discoverer of the malaria transmission by mosquitoes, led at the beginning of the 20^{th} century a difficult campaign and often acrimonious to be accepted by the medical community, what he called his "mosquito theorem". This theorem implies that the reduction of the anopheles population would be a way to prevent malaria [144, 145, 146]. Ross identified the main factors in malaria transmission and calculated the number of new infections arising per month as the product of these factors, he deduced that there is a critical density of mosquitoes, below which the malaria parasite can not be sustained. Kermack and McKendrick continued the work of Ross, and extended the concept of threshold to the transmission of diseases.

In 1955 MacDonald gave an expression for the basic reproduction rate in terms of ingredients identified by Ross by rewriting the resulting expression. He obtained the critical level already derived by Ross. He started using symbol z_0 for his quantity, and he was the first who introduced the "basic reproduction rate" in epidemiology, even if he did not see the connection with demography [84]. The concept of basic reproduction ratio was rediscovered in epidemiology in 1974 (see [62, 85]) and definitely established in the Dahlem Workshop Proceedings [3]. Furthermore Diekmann and Heesterbeek have given a precise mathematical definition of $\mathcal{R}_0$[59], extendable to systems in any dimension.

1.3.1 The next generation method

The next-generation method, developed by Diekmann et al. [59], Diekmann and Heesterbeek [58], and popularised by van den Driessche and Watmough [157], is a generalisation of the Jacobian method, and was improved more recently in [60]. It is significantly easier to use than Jacobian-based methods (e.g. based on Jacobian matrices), since it only requires the infection states (such as the exposed class, the infected class and the asymptomatically infected class) and ignores all other states (such as susceptible and recovered individuals). This keeps the size of the matrices in many cases relatively manageable. By definition, the basic reproduction ratio concept is related to the possibility of the existence of a population entirely constituted of susceptible individuals. This involves some specific structures for the models. As a rule, several traits of individuals are epidemiologically relevant in an infectious agent/host system, for example age, sex, species. Only the case where these traits divide the population into a finite number of discrete categories is considered. One can then define a matrix called the next-generation matrix (NGM) denoted by K that relates the numbers of newly infected individuals in the various categories in consecutive generations. We will make the following assumption: all recruitments in the total population are made in the susceptibles classes. This implies already the existence of susceptible and infected compartments, and also the existence of a disease free equilibrium (DFE).

Let the variables $x = (x_1, ..., x_n)^T$ represent the sizes of n population classes based on their epidemiological status w.r.t. an infectious disease. x_i could be the prevalence of class i (percentage of person in the class), a density, or the number of individuals w.r.t. an infectious disease. We assume that compartments are arranged in such a way that the first p are composed of individuals "not infected" or, more precisely, do not carry or do not contribute to the transmission of the germ (virus, protozoan, parasitic, ...). In these p classes, there are in fact all those who do not progress to the disease without effective contact to a compartment of infectious individuals or are not directly involved in the spread of the disease. There may be susceptibles, vaccinated, quarantined people, without vertical and horizontal trans-

mission (e.g. no transmission from mother to child). The $n-p$ other compartments consist of "infected" (latently infected, infectious, asymptomatic carrier, etc.).

The involved ODE is defined by

$$\dot{x} = f(x), \qquad f \in \mathcal{C}^1(\mathbb{R}^n) \tag{1.7}$$

We need the following result

Proposition 1.3.1. *If f is a $\mathcal{C}^k$ function from $\mathbb{R}^n$ to $\mathbb{R}^m$, such that $f(x_0) = 0$, then there exists a $\mathcal{C}^{k-1}$ function $M(x)$ from $\mathbb{R}^n$ to $\mathcal{M}_{mn}(\mathbb{R})$ such that for all $x \in \mathbb{R}^n$, we have*

$$f(x) = M(x)(x - x_0)$$

Proof : Let us consider the $\mathcal{C}^k$ function defined from $\mathbb{R}$ to $\mathbb{R}^m$ by

$$\psi(t) = f(x_0 + t(x - x_0)).$$

One has

$$\begin{aligned} f(x) &= \psi(1) - \psi(0) \\ &= \int_0^1 \psi'(s)ds \\ &= \int_0^1 Df(s,x)(x - x_0)ds \\ &= \left(\int_0^1 Df(s,x)ds\right)(x - x_0). \end{aligned} \tag{1.8}$$

Thus $M(x) = \int_0^1 Df(s,x)ds$ satisfies the claim. □

In the following we define the input and output of each compartment.

- Let $\mathcal{F}_i$ be the rate of appearance of new infections in compartment i, $\mathcal{F}_i \in \mathcal{C}^1(\mathbb{R})$;
- $\mathcal{V}_i(x) = \mathcal{V}_i^-(x) - \mathcal{V}_i^+(x)$, $\mathcal{V}_i^+, \mathcal{V}_i^- \in \mathcal{C}^1(\mathbb{R})$ where $\mathcal{V}_i^-$ denotes the transfer rates of individuals out of compartment i (mortality, change in epidemiological status, movement, etc.) and $\mathcal{V}_i^+(x)$ is the transfer rate of individuals in the compartment i (recovery, aging, movement, etc.). $\mathcal{V}_i(x)$ is the transfer rate out and in the compartment i.

Using the previous notation, it follows that equation (1.7) can be written in the form

$$\dot{x}_i = f_i(x) = \mathcal{F}_i(x) - \mathcal{V}_i(x), \quad i = 1, ..., n. \tag{1.9}$$

Definition 1.3.1. (*Disease free equilibrium*) Let

$$X_s = \{x \geq 0 | x_i = 0; \;\; i = p+1, ..., n\}$$

is the disease free equilibrium (DFE) of the model 1.7 if $f(X_s) = 0$.

Corresponding to the nature of the epidemiological models, the following general assumptions are introduced:

A_1**:** $x \geq 0$, $\mathcal{F}_i(x) \geq 0$, $\mathcal{V}_i^+(x) \geq 0$ and $\mathcal{V}_i^-(x) \geq 0$ for $i = p+1, ..., n$. Each component, represents a net outflow or inflow from compartment i and must be positive whenever the compartment is empty. The functions $\mathcal{F}_i(x)$ represent "new" infections and cannot be negative.

A_2**:** If $x = 0$, then $\mathcal{V}_i^- = 0$. If there is nothing inside a compartment, then there is no outflow.

A_3**:** If $i \leq p$, $\mathcal{F}_i = 0$. There is no new infection inside "non infective" classes.

A_4**:** If $x \in X_s$ i.e. $x_i = 0$, $i > p$, then $\mathcal{V}_i^+ = 0$. If there is no infection at all, there are no inflows inside the infectious classes

A_5**:** If $\mathcal{F}(x)$ is set to zero, then all eigenvalues of $Df(\mathbf{x}_0)$ have negative real parts, where $Df(\mathbf{x}_0)$ is the Jacobian matrix evaluated at the DFE $\mathbf{x}_0$.

Generally, there may be several DFE (see [32] for an example). We are only interested in those that are stable in absence of the pathogen. One question which is usually asked, is under which conditions a pathogen can invade a DFE.

Let $\mathbf{x}_1 = (x_1, ..., x_p)^T$ be the "noninfected" population and $\mathbf{x}_2 = (x_{p+1}, ..., x_n)^T$ the "infected" population. Then, equation (1.7) can be write in the form

$$\begin{cases} \dot{\mathbf{x}}_1 &= f_1(\mathbf{x}_1, \mathbf{x}_2), \\ \\ \dot{\mathbf{x}}_2 &= f_2(\mathbf{x}_1, \mathbf{x}_2). \end{cases} \tag{1.10}$$

Then, one has $\mathbf{x}_0 = (\mathbf{x}_1^0, 0)$ as the DFE of the model.

Lemma 1.3.1. *If* $\mathbf{x}_0 = (\mathbf{x}_1^0, 0)$ *is a DFE of (1.10) and* $f_i(x)$ *satisfies* (A_1)-(A_5)*, then the Jacobian matrix of the system at* $\mathbf{x}_0$ *is partitioned as*

$$J = \begin{bmatrix} D_{\mathbf{x}_1} f_1(\mathbf{x}_0) & D_{\mathbf{x}_2} f_1(\mathbf{x}_0) \\ 0 & F - V \end{bmatrix}$$

where $F = \left[\dfrac{\partial \mathcal{F}_i}{\partial x_j}(\mathbf{x}_0)\right]$ *and* $V = \left[\dfrac{\partial \mathcal{V}_i}{\partial x_j}(\mathbf{x}_0)\right]$ *for* $i = p+1, ..., n$. *Further,* F *is non-negative,* V *is a non-singular M-matrix and all eigenvalues of* $D_{\mathbf{x}_1} f_1(\mathbf{x}_0, 0)$ *have negative real part.*

Proof : By the definition of $\mathbf{x}_0$, one has

$$f_1(\mathbf{x}_1^0, 0) = 0$$

and, using assumption (A_3)-(A_4), it follows for all $\mathbf{x}_1 \in \mathbb{R}^p$ that

$$f_2(\mathbf{x}_1^0, 0) = 0.$$

It follows that $D_{\mathbf{x}_1} f_2(\mathbf{x}_0) = 0$. Since for $x = (\mathbf{x}_1, \mathbf{x}_2)$, $f(x)$ is $\mathcal{C}^1$, and applying proposition 1.3.1, there exists$M_1(x) = [M_{11}(x), M_{12}(x)]$ and $M_2 = M_{22}(x)$ with

$$\begin{cases} f_1(x) &= M_1 \begin{bmatrix} \mathbf{x}_1 - \mathbf{x}_1^0 \\ \mathbf{x}_1 \end{bmatrix} = M_{11}(x)(\mathbf{x}_1 - \mathbf{x}_1^0) + M_{12}(x)\mathbf{x}_2, \\ \\ f_2(x) &= M_2(x)\mathbf{x}_2 = M_{22}(x)\mathbf{x}_2 \end{cases}$$

Then, system (1.10) becomes

$$\begin{cases} \dot{\mathbf{x}}_1 &= M_{11}(x)(\mathbf{x} - \mathbf{x}_1^0) + M_{12}(x)\mathbf{x}_2, \\ \\ \dot{\mathbf{x}}_2 &= M_{22}(x)\mathbf{x}_2, \end{cases} \tag{1.11}$$

and the Jacobian at the DFE is given by

$$J = J(\mathbf{x}_0) = \begin{bmatrix} M_{11}(\mathbf{x}_0) & M_{12}(\mathbf{x}_0) \\ 0 & M_{22}(\mathbf{x}_0) \end{bmatrix} = \begin{bmatrix} D_{\mathbf{x}_1} f_1(\mathbf{x}_0) & D_{\mathbf{x}_2} f_1(\mathbf{x}_0) \\ 0 & F - V \end{bmatrix}.$$

The non-negativity of F follows from (A_1) and (A_4). Let $\{e_j\}$ be the Euclidean basis vectors, where e_j is the j^{th} column of the $n \times n$ identity matrix. Then, for $j \in p+1, ..., n$

$$\frac{\partial \mathcal{V}_i}{\partial x_j}(\mathbf{x}_0) = \lim_{h \longrightarrow 0} \frac{\mathcal{V}_i(\mathbf{x}_0 + he_i) - \mathcal{V}_i(\mathbf{x}_0)}{h}$$

To show that $\mathcal{V}$ is a non-singular M-matrix, note that if $\mathbf{x}_0$ is a DFE, then by (A_2) and (A_4), $\mathcal{V}_i(\mathbf{x}_0) = 0$ for $i = p+1, ..., n$, and if $i \neq j$, then the i^{th} component of $\mathbf{x}_0 + he_j = 0$ and $\mathcal{V}_i(\mathbf{x}_0 + he_j) = -\mathcal{V}_i^+(\mathbf{x}_0 + he_j) \leq 0$, by (A_1) and (A_2). Hence,

$$\frac{\partial \mathcal{V}_i}{\partial x_j}(\mathbf{x}_0) = \lim_{h \longrightarrow 0} \frac{\mathcal{V}_i(\mathbf{x}_0 + he_i)}{h} \leq 0$$

This show that off-diagonal elements of V are negative and therefore, V is a non singular M-matrix. □

The assumed stability of the disease-free subsystem implies $\alpha(D_{\mathbf{x}_1} f_1(\mathbf{x}_0)) < 0$. Thus, the system is locally asymptotically stable if $\alpha(F - V) < 0$. The following result is a consequence of the Varga Theorem [158].

Theorem 1.3.1. *[157]*

$\alpha(F - V) < 0$ if and only if $\rho(F \cdot V^{-1}) < 1$. Moreover, Consider the disease transmission model given by (1.7) with $f(x)$ satisfying conditions (A_1)-(A_5). If $\mathbf{x}_0$ is a DFE of the model, then $\mathbf{x}_0$ is locally asymptotically stable if $\rho(F \cdot V^{-1}) < 1$, but unstable if $\rho(F \cdot V^{-1}) > 1$.

Slight modification of the proof can be find in [157]

Proof : Let $M = F - V$. If assuming that $\alpha(M) = \alpha(F - V) < 0$, then $F - V$ is asymptotically stable. Applying Theorem 1.2.3, it follows that $M^{-1} > 0$. Since matrices $V = F - M$ and M are non-singular, one can write that $-M$ is a non-singular M-matrix once $\alpha(M) < 0$. Since $F \cdot V^{-1}$ is non-negative, $-MV^{-1} = I - F \cdot V^{-1}$ is a Metzler matrix. Applying Lemma 1.2.1, it follows that $I - F \cdot V^{-1}$ is a non-singular M-matrix. Finally, since $F \cdot V^{-1}$ is non-negative, all eigenvalues of $F \cdot V^{-1}$ have magnitude less than or equal to $\rho(F \cdot V^{-1})$. Thus, $F \cdot V^{-1}$ is a non-singular M-matrix if and only if $\rho(F \cdot V^{-1}) < 1$.

Hence, $\alpha(F - V) < 0$ if and only if $\rho(F \cdot V^{-1}) < 1$. Similarly, it follows that $\alpha(F-V) = 0$ if and only if $I-F\cdot V^{-1} < 0$ is a singular M-matrix. This is equivalent to $\rho(F\cdot V^{-1}) = 1$. The second equivalence follows from Lemma 1.2.2. The remainder of the equivalences follow as in the non-singular case. Hence, $\alpha(F - V) \leq 0$ if and only if $\rho(F \cdot V^{-1}) < 1$. It follows that $\alpha(F - V) > 0$ if and only if $\rho(F \cdot V^{-1}) > 1$. □

Definition 1.3.2. (*The basic reproduction ratio*)
If the transmission matrix V is a M-matrix, then the basic reproduction ratio is defined by

$$\mathcal{R}_0 = \rho(F \cdot V^{-1}). \tag{1.12}$$

This is the mathematical definition of the basic reproduction ratio. In the following we also give the biological interpretation of $\mathcal{R}_0$.

1.3.2 Biological interpretation of $\mathcal{R}_0$

We introduce a small number of infectious individuals in a entirely susceptible population regarding an infectious disease. To determine the fate of a small number of infected individuals, we consider the dynamical system with no reinfection, since we are interested only in secondary cases. Because we want to analyze the behavior after an infinitesimal time step, we consider the linearized system approaching an equilibrium. f_1 is near the equilibrium. The system behavior is approximated by the linearized system (Grobman and Hartman, Theorem 1.2.1).

The linearized system without F is given by

$$\dot{x} = \begin{bmatrix} D_{\mathbf{x}_1} f_1(\mathbf{x}_0) & D_{\mathbf{x}_2} f_1(\mathbf{x}_0) \\ 0 & -V \end{bmatrix} x \tag{1.13}$$

If $(0, \mathbf{x}_2^0)$ is a small number of infected individuals introduced at the initial time, then by integrating the linear system (1.13) w.r.t. time at t, the number of infectious individuals will be

$$e^{Vt} \cdot \mathbf{x}_2^0.$$

And for $t \to \infty$,

$$\int_0^\infty (0, e^{Vt} \cdot \mathbf{x}_2^0) = (0, V^{-1} \cdot \mathbf{x}_2^0).$$

This set of infected cases will lead to further transmission. The number of new cases will be

$$F \cdot V^{-1} \cdot \mathbf{x}_2^0$$

By linearization, we consider the transmission matrix given by the Jacobian matrix F. Components of $F \cdot V^{-1}$ will have some interpretations. If one considers an infected compartment j, then the entry (k, j) of $F \cdot V^{-1}$ is the average time that this individual will remain in the compartment k during its infectiousness period. The entry (i, j) of F is the speed by which an individual in the compartment k produces new infections in the compartment i. Therefore the entry (i, j) of $F \cdot V^{-1}$ is the expected number of new infections of type i produced by an infected individual of type j. If $K = F \cdot V^{-1}$ is called the "next generation matrix", we have just seen that K_{ij} is the expected number of new infections of type i produced by an infected individual of type j. The matrix K is a positive square matrix of the dimension of the number of "types" (i.e., compartments) of infected. Approximately $F \cdot V^{-1}$ and x_0, expressed in vectorial way, the "number" of new secondary cases. One is led to consider, at the generation n, the quantity $K^n x_0$. By the Perron-Frobenius theorem 1.2.2, the dominant mode (mode is the term for engineers or physicists designate eigenvalues) is just the spectral radius.

1.4 Optimal control applied to epidemiological models

Optimal control theory is a mathematical optimization method for deriving control policies. The method is largely due to the work of Lev Pontryagin and Richard Bellman. Optimal control deals with the problem of finding a control law for a given system such that a certain optimality criterion is achieved. A control problem includes a cost functional which is a function of state and control variables. In the 1950's, motivated especially by aerospace problems, engineers became interested in the problem of controlling a system governed by a set of differential equations. It was natural to want to control the problem such that a given performance index would be minimized. Since some practical techniques were developed for the computation and implementation of optimal controls, the use of this theory became common in a large number of fields.

In epidemiology, large savings in cost could be obtained with a small improvement of strategy to prevent disease or to cure, so that optimal control became very important. An optimal control problem is a set of differential equations describing the paths of the control variables that minimize the cost functional. The optimal control can be derived using Pontryagin's maximum principle [135, 143], or by solving the Hamilton-Jacobi-Bellman equation which is a sufficient condition. In population dynamic and epidemiology, many work has been done on the theory of optimal control [111]. In this part of our work, we will call back necessary theory for the control of epidemiological models. Before beginning, it is advantageous to quickly review a few fundamental results. These results can be found in [111, 75].

1.4.1 Controlled dynamics

Let us considering an ODE having the form

$$\begin{cases} \dot{y} = f(y(t), u(t)), \\ y(t_0) = y_0 \end{cases} \tag{1.14}$$

where the function $f : \mathbb{R}^n \times \mathcal{U} \longrightarrow \mathbb{R}^n$, $y : [t_0, \infty) \longrightarrow \mathbb{R}^n$, $\mathcal{U} \subset \mathbb{R}^m$ and $t > t_0$. Here, the dot represents differentiation w.r.t. time t. We obtain the evolution of our system when the parameter is constantly set to the value $u(t)$. The trajectory $y(\cdot)$ will be regard as the response of the system corresponding to the control $u(t)$. We introduce

$$\mathcal{U} = \{u : [t_0, \infty) \longrightarrow \mathbb{R}^m \mid \ u \ \ measurable\}$$

to denote the set of all admissible controls, when $u(t) = (u_1(t), u_2(t), \cdots, u_m(t))^T$. Note that the solution $y(t)$ of equation (1.14) depends upon u and the initial condition. Consequently our notation would be more precise, but more complicated, if

we were to write

$$y(t) = y(t, u(t), y_0),$$

displaying the dependence of the response upon the control and the initial value. We can consider the application $u(t) \mapsto y(t) = y(u)(t)$ to remind that $y(t)$ is a function of $u(t)$. The optimal control problem consist of to determine what is the "best" control for our system. For this we need to specify a specific objective (or payoff) criterion. Let us define the *objective function*

$$J(u) = \int_{t_0}^{t_f} g(t, y(t), u(t))dt + h(y(t_f)) \tag{1.15}$$

where $y(t)$ is the solution of equation (1.14) for the control $u \in \mathcal{U}$. Here $g : [t_0, \infty) \times R^n \times \mathcal{U} \longrightarrow \mathbb{R}$ and $h : \mathbb{R}^n \longrightarrow \mathbb{R}$ are given, and we call g the *running payoff* and h the *terminal payoff*. The terminal time $t_f > t_0$ is given as well, or can be include in h. We want to find a control $\bar{u}$, which minimizes the objective function

$$J(y, \bar{u}) \leq J(u) \quad \forall u \in \mathcal{U}.$$

In other words, our basic optimal control problem consist to finding a piecewise continuous control function $u(t)$ and the associated state variable $y(t)$ such that

$$\begin{aligned} J(u) \quad = \quad & \int_{t_0}^{t_f} g(t, y(t), u(t))dt + h(y(t_f)) \longrightarrow \min_u \\ & \text{subject to} \\ & \begin{cases} \dot{y} = f(t, y(t), u(t)), \\ y(t_0) = y_0. \end{cases} \end{aligned} \tag{1.16}$$

Such a control $\bar{u}$ is called *optimal* and the state trajectory $\bar{y}$ is called the corresponding optimal trajectory. The optimal value of the objective function will be denoted as $J(\bar{y}, \bar{u},)$ or $\bar{J}$. Problem (1.16) is said to be in the *Bolza* form [149]. Usually the control variable u will be constrained. Throughout this thesis, we shall allow these constraints to depend on state variables. These are so-called mixed inequality constraints and written as

$$c_1(t, y(t), u(t)) \geq 0, \quad t \in [t_0, t_f], \tag{1.17}$$

where $c_1 : [t_0, +\infty) \times \mathbb{R}^n \times \mathbb{R}^m \longrightarrow \mathbb{R}^p$ is a given function of u, t and possibly y. There is another type of constraints involving only state variables. These are written as

$$c_2(t, y(t)) \geq 0, \quad t \in [t_0, t_f] \tag{1.18}$$

where $c_2 : [t_0, +\infty) \times \mathbb{R}^n \longrightarrow \mathbb{R}^q$ is a given function of y and t. These are the most difficult type of constraints to deal with, and are known as pure state inequality

constraints. Finally, another type of constraints limit the values the terminal state $y(t_f)$ may be took. We denote this by choosing

$$y(t_f) \in Y,$$

where Y is called the reachable set of the state variable at time t_f. Note that Y depends on the initial value y_0. Here Y is the set of possible terminal values that can be reached when $y(t)$ and $u(t)$ obey imposed constraints.

Richard Bellman (1957) [14, 63, 13, 149] states in his book on dynamic programming the principle of optimality as follows:

"An optimal policy has the property that whatever the initial state and initial decision are, the remaining decisions must constitute an optimal policy with regard to the state resulting from the first decision."

That principle can be translate into the following theorem.

Theorem 1.4.1. *(Bellman optimality principle)*

If $\bar{u} : [t_0, t_f] \longrightarrow \mathbb{R}_+$ is an optimal control of problem (1.16) over the interval $[t_0, t_f]$, starting at state $y(t_0)$, then the restriction of $\bar{u}$ over the time interval $[t_1, t_f]$ denotes $\bar{u}^* : [t_1, t_f] \longrightarrow \mathbb{R}_+$ is necessarily optimal over the sub-interval $[t_1, t_f]$ for any t_1 such that $t_0 \leq t_1 \leq t_f$.
Further, if $\bar{u}$ is the unique optimal control for problem (1.16), then $\bar{u}^*$ is the unique optimal control for problem (1.16) over $[t_1, t_f]$

The proof of this theorem used simply the definition of the optimal control and can be found in [149, 111, 54].
Intuitively this principle is obvious, for if we were to start in state y at time t and did not follow an optimal path from there on, then there would exist (by assumption) a better path from t to T, hence we could have followed. The basic assumption underlying the Bellman's principle of optimality is that the system can be characterized by its state $y(t_0)$ at time t_0, which completely summarizes the effect of all inputs $u(t)$ prior to time t.

1.4.2 Necessary condition

The previous section presented the optimal control problem. In this subsection, we will study sufficient conditions to guarantee the existence (and the uniqueness) of a finite objective optimal control and state.

1.4.2.1 Existence of an optimal control pair

The questions of existence and uniqueness have been solved in [75].

Theorem 1.4.2. *(Existence of the optimal control pair [75])*

Suppose f is continuous; Moreover, there exist positive constants $C_1,\ C_2,\ C_3,\ C_4$ such that for all $t \in \mathbb{R}_+$, $y \in \mathbb{R}^n$ and $u \in \mathcal{U} \subset \mathbb{R}^m$

$A:\ \|f(t,y,u)\| \leq C_1(1 + \|u\| + \|y\|)$;

$B:\ \|f(t,y_1,u) - f(t,y,u)\| \leq C_2\|y_1 - y\|(1+\|u\|)$;

$C:\ \mathcal{U}$ *is closed;*

$D:\ \mathcal{U}$ *is convex;* $f(t,y,u) = \alpha(t,y) + \beta(t,y)u$, *where* α *and* β *are functions;*

$E:\ g(t,y,\cdot)$ *is convex on* $\mathcal{U}$

$F:\ g(t,y,u) \geq C_3\|u\|^\gamma - C_4;\ \gamma > 0.$

Then, the optimal control pair $(\bar{u}, \bar{y})$ *exists.*

The proof of this theorem comes from the general case of the existence of an optimal control solution with payoff function showed by W. Fleming and Rishel (see [75]). The principle technique to solve such optimal control problem is to solve a set of necessary conditions satisfying the optimal control function. The necessary conditions derive here come from Pontryagyn and co-workers [135]. Pontryagin introduced the idea of adjoint function in other to append the differential equation to the objective functional.

Considering the existence of a piecewise optimal control for problem (1.16), the following proposition shows importance and origin of optimality condition, tranversality condition and the adjoint equation. The following result has been shown in dimension one by Lehnart and Workman (cf. [111]).

Proposition 1.4.1. *Considering the optimal control problem (1.16), let* $(\bar{y}(t), \bar{u}(t)) \in \mathbb{R}^n \times \mathbb{R}^m$ *be a pair of optimal control, with* $\bar{y}$ *corresponding to the state, then there exists a piecewise function* $\lambda(t) \in \mathbb{R}^n$ *such that*

$$\begin{aligned}
(D_u g(t,\bar{y}(t),\bar{u}(t)))^T + \lambda^T \cdot D_u f(t,\bar{y}(t),\bar{u}(t)) &= 0, \ \textit{(optimality condition)} \\
\frac{d\lambda}{dt} &= -(D_y g^T + D_y f^T \lambda) \ \textit{(adjoint equation)}, \\
\lambda(t_f) &= D_y h(t_f) \ \textit{(transversality condition)},
\end{aligned} \tag{1.19}$$

where $D_u f$, $D_u g$, $D_y f$, $D_y g$ and $D_y h$ denote the Jacobian matrix of f, g and h.

In [111], authors showed that the proposition 1.4.1 is true in dimension one in the absence of constraints on the terminate state. The following proof is adapted from the one dimensional proof in [111].

Proof :
Let $(\bar{y}, \bar{u})$ be the pair of optimal control, with $\bar{y}$ corresponding to the state. Thus, one has for all (y, u) that $-\infty < J(\bar{u}) < J(u)$. Let $\gamma(t) : [t_0, +\infty) \longrightarrow \mathbb{R}^m$ be a piecewise continuous variation function and $\varepsilon \in \mathbb{R}$. Then,

$$u_\varepsilon = \bar{u}(t) + \varepsilon\gamma(t)$$

is another piecewise continuous control, and let y_ε be the state corresponding to the control function u_ε, namely, y_ε satisfies

$$\frac{dy_\varepsilon}{dt} = f(t, y_\varepsilon, u_\varepsilon).$$

It is easy to see that $y_\varepsilon \longrightarrow \bar{y}$ when $\varepsilon \longrightarrow 0$ and the derivative $\left(\frac{dy_\varepsilon}{d\varepsilon}(t)\right)_{\varepsilon=0}$ exists for each t. The objective functional corresponding to u_ε is

$$J(u_\varepsilon) = \int_{t_0}^{t_f} g(t, y_\varepsilon(t), u_\varepsilon(t))dt + h(y(t_f)).$$

Let $\lambda(t) : \mathbb{R}^n \longrightarrow \mathbb{R}^n$ be a piecewise differentiable function on $[t_0, t_f]$ to be determined. By the fundamental theorem of calculus,

$$\int_{t_0}^{t_f} \frac{d}{dt}[\lambda^T \cdot y_\varepsilon](t)dt = \lambda^T(t_f) \cdot y_\varepsilon(t_f) - \lambda^T(t_0) \cdot y_\varepsilon(t_0).$$

This relation implies that

$$\int_{t_0}^{t_f} \frac{d}{dt}[\lambda^T \cdot y_\varepsilon](t)dt + \lambda^T(t_0) \cdot y_\varepsilon(t_0) - \lambda^T(t_f) \cdot y_\varepsilon(t_f) = 0.$$

Adding this zero expression to $J(u_\varepsilon)$, one has

$$\begin{aligned} J(u_\varepsilon) &= \int_{t_0}^{t_f} \left[g(t, y_\varepsilon(t), u_\varepsilon(t)) + \frac{d}{dt}[\lambda^T \cdot y_\varepsilon](t) \right] dt + \lambda^T(t_0) \cdot y_0 - \lambda^T(t_f) \cdot y_\varepsilon(t_f) + h(y_\varepsilon(t_f)) \\ &= \int_{t_0}^{t_f} \left[g(t, y_\varepsilon(t), u_\varepsilon(t)) + \left(\frac{d\lambda}{dt}(t)\right)^T \cdot y_\varepsilon(t) + \lambda(t)^T \cdot f(t, y_\varepsilon(t), u_\varepsilon(t)) \right] dt \qquad (1.20) \\ &+ \lambda^T(t_0) \cdot y_0 - \lambda^T(t_f) \cdot y_\varepsilon(t_f) + h(y_\varepsilon(t_f)). \end{aligned}$$

Since the maximum of J w.r.t. the control u occurs at $\bar{u}$, the derivative of $J(u_\varepsilon)$ w.r.t. ε is zero, e.g.

$$\lim_{\varepsilon \longrightarrow 0} \frac{J(u_\varepsilon) - J(\bar{u})}{\varepsilon} = 0.$$

Since the interval $[t_0, t_f]$ is compact, and the integrand term is piecewise differentiable, applying the Lebesgue dominated convergence theorem allows us to move the limit and then the derivative inside the integral. Therefore,

$$\begin{aligned}
&\left(\frac{d}{d\varepsilon} J(u_\varepsilon)\right)_{\varepsilon=0} = \lim_{\varepsilon \longrightarrow 0} \frac{J(u_\varepsilon) - J(\bar{u})}{\varepsilon} \\
= &\int_{t_0}^{t_f} \left(\frac{\partial}{\partial \varepsilon} \left[g(t, y_\varepsilon(t), u_\varepsilon(t)) + \left(\frac{d\lambda}{dt}(t)\right)^T \cdot y_\varepsilon(t) + \lambda^T(t) \cdot f(t, y_\varepsilon(t), u_\varepsilon(t)) \right] dt \right)_{\varepsilon=0} \\
- &\lambda^T(t_f) \cdot \left(\frac{dy_\varepsilon}{d\varepsilon}(t_f)\right)_{\varepsilon=0} + (D_y h(y_\varepsilon(t_f)))^T \cdot \left(\frac{dy_\varepsilon}{d\varepsilon}(t_f)\right)_{\varepsilon=0}, \\
= &\int_{t_0}^{t_f} \left(\left[(D_y g)^T \cdot \frac{dy_\varepsilon}{d\varepsilon} + (D_u g)^T \cdot \frac{du_\varepsilon}{d\varepsilon} + \left(\frac{d\lambda}{dt}\right)^T \cdot \frac{dy_\varepsilon}{d\varepsilon} \right](t) \right)_{\varepsilon=0} dt \\
+ &\int_{t_0}^{t_f} \left(\left[\lambda^T \cdot \left(D_y f \cdot \frac{dy_\varepsilon}{d\varepsilon} + D_u f \cdot \frac{du_\varepsilon}{d\varepsilon} \right) \right](t) \right)_{\varepsilon=0} dt \\
- &\lambda^T(t_f) \left(\frac{dy_\varepsilon}{d\varepsilon}(t_f)\right)_{\varepsilon=0} + (D_y h(y(t_f)))^T \cdot \left(\frac{dy_\varepsilon}{d\varepsilon}(t_f)\right)_{\varepsilon=0}.
\end{aligned} \tag{1.21}$$

Finally, from equation (1.21) one has

$$\begin{aligned}
&\left(\frac{d}{d\varepsilon} J(u_\varepsilon)\right)_{\varepsilon=0} = \lim_{\varepsilon \longrightarrow 0} \frac{J(u_\varepsilon) - J(\bar{u})}{\varepsilon} \\
= &\int_{t_0}^{t_f} \left[\left(D_y g + \frac{d\lambda}{dt}^T + \lambda^T \cdot D_y f \right) \cdot \left(\frac{dy_\varepsilon}{d\varepsilon}(t)\right)_{\varepsilon=0} + ((D_u g)^T + \lambda^T \cdot D_u f) \cdot \gamma(t) \right] dt \\
- &\left(\lambda^T(t_f) - (D_y h(\bar{y}(t_f)))^T\right) \cdot \left(\frac{dy_\varepsilon}{d\varepsilon}(t_f)\right)_{\varepsilon=0},
\end{aligned} \tag{1.22}$$

where $D_u f$, $D_u g$, $D_y f$ and $D_y g$ denote the Jacobian matrix of f and g, evaluated in $(t, \bar{y}(t), \bar{u}(t))$. The adjoint function has to be chosen in order to simplify equation (1.22) by making the coefficient of

$$\left(\frac{dy_\varepsilon}{d\varepsilon}(t)\right)_{\varepsilon=0}$$

equal to zero. Thus, we choose the adjoint function $\lambda(t)$ such that

$$\frac{d\lambda}{dt} = -((D_y g)^T + (D_y f)^T \cdot \lambda) \text{ (adjoint equation)} \tag{1.23}$$

and the transversality condition

$$\lambda(t_f) = D_y h(\bar{y}(t_f)).$$

Therefore, equation (1.22) is reduced to

$$0 = \int_{t_0}^{t_f} \left((D_u g(t, \bar{y}(t), \bar{u}(t)) + \lambda^T \cdot D_u f(t, \bar{y}(t), \bar{u}(t))) \cdot \gamma(t) \right) dt. \tag{1.24}$$

Since $\gamma(t)$ have been chosen arbitrarily, its specially holds also for

$$\gamma(t) = (D_u g(t, \bar{y}(t), \bar{u}(t)) + \lambda^T \cdot D_u f(t, \bar{y}(t), \bar{u}(t))).$$

In this case,

$$0 = \int_{t_0}^{t_f} \left((D_u g(t, \bar{y}(t), \bar{u}(t)) + \lambda^T \cdot D_u f(t, \bar{y}(t), \bar{u}(t))) \right)^2 dt, \tag{1.25}$$

Which implies the optimality condition

$$D_u g(t, \bar{y}(t), \bar{u}(t)) + \lambda^T D_u \cdot f(t, \bar{y}(t), \bar{u}(t)) = 0. \tag{1.26}$$

This ends our proof □

In practical cases, one does not need to re-derive the above equation in the way developed in proposition 1.4.1 for a particular problem. In fact, we can generate the necessary conditions from the Hamiltonian H defined as follows:

$$\begin{array}{rcl} H(t, y, u, \lambda) & = & g(t, y, u) + \langle \lambda \mid f(t, y, u) \rangle \\ & = & \text{(integrand)} + \text{(adjoint)} \times \text{(RHS of the ODE)}, \end{array} \tag{1.27}$$

where RHS denotes the right hand side of the ODE. The definition of the adjoint function comes from the result.

1.4.2.2 Pontryagin Principle

The following result is quite long and difficult to prove, and come from the original result of Pontryagin, Boltyankii and Mitshchenko result [135].

Theorem 1.4.3. *(Pontryagin Principle)*

Let $\bar{u}(t)$ and the corresponding state $\bar{y}(t)$ be optimal for problem (1.16). Then there exists a piecewise differentiable adjoint variable $\lambda(t)$ such that

$$H(t, \bar{y}, u, \lambda) \leq H(t, \bar{y}, \bar{u}, \lambda)$$

for all controls $\bar{u}$ at each time t, where the Hamiltonian is defined by

$$H(t, y, u, \lambda) = g(t, y, u) + \langle \lambda \mid f(t, y, u) \rangle,$$

and

$$\begin{aligned} \frac{d\lambda}{dt} &= -D_y H(t, \bar{y}, \bar{u}, \lambda)^T \\ \lambda(t_f) &= 0. \end{aligned}$$

One has following results.

Theorem 1.4.4. *Let us consider the Hamiltonian of problem (1.16) defines by*

$$H(t, y, u, \lambda) = g(t, y, u) + \langle \lambda \mid f(t, y, u) \rangle.$$

1. *H is Lipschitz continuous w.r.t. t on the optimal path.*
2. *If problem (1.16) is autonomous, then H is a constant function of time along the optimal path.*

The proofs of results in theorem 1.4.4 use the mean value theorem for the first part, the differentiability of H and the maximum principle for the second part. They can be found in [111]. Considering problem (1.16) mixed inequality constraints (1.17), the Lagrangian function

$$L : [t_0, +\infty) \times \mathbb{R}^n \times \mathbb{R}^m \times \mathbb{R}^n \times \mathbb{R}^p \longrightarrow \mathbb{R}$$

as

$$L(t, y, u, \lambda, \mu) := H(t, y, u, \lambda) + \langle \mu \mid c_2(t, y, u) \rangle,$$

where $\mu \in \mathbb{R}^p$ is a row vector, whose components are called Lagrange multipliers. Lagrange multipliers satisfy the complimentary slackness conditions

$$\mu \geq 0, \qquad \mu \cdot c_2(t, y, u) = 0.$$

The adjoint vector satisfies the differential equation

$$\frac{d}{dt}\lambda(t) = -D_y L(t, y, u, \lambda, \mu).$$

1.5 Forward backward sweep method (FBSM)

Considering an optimal control problem, it is often difficult to find a solution attributable to the non-linearity of the RHS of the equation. Numerical techniques for optimal control problems may often be classified as either direct or indirect. For a direct method, the differential equation and the integral are discretized and the problem is converted into a nonlinear programming problem. Many choices are available for discretizing the integral, the differential equation, and for solving the nonlinear programming problem resulting in several different numerical methods. Indirect methods approximate solutions to optimal control problems by numerically solving the boundary value problem for the differential-algebraic system generated by the maximum principle. In their book [111], Lenhart and Workman presented a simple numerical scheme called FBSM, that can produce a numerical approximation to solutions for some problems. The FBSM runs quickly. In their paper (cf. [114]), McAssey and colleagues proved two convergence theorems for a basic type of optimal control problem. The first theorem showed that recursively solving the system of differential equations will produce a sequence of iterates converging to the solution of the system and the second theorem shows that a discretized implementation of the continuous system also converges as the iteration and number of sub-intervals increases. The FBSM method is designed to solve the differential algebraic system generated by the maximum principle that characterizes the solution. Let us consider the following optimization problem:

$$J(u) = \int_{t_0}^{t_f} g(t, y(t), u(t))dt \longrightarrow \min \tag{1.28}$$

Subject to

$$\begin{aligned} \dot{y} &= f(t, y(t), u(t)) \\ y(t_0) &= y_0, \end{aligned} \tag{1.29}$$

where f and g are continuously differentiable in all three variables. The maximum principle says that there is an adjoint variable $\lambda(t)$, such that an optimal state $y(t)$, and optimal control $u(t)$ must necessarily satisfy the state equation,

$$\dot{y}(t) = f(t, y(t), u(t)), \tag{1.30}$$

$$y(t_0) = y_0, \tag{1.31}$$

The adjoint equation

$$\dot{\lambda} = D_y H, \quad \lambda(t_f) = 0; \tag{1.32}$$

with

$$H(t, y, u, \lambda) = g(t, y, u) + \lambda(t) f(t, y, u)$$

and minimize the Hamiltonian $H(t, y, u, \lambda)$, considered as a function of the control $u(t)$. The FBSM first solves the state equation (1.30) with a Runge-Kutta routine, then solves the adjoint equation (1.32) backwards in time with the Runge-Kutta

solver, and then updates the control [111, 114]. This produces a new approximation of the state, adjoint and control (y, λ, u). The method continues by using these new updates and calculating new Runge-Kutta approximations and control updates with the goal of finding a "fixed point" (y, λ, u). The method terminates when there is sufficient agreement between the states, costates, and controls of two passes through the approximation loop.

Remark 1.5.1. As H is non-linearly dependent on u, one could determine u from $H_u = 0$. Then one has $u = c_3(y, \lambda)$, and one could replace in system (1.22) and (1.30). However, in our example, one has a positivity constraint for the control function (see equation (4.16 and 4.17) below).

The rough outline of the algorithm presented by Lenhart and Workman [111] is given by :

1. Give an initial value to u over the interval and store the initial guess u.
2. Using the initial condition $y(0) = y_0$ and the store value of u, solve y according to its differential equation in the optimality system.
3. Using the transversal condition $\lambda(t_f) = 0$, solve backward the adjoint equation according to its differential equation in the optimality system.
4. Update the control by introducing the new y and λ into the characterization of u.
5. Check convergence by looking if values of variables in the iteration are negligibly small and output the solution. If it is not small, then go back to 2.

A specified value δ is requiring as a stopping criteria to find the relative errors for the state, the adjoint and the control. The desired relative error for the state variable, for example, is

$$\frac{\|y - y_{old}\|}{\|y\|} < \delta$$

where $\|.\|$ is the l^1-norm $\|y\| = \sum_{i=1}^{m} |y_i|$, y_{old} the old value of y.

Convergence of the FBSM

For the sake of simplicity, problem (1.28) will be rewritten using the maximum principle in the following form:

Find $(y(t); \lambda(t); u(t))$ such that

$$\begin{aligned} \dot{y} &= f(t, y(t), u(t)), \;\; y(t_0) = y_0, && (1.33)\\ \dot{\lambda} &= g_1(t, y(t), u(t)) + \lambda g_2(t, y(t), u(t)), \;\; \lambda(t_f) = 0, && (1.34)\\ u(t) &= c(t, y(t), \lambda(t)), && (1.35) \end{aligned}$$

where g_1, g_1 and c are given functions satisfying the continuity properties so that the system (1.33)-(1.35) has a unique solution. The FBSM is given by the following algorithm.

Algorithm 1.5.1. *Initialization: choose an initial control $u^0 = u^0(t)$;*
Iteration: for $n \geq 0$, solve

$$\begin{aligned} \frac{dy^{n+1}}{dt} &= f(t, y^{n+1}(t), u^n(t)), \;\; y^{n+1}(t_0) = y_0 && (1.36)\\ \frac{d\lambda^{n+1}}{dt} &= g_1(t, y^{n+1}(t), u^n(t)) + \lambda^{n+1} g_2(t, y^{n+1}(t), u^n(t)), \\ & \quad \lambda^{n+1}(t_f) = D_y h(y^{n+1}(t_f)), && (1.37)\\ u^{n+1}(t) &= c(t, y^{n+1}(t), \lambda^{n+1}(t)). && (1.38) \end{aligned}$$

We make the following assumptions.

Assumption 1.5.1. *The functions g_1, g_2 and c are Lipschitz continuous with respect to their second and third arguments, with Lipschitz constants k_{g_1}, k_{g_2} and k_c. Moreover, $\kappa = \|\lambda\|_\infty < \infty$ and $\zeta = \|g_2\|_\infty < \infty$.*

The following theorem discusses convergence of the FBSM.

Theorem 1.5.1. *Under the assumptions (1.5.1), if*

$$\alpha_0 \equiv k_c \left\{ \left[e^{k_f(t_1 - t_0)} - 1 \right] + (k_{g_1} + \kappa k_{g_2}) \frac{1}{\zeta} \left[e^{\zeta(t_1 - t_0)} - 1 \right] \left[e^{k_f(t_1 - t_0)} + 1 \right] \right\} < 1 \tag{1.39}$$

then

$$\lim_{n \to \infty} \max_{t_0 \leq t \leq t_f} |y(t) - y^n(t)| + \max_{t_0 \leq t \leq t_f} |\lambda(t) - \lambda^n(t)| + \max_{t_0 \leq t \leq t_f} |u(t) - u^n(t)| = 0. \tag{1.40}$$

The proof of this theorem, using a consequence of Gronwall's lemma, can be found in [114]. The essence is to find bounds for the errors in y and λ in terms of the error in u and then to show that this last error can be made small. The following theorem shows the convergence of the numerical approximations of the solutions at discrete points in the interval when the Lipschitz constants are small

enough or the time interval is short enough. Since the FBSM solves forward the state equation and backward the costate equation, we use the following notation:

$$\Delta_i y = y_i - y_{i-1};\ \ \delta_i y = y_{i-1} - y_i, \quad i = 1, \cdots, N.$$

Consider a discrete approximation to a general initial value problem, the FBSM is given by the following algorithm.

Algorithm 1.5.2. *Initialization: Choose an initial control value* $u_i^0 = u^0(t_i),\ i = 1, \cdots, N$;
Iteration: for $n \geq 0$ *and* $i = 1, \cdots, N$, *solve*

$$\begin{aligned} \Delta_i y^{n+1} &= h_N F(t_i, y_i^{n+1}, u_i^n),\ \ y_0^{n+1} = y_0 && (1.41)\\ \delta_{i-1}\lambda^{n+1} &= h_N G(t_i, y^{n+1}, u^n, \lambda^{n+1}), \lambda_N^{n+1} = D_y h(y_N^{n+1}), && (1.42)\\ u_i^{n+1} &= c(t_i, y_i^{n+1}, \lambda_i^{n+1}), && (1.43) \end{aligned}$$

where $h_N = 1/N$, F *and* G *are chosen according to a discretization scheme (Euler, Runge-Kutta).*

The following theorem and its proof can be found in [114].

Theorem 1.5.2. *Under the assumptions (1.5.1), supposing that either the Lipschitz constants are small or* t_f *is small for all* $\varepsilon > 0$, *there exist* $n_\varepsilon, N_\varepsilon \in \mathbb{N}$ *such that*

$$\max_{i=1,\cdots,N} \{|y(t_i) - y_i^n| + |\lambda(t_i) - \lambda_i^n| + |u(t_i) - u_i^n|\} < \varepsilon, \tag{1.44}$$

when $N > N_\varepsilon$ *and* $i \geq n_\varepsilon$.

The idea of the proof includes the discrete Gronwall inequalities. The proof follows the general outline of the proof of the continuous approximation. The essence is to find bounds for the errors in y and λ in terms of the error in u and then to show that this last error can be made small. For that, one takes into account an average approximation error on y_i^n and λ_i^n.

Adapted Forward-Backward Sweep Method

The FBSM previously presented is somewhat limited w.r.t. the optimal control problems that can solve. For example, the method is not appropriate to problems with a fixed state endpoint. Other optimal control problems are solved using an adapted method from the FBSM. Bounded control problems, when $a \leq u(t) \leq b$

run quickly with the adapted FBSM. In the same way, problem system (1.16) can run very quickly with the adapted FBSM. It could be solved by expressing u from

$$u(t) = c_3(t, y(t), u(t))$$

in equation (1.28) to

$$u(t) = \min(b, \max(a, c_3(t, y(t))(t))).$$

The Adapted FBSM is used when there is box constraints on the optimal control.

Chapter 2

Tuberculosis Transmission Model

2.1 Tuberculosis biology

Tuberculosis is an infection, primarily in the lungs (a pneumonia), mostly caused by bacteria called *Mycobacterium tuberculosis*. TB is spread usually from person to person by breathing infected air during close contact. The life cycle of MTB is presented in Figure 2.1.

The infection can remain in an inactive (dormant) state for years without causing symptoms or spreading to other people. When a patient immune system with dormant TB is weakened, the TB can become active (reactivate) and cause infection in the lungs or other parts of the body. The risk factors for acquiring TB include close-contact situations, alcohol and drug abuse, and certain diseases (such as diabetes, cancer, and HIV) and occupations (such as health-care workers). The most common symptoms and signs of TB are fatigue, fever, weight loss, cough, and night sweat. The diagnosis of TB involves skin tests, chest X-rays, sputum analysis (smear and culture), and Polymerase Chain Reaction (PCR) tests to detect the genetic material of the causative bacteria. Antibiotics such as isoniazid (INH) maybe used to treat inactive (dormant) TB to prevent the TB infection from becoming active [131]. Combining INH with one or more of several drugs, including rifampin (Rifadin), ethambutol (Myambutol), pyrazinamide, and streptomycin can usually successfully treat active TB. Drug-resistant TB is a serious, as yet unsolved, public-health problem, especially in south-east Asia, the countries of the former Soviet Union, Africa, and in prison populations. Poor patient compliance, lack of detection of resistant strains, and unavailable therapy are key reasons for in-

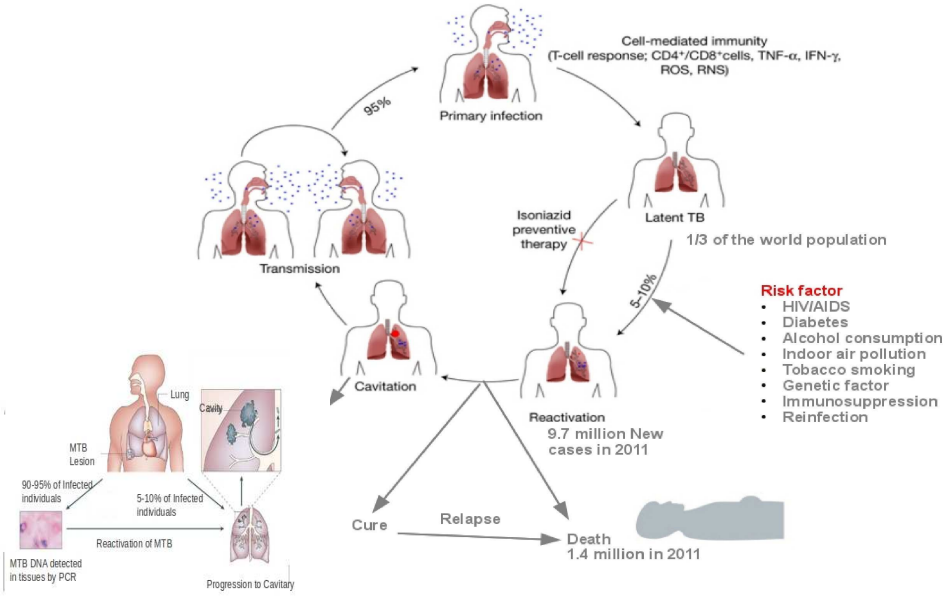

Figure 2.1: Life cycle of Mycobacterium tuberculosis. Illustrations from [101, 142].

creasing drug-resistance to TB. Furthermore, HIV occurrence has been responsible for an increased frequency of tuberculosis. Control of HIV in the future, however, should substantially decrease the incidence of TB.

In the following, we construct a mathematical model for the spread of tuberculosis incorporating constant recruitment, slow and fast progression, effective chemoprophylaxis, diagnosis and treatment of infectious, exogenous reinfections and traditional medicine, in sub-Saharan Africa. Based on epidemiological status, the simplest models include classes of susceptible, infected, infective and recovered individuals and hence are known as SEIR (Susceptible-Infected-Infective-Recovered) models [3, 4, 37]. Parameter identification using the software POEM/BioParkin will be computed and the impact of any parameter change on the TB dynamics will be discussed.

Mycobacterium tuberculosis life cycle

When MTB reach human lungs, they are usually engulfed and destroyed by the macrophage cells of the immune system. But MTB have developed mechanisms to survive these assaults. The life cycle of MTB is as follows.

- First, MTB bacilli are inhaled by their victim and phagocytosed by resident alveolar macrophages in the lung, e.g. through exhaled droplets.
- Next, the infected cells invade the subtending epithelium. This recruits monocytes from the blood circulation, leads to neovascularization, and the formation of granulomas.
- Many of the granulomas persist in a balanced state, whereas progression towards disease is characterized by the loss of vascularisation and the increase of necrosis.
- Finally, infectious bacilli are released into the airways after the cavitation of the granulomas and its collapse into the lungs.

This life cycle has been published by many authors (cf. [100]).

2.2 Suggested model

Data availability and the study objectives generally determine the modelling approach to be used. Following, the mathematical model formulation and the data characteristics are presented.

Data characteristics

The key characteristics of data stored by the TB service of WHO can be classified into two major groups corresponding to the TB countries burden (estimations) and TB countries notification.

The notification group includes data of DOTS strategy for TB. It consists of diagnosing cases, treating patients for 6-8 months with drugs, information about the issue of the treatment and about the promotion adherence to the relatively difficult treatment regimen. We can therefore find the number of new cases, retreatment cases, smear positive cases, smear negative cases and their HIV/AIDS status according to the DOTS strategy.

Parameters	Symbol
Class of susceptible population	S
Class of latently infected population	E
Class of diagnosed infectious population	I
Class of undiagnosed infectious population	J
Class of lost sight population	L
Class of recovered population	R
Total human population	N

Table 2.1: States variables for the TB model

The TB data burden group contains information about the TB estimations. One can find estimated information such as the case detection rate, the number of incident cases, the mortality of TB cases, the total population size, the prevalence of non HIV infected cases and of HIV/AIDS cases. Unstructured data sets and data values that change frequently are not stored by WHO. Using those two types of data, some parameters and state values could be estimated.

Modelling approach

We consider a finite total population at time t, denoted by $N(t)$, sub-divided into following mutually exclusive sub-populations: infectious, susceptible, recovered and latently infected.

The infectious class is divided into three sub-classes with different properties: diagnosed infectious (I), undiagnosed infectious (J) and lost sight (L). At any given time, an individual is in one of the following states: susceptible, latently infected (exposed to TB but not infectious) (E), diagnosed infectious (has active TB confirmed after a sputum examination in the hospital), undiagnosed infectious (i.e., never been to the hospital for diagnosis and have active for confirmation by a sputum examination in hospital), lost sight (people who have been diagnosed from an active TB , begun their treatment and quit before the end, and the health personal do not know their epidemiological status) and recovered people (cured after a therapy of treatment in the hospital) and we will denote these states by S, E, I, J, L and R respectively. We summarize these definition in the following Table 2.2.

In fact, a definitive diagnosis of tuberculosis can only be made by culturing MTB organisms from a specimen taken from the patient (most often sputum, but may also include pus, Cerebro-Spinal Fluid (CSF), biopsied tissue, etc.). A diagnosis made therefore other than by culture may only be classified as "probable" or "presumed".

For TB diagnosis, most protocols require that two separated cultures both are tested negative [105]. Many countries still rely on a long-used method called sputum smear microscopy to diagnose TB. Trained laboratory technicians look at sputum samples under a microscope to see if TB bacteria are present. With three such tests, diagnosis can be made within a day, but this test does not detect numerous cases of less infectious forms of TB [131]. So, the model is based on the following assumptions.

Assumption 2.2.1. *1. TB transmission from diagnosed infectious detected in the hospital to susceptible population obeyed to the standard mass action or frequency-dependent.*

2. TB transmission from undiagnosed infectious to susceptible population is density-dependent.

This argument abides on account of the fact that diagnosed infectious people are not inside the residence in most cases (since their are hospitalize for at least 2 months) or are advised to lessen their infectiousness in their residing neighbourhood. We can then consider that their distribution in the population is not necessarily homogeneous. Since undiagnosed infectious remain inside the population, there is an unlimited possibility of contacts with the susceptible population. We concluded a density dependent force of infection for this inmate [12].

All recruitment is into the susceptible class and occurs at an average scale Λ. The fixed survey for non-disease related death is μ, thus, $1/\mu$ is the average life-time. Diagnosed infectious, undiagnosed infectious and lost sight have the additional constant death rates due to the disease defined by d_1, d_2 and d_3, respectively. Transmission of MTB occurs due to adequate contacts among susceptible, diagnosed and undiagnosed infectious, and lost sight populations. Thus, susceptible individuals acquire TB infection from individuals with active TB and lost sight at a rate $\nu(I, J, L)$ given by

$$\nu(I, J, L) = \beta_1 \frac{I}{N} + \beta_2 \frac{L}{N} + \beta_3 J, \tag{2.1}$$

where β_i, $i = 1, 2, 3$ are respectively the effective contact rate of diagnosed, lost sight and undiagnosed infectious sufficient to transmit infection to susceptible. An effective contact can be defined as any kind of contact between two individuals such that, if one individual is infectious and the other susceptible, then the first individual infects the second. Whether or not a particular kind of contact will be effective depends on the infectious agent and its route of transmission. The effective contact rates β_i in a given population for tuberculosis measured in effective contacts per unit time. This may be expressed as the product of the total contact rate per unit time (η_i) by the risk of infection, given contact between an infectious and a susceptible individual (ϕ_i). This risk is called the transmission risk. Thus, $\beta_i = \eta_i \phi_i$.

Further to adequate contacts with active TB, a susceptible individual becomes first infected but not yet infectious. A proportion p of the latently-infected individuals develop fast active TB and the remainder $(1-p)$ develop latent TB and enter the latent class E. Among latently-infected individuals developing active TB, a fraction f is assumed to undergo a fast progression directly to the diagnosed infectious class I, while the remainder $(1-f)$ enters the undiagnosed infectious class J. We set $p_1 = pf$ and $p_2 = p(1-f)$. Once latently infected with MTB, an individual will remains so for life unless reactivation occurs. Latently infected individuals are assumed to acquire some immunity as a result of infection, which reduces the risk of subsequent infection but does not fully prevent it.

Due to endogenous reactivation, a fraction $1-r_1$ of latently infected individuals who did not received effective chemoprophylaxis become infectious with a constant rate k, and reinfect after effective contact with individuals in the active TB classes or lost sight at a rate $\lambda_e = \sigma_1\nu(I, J, L)$, where σ_1 is the factor reducing the risk of infection as a result of acquiring immunity for latently infected individuals. Among latently infected individuals who become infectious, the fraction h is diagnosed and treated under the "Stop TB" program, while the remaining $1-h$ is not diagnosed and becomes undiagnosed infectious J. We assume that after some time suffering from TB, some undiagnosed infectious decide to go to hospital with a rate θ. Also, we assume that among diagnosed infectious who had begun their treatment therapy, a fraction r_2 of I have taken all the dose and have made all the sputum examinations and will declared cured of the disease. Some diagnosed infectious who have not finished their dose of drugs and sputum examinations or whose treatment was unsuccessful, will not return to the hospital for the rest of sputum examinations and check-up. They will enter the class of lost sight L at a constant rate α. Lost sight can return to the hospital at a constant rate δ.

As suggested by Murray et al. [118], recovered individuals can only have partial immunity. Hence, they can undergo a MTB reactivation or relapse with a constant rate γ. The remainder can be reinfected (exogenously) after an effective contact with individuals in the active TB classes and lost sight at a rate $\lambda_r = \sigma_2\nu(I, J, L)$, where σ_2 is the factor reducing the risk of infection as a result of acquiring partial immunity for recovered individuals. Due to their own immunity, traditional medicine, natural recovery and drugs bought in the street (practised in sub-Saharan Africa), a fraction remainder lost sight and undiagnosed infectious can spontaneously recovered at constant rates ρ and ω, respectively and enter the latent class E and recovery class R respectively. A desciption of the parameters of model (2.2) are summarize in Table 2.2. The whole model flow diagram is shown in Figure 2.2.

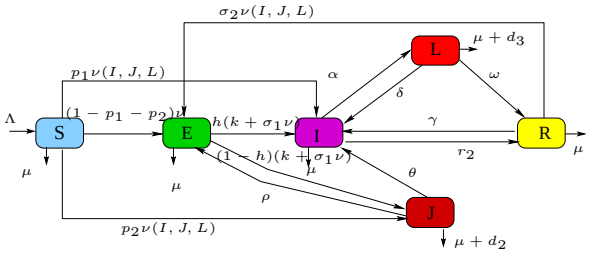

Figure 2.2: Transfer diagram for a transmission dynamics of tuberculosis.

The flow diagram Figure 2.2 yields the following differential equations:

$$\begin{cases} \dot{S} &= \Lambda - \nu(I,J,L)S - \mu S, \\ \dot{E} &= (1-p_1-p_2)\nu(I,J,L)S + \rho J + \sigma_2\nu(I,J,L)R - \sigma_1(1-r_1)\nu(I,J,L)E - A_1E, \\ \dot{I} &= p_1\nu(I,J,L)S + \delta L + \theta J + \gamma R + h(1-r_1)(k+\sigma_1\lambda_T)E - A_2I, \\ \dot{J} &= p_2\nu(I,J,L)S + (1-h)(1-r_1)(k+\sigma_1\nu(I,J,L))E - A_3J, \\ \dot{L} &= \alpha I - A_4L, \\ \dot{R} &= r_2I + \omega L - \sigma_2\nu(I,J,L)R - A_5R, \end{cases} \tag{2.2}$$

where

$$A_1 = \mu + k(1-r_1), \qquad A_2 = \mu + d_1 + r_2 + \alpha,$$

$$A_3 = \mu + d_2 + \theta + \rho, \qquad A_4 = \mu + d_3 + \delta + \omega \qquad \text{and} \qquad A_5 = \gamma + \mu.$$

2.3 Basic properties of the model

The model (2.2) monitors a human population and then, all its associated parameters and state variables are assumed to be non-negative for all $t \leq 0$ and do not go to infinity. Before analyzing the model, it is instructive to show that the state variables of the model remain non-negative for all non-negative initial conditions. In this section, we show that the model is mathematically well-posed and epidemiologically reasonable [86]. The model Eq. (2.2) can be written in the following compact form:

$$\begin{cases} \dot{x} &= \varphi(x) - \nu(I,J,L)x, \\ \dot{y} &= \nu(I,J,L)[B_1x + B_2\langle e_1 \mid y\rangle + B_3\langle e_5 \mid y\rangle] + A\,y, \end{cases} \tag{2.3}$$

where $x = S \in \mathbb{R}_{\geq 0}$ is a state representing the compartment of non transmitting individuals (susceptible), $y = (y_1, y_2, y_3, y_4, y_5) = (E, I, J, L, R)^T \in \mathbb{R}^5_{\geq 0}$ is the vector representing the state compartment of different infected individuals (latently infected, diagnosed and undiagnosed infectious, lost sight, and recovered individuals), $\varphi(x) = \Lambda - \mu\, x$ is a function that depends of x, $\nu(I, J, L) = \dfrac{\langle e_1 \mid y\rangle}{N} + \langle e_2 \mid y\rangle$ is the force of infection, $N = x + y_1 + y_2 + y_3 + y_4 + y_5$ is the size of the total population, $e_1 = (0, \beta_1, \beta_2, 0, 0) \in \mathbb{R}^5$, $e_2 = (0, 0, 0, \beta_3, 0) \in \mathbb{R}^5$, $e_3 = (1, 0, 0, 0, 0) \in \mathbb{R}^5$, $e_4 = (0, 0, 0, 0, 1) \in \mathbb{R}^5$, $B_1 = (1 - p_1 - p_2, p_1, p_2, 0, 0)^T \in \mathbb{R}^5$, $B_2 = (-\sigma_1(1 - r_1), h\sigma_1(1 - r_1), \sigma_1(1 - h)(1 - r_1), 0, 0)^T \in \mathbb{R}^5$, $B_3 = (-\sigma_2(1 - \gamma), 0, 0, 0, \sigma_2(1 - \gamma))^T \in \mathbb{R}^5$, $\langle . \mid . \rangle$ is the usual scalar product and A is the constant matrix:

$$A = \begin{bmatrix} -A_1 & 0 & \rho & 0 & 0 \\ kh(1 - r_1) & -A_2 & \theta & \delta & \gamma \\ k(1 - h)(1 - r_1) & 0 & -A_3 & 0 & 0 \\ 0 & \alpha & 0 & -A_4 & 0 \\ 0 & r_2 & 0 & \omega & -A_5 \end{bmatrix},$$

with A_1, A_2, A_3, A_4 and A_5 defined as in Eq. (2.2).

It should be pointed out that A is a Metzler matrix because all its off-diagonal entries are non-negative. A is also non-singular because it is column diagonally dominant. Using the fact that$A$ is a non-singular Metzler matrix, we can deduce therefore that the matrix$-A^{-1}$ is non-negative [15, 152]. This property is very useful for the positivity of eigenvalues and the positivity of the basic reproduction ratio number.

Positivity of the solution

The following theorem shows that state variables are non-negative and dissipative.

Lemma 2.3.1. *Let the initial values be $S(0) > 0$, $E(0) > 0$, $I(0) > 0$, $J(0)$, $L(0) > 0$ and $R(0) > 0$ then, solutions (S, E, I, J, L, R) of model system (2.2) are positive for all $t > 0$. Furthermore,*

$$\limsup_{t \longrightarrow \infty} N(t) \leq \frac{\Lambda}{\mu},$$

with $N(t) = S(t) + E(t) + I(t) + J(t) + L(t) + R(t)$.

Proof:

Assume that $\bar{t} = \sup\{t > 0 :\ S > 0, E > 0, I > 0, J > 0, L > 0, R > 0\} \in [0, t]$. Thus, $\bar{t} > 0$ and it follows from the first equation of model system (2.2), that

$$\frac{dS}{dt} = \Lambda - (\mu + \nu(I, J, L))S,$$

where $\nu(I, J, L)$ is defined as in Eq.(2.1). The above equation can be rewritten as,

$$\frac{d}{dt}\left[S(t)\exp\left\{\mu t + \int_0^t \nu(I,J,L)(s)ds\right\}\right] = \Lambda\exp\left\{\mu t + \int_0^t \nu(I,J,L)(s)ds\right\}.$$

Hence,

$$S(\bar{t})\exp\left\{\mu\bar{t} + \int_0^{\bar{t}} \nu(I,J,L)(s)ds\right\} - S(0) = \int_0^{\bar{t}} \Lambda\exp\left\{\mu u + \int_0^u \nu(I,J,L)(w)dw\right\}du,$$

so that

$$\begin{aligned} S(\bar{t}) &= S(0)\exp\left\{-\left(\mu\bar{t} + \textstyle\int_0^{\bar{t}} \nu(I,J,L)(s)ds\right)\right\} \\ &+ \exp\left\{-\left(\mu\bar{t} + \textstyle\int_0^{\bar{t}} \nu(I,J,L)(s)ds\right)\right\} \cdot \textstyle\int_0^{\bar{t}} \Lambda\exp\left\{\mu u + \int_0^u \nu(I,J,L)(w)dw\right\}du \;>\; 0. \end{aligned}$$

Similarly, it can be shown that $E(t) \geq 0$, $I(t) \geq 0$, $J(t) \geq 0$ $L(t) \geq 0$ and $R(t) \geq 0$ for all $t > 0$. Now, adding all equations in the differential system (2.2), one gets

$$\dot{N} = \Lambda - \mu N(t) - d_1\, I(t) - d_2 J(t) - d_3 L(t). \tag{2.4}$$

Thus, we can deduce from equation (2.4) that

$$\Lambda - \mu N(t) - (d_1 + d_2 + d_3)N(t) \leq \dot{N} \leq \Lambda - \mu N(t).$$

In particular, it follows by the standard comparison theorem [21, 106, 89] that $N(t) \leq N(0)e^{-\mu t} + \dfrac{\Lambda}{\mu}(1 - e^{-\mu t})$ and thus,

$$\frac{\Lambda}{\mu + d_1 + d_2 + d_3} \leq \liminf_{t\longrightarrow\infty} N(t) \leq \limsup_{t\longrightarrow\infty} N(t) \leq \frac{\Lambda}{\mu},$$

so that

$$\limsup_{t\longrightarrow\infty} N(t) \leq \frac{\Lambda}{\mu}.$$

This completes the proof. □

Invariant Region

The following steps established the positive invariance of the set

$$\Omega_\rho = \left\{(S, E, I, J, L, R) \in \mathbb{R}^6_{\geq 0}, \quad N(t) \leq \frac{\Lambda}{\mu} + \rho\right\}, \quad \rho > 0 \tag{2.5}$$

i.e., that solutions remain in Ω_ρ for all $t \geq 0$.

From equation (2.4), it follows by the standard comparison theorem [21, 106, 89] that $\lim_{t\to+\infty} N(t) \leq \frac{\Lambda}{\mu}$.

This implies that the trajectories of model system (2.2) are bounded. On the other hand, integrating the differential inequality $\dot{N} \leq \Lambda - \mu N$ yields $N(t) \leq N(0)e^{-\mu t} + \frac{\Lambda}{\mu}(1 - e^{-\mu t})$. In particular $N(t) \leq \frac{\Lambda}{\mu}$ if $N(0) \leq \frac{\Lambda}{\mu}$. In other hand, if $N(0) \geq \frac{\Lambda}{\mu}$, then $\Lambda - \mu N(0) \leq 0$, since

$$\dot{N} \leq \Lambda - \mu N(t) \leq 0,$$

the total population $N(t)$ will decrease until

$$N(t) \leq \frac{\Lambda}{\mu}.$$

Then, the simplex Ω_ρ is a compact forward invariant set for model system (2.2), and for $\rho > 0$, this set is absorbing. So, we limit our study to this simplex for $\rho > 0$.

The prevalent existence, uniqueness and continuation results hold for model system (2.2) in Ω_ρ. Thus, the total population is asymptotically constant. The well-posedness of the model follows from a straight forward application of the classical theory [134]. Hence, model system (2.2) is mathematically and epidemiologically well-posed and it is enough to observe the dynamics of the flow generated by model (2.2) in Ω_ρ.

2.4 Sensitivity analysis

Sensitivity analysis generates essential information for parameter estimation, optimization, control, model simplification and experimental design. Model (2.2) studies the dynamical evolution of TB within a well-defined, biology-related context. For TB for example, models described many interactions among differential infectivity of TB in a population with lack of information on some classes.

Through sensitivity analysis, the systematic study of the effects of parameter values on the predictions of mathematical models is a valuable tool for model evaluation and validation as well as for quantifying the effect of parametric uncertainly and variability [103, 156, 87, 57, 137]. This mathematical enable as major topic in systems biology, enables to identify the most sensitive parameters used for parameter identification, optimal control strategy, and for the model validation. Much research has been performed on the sensibility of ODEs (See for example [103, 156, 87, 57, 137, 53]).

Sensitivity equations for ODE systems

A parameter dependent initial value problem (IVP) for ODEs can be written as

$$\begin{cases} \dfrac{d}{dt}y(t,p) &= f(t,y,p), \qquad t \geq 0, \\ \\ y(0,p) &= y_0, \end{cases} \tag{2.6}$$

where p is the vector of parameters, the right-hand side, f, denotes dependency of the change in the states vector, y_0, on both the states, $y \in \mathbb{R}^n$, and the parameter vector, $p \in \mathbb{R}^q$. The initial condition vector, y_0, has the same dimension as the states vector y. The TB model equation(2.2) can be written in the form equation (2.2) where $y(t,p) = (S(t,p), E(t,p), I(t,p), J(t,p), L(t,p), R(t,p)) \in \mathbb{R}^6$ and $p = (\Lambda, \beta, \cdots, \mu) \in \mathbb{R}^{23}$.

Sensitivity here describes the influence of changes in the parameter vector p on the solution vector y. A parameter is called sensitive if small changes in its value lead to large changes in the solution [54, 56]. The parameter vector p may include initial conditions y_0, although y_0 does not enter explicitly in f. We can next introduce the variable

$$S_{ij} := \frac{\partial y_i}{\partial p_j}(t), \qquad i = 1, \cdots, n, \;\; j = 1, \cdots, q. \tag{2.7}$$

This variable will be found as the solution of a new set of differential equations, which we derive below. The system of differential equation (2.7) will be solved simultaneously with the system (2.6). Applying the chain rule for differentiation and the rule to interchanging the order of differentiation for certain mixed partials, we have

$$\dot{S}_{ij} = \frac{d}{dt}(S_{ij}) = \frac{d}{dt}\frac{\partial y_i}{\partial p_j} = \frac{\partial}{\partial p_j}\frac{dy_i}{dt} = \frac{\partial f_i(t, y(t,p), p)}{\partial p_j}$$

or finally

$$\dot{S}_{ij} = \frac{\partial f_i}{\partial p_j} + \sum_{k=1}^{n} \frac{\partial f_i}{\partial y_k} S_{kj}, \;\; i = 1, \cdots, n, \;\; j = 1, \cdots, q. \tag{2.8}$$

The term $\frac{\partial f_i}{\partial y_k}$ is recognized to be an element of the Jacobian matrix of f. Matrix S can be written also as solution to the variational equation

$$S' = f_y(y,p)S + f_p(y,p), \qquad S(t_0) = 0. \tag{2.9}$$

It should be noted that if the parameter p_j does not appear explicitly in the f_i, then equatio (2.8) will be write in the form $\dot{S}_{ij} = \sum\limits_{k=1}^{n} \frac{\partial f_i}{\partial y_k} S_{kj}, \;\; i = 1, \cdots, n, \;\; j = 1, \cdots, q.$

This may be the case, for example for the initial values of the system. Generally, the dependence of the solution, $y(t,p)$, on the parameters p, is characterized by the sensitivity (n,m)-matrix, $S = S(t)$ [53].

Solving sensitivity systems

The sensitivities in this dissertation are valued for all components of the system in order to perform parameter identification. However, only the elements for which experimental data are available are considered in the subsequent analysis. The sensitivities must then be calculated at the measure time points [53].

Parameters are only simultaneously identifiable if the systems sensitivity with respect to these parameters is high enough compared to the most sensitive one. In order to be able to compare the different sensitivities, the condition, or more precisely the sub-condition has to be computed. Parameters that are not sensitive with respect to the remaining parameters do not significantly influence the system at a giving state, thus a change in their values can be considered as negligible for the solution. However, it is important not to set their values to zero. Sensitivities are calculated for all elements of the system and for all parameters that should be estimated. The solution is given for all grid points in a defined time interval. Sensitivities holds only in a vicinity of the state determined by y and p. The sensitivity analysis of a parameter is therefore local. The term local refers to the fact that these sensitivities describe the system around a given set of values for the parameters p_i. The system is considered to respond linearly for small perturbations, if the measures of the ratio between the Δy_i (absolute variation of the output y_i) and the cause Δp_j (absolute variation of the input p_j) denoted S_{ij} is big enough with respect to the biggest sensitivity parameter $p_{j_{max}}$,$j \neq j'$. It is straightforward to extend the solution algorithm developed for system (2.6) to the variational problem (2.6). By solving the variational problem, one can find solutions giving the dynamics of the sensitivities for all time points.

In a more practical way, in this thesis, sensitivity is computed for parameter identification and optimal control. The sensitivity must be considered at a measured time point. Let n_y be the number of components for which data are available. If data are available for all states, then set $n_y = n$. Let $(t_k)_{k=0,\cdots,M}$ be the discretization grid on the considered time interval $[t_0; t_f]$, where $t_f = t_M$ and $T^j = \{t_k^j,\ k = 1,\cdots,M_j\}$, where $t_k^j < t_{k+1}^j$ for all $k = 1,\cdots,m_d^j - 1$ the set of time points where experimental data are available for the element $j \leq n_y$ and m_d^j the number of data point for state j. we set $M = \sum_{l=1}^{n_y} m_d^l$ the number of data point available. If the measure time points are the same for all states, set $M = M^j$ as the number of data

for each states. The sensitivities are therefore defined point by point, corresponding to the data availability and the given time point. For sake of simplicity, one assumes the notation $M_j = M$ for all time points and for all components. In the following, we define the special, the normalized and the relative sensitivities for a given j^{th} element at a given t_k time point. The following definitions can be found in [54].

Definition 2.4.1. (sensitivity)

- The **sensitivity** of the i^{th} chosen element and the k^{th} chosen time-point with respect to the j^{th} chosen parameter is given by

$$\begin{aligned} S_{i_k j} &:= S_{ij}(t_k^i, p), \\ k &= 1, \cdots, M, \;\; i = 1, \cdots, n_y, \;\; j = 1, \cdots, q. \end{aligned} \tag{2.10}$$

- The **normalized sensitivity** of the i^{th} chosen element and the k^{th} chosen time-point with respect to the j^{th} chosen parameter is given by

$$\begin{aligned} S_{i_k j}^{norm} &:= S_{ij}(t_k^i, p)\frac{|p_j|}{\|y_i\|}, \\ k &= 1, \cdots, M, \;\; i = 1, \cdots, n_y, \;\; j = 1, \cdots, q. \end{aligned} \tag{2.11}$$

  where $\|y_i\| = \|(y_i(t_1), \cdots, y_i(t_{M^i}))\|_{l^2}$

- Let p^{trsh} and y^{trsh} been threshold values for parameters p and y respectively. The **relative sensitivity** of the i^{th} chosen element and the k^{th} chosen time-point with respect to the j^{th} chosen parameter is given by

$$\begin{aligned} S_{ij}^{*} &:= S_{ij}(t_k, p)\frac{\max(|p_j|, p_j^{trsh})}{\max(\|y_i\|, y_i^{trsh})}, \\ k &= 1, \cdots, M, \;\; i = 1, \cdots, n_y, \;\; j = 1, \cdots, q. \end{aligned} \tag{2.12}$$

  where $\|y_i\| = \|(y_i(t_1), \cdots, y_i(t_{n_d^i}))\|_{l^2}$

The sensitivity vectors $S_j(t_k) := (s_{1j}(t_k), \cdots, S_{Mj}(t_k))^T,\; M \leq n_y \cdot \sum_{l=1}^{n_y}$ result in the columns of the sensitivity matrix $S := (S_{ij}^*)_{i=1,\cdots,N, j=1,\cdots,m_d}$. This matrix must be computed in order to determine which parameters are sensitive. The column sum norm for a parameter p_j is given by the l^2 norm of the column vector S_j (see [53]).

Analysis of the sensitivity matrix

The sensitivity matrix S can be linearly column dependent, then it is singular or numerically singular. Then, some parameters influence the solution in a comparable manner and cannot be estimated simultaneously. In order to detect linear dependencies, a more detailed analysis most be performed. The following result and its proof can be found in [55].

Theorem 2.4.1. *Let $S \in \mathcal{M}_{Nq}(\mathbb{R})$ be an arbitrary and real matrix. There exists two orthogonal matrices $U \in \mathcal{M}_N(\mathbb{R})$ and $V \in \mathcal{M}_q(\mathbb{R})$ such that*

$$S = U\Sigma V^T, \tag{2.13}$$

where $\Sigma = diag(\sigma_1, \cdots, \sigma_{\min(q,N)}) \in \mathcal{M}_{Nn}(\mathbb{R})$ with $\sigma_{\min(m,N)} \leq \cdots \leq \sigma_1 \leq 0$.

σ_i are called the *singular values* of S and we call the factorization (2.13) the singular value decomposition (SVD) of S. In the special but common case in which $S \in \mathcal{M}_q(\mathbb{R})$ is a square matrix with with real numbers and positive determinant, then U, V^T, and Σ are elements of $\mathcal{M}_q(\mathbb{R})$ as well. Σ can be regarded as a scaling matrix, and U and V^T can be viewed as rotation matrices. If the above-mentioned conditions are met, the expression $U\Sigma V^T$ can thus be intuitively interpreted as a composition of three geometrical transformations: a rotation, a scaling, and another rotation.

The condition number for an invertible matrix $M \in \mathcal{M}_q(\mathbb{R})$ with respect to a matrix norm is defined by

$$\kappa(M) = \|M\| \cdot \left\|M^{-1}\right\|. \tag{2.14}$$

If M is non-singular, and $\kappa(M) := +\infty$ if M is singular. For non square matrices as S, a more general definition of the condition number (cf. [55]) states that

$$\kappa(S) := \frac{\max\limits_{\|x\|=1} \|Sx\|}{\min\limits_{\|x\|=1} \|Sx\|} \in [0, \infty].$$

The condition number is a measure of stability or sensitivity of a matrix (or the linear system it represents) to numerical operations. It has the advantage of been well-defined for non-invertible and rectangular matrices as well. The condition numbers of matrix has the following properties:

(*i*) $\kappa(S) \geq 1$;

(*ii*) $\kappa(\alpha S) = \kappa(S)$ for all $\alpha \in \mathbb{R}, \alpha \neq 0$;

(*iii*) $S \neq 0$ is singular if and only if $\kappa(S) = \infty$.

Matrices with condition numbers near 1 are said to be well-conditioned. Matrices with condition numbers much greater than one are said to be ill-conditioned (cf. [45]). Properties ((*i*) and (*iii*)) favours condition numbers rather than determinants for characterizing the solvability of a linear system because condition numbers are invariant under multiplication.

In the following, we will use only the Euclidian matrix norm or L^2-norm:

$$\|M\| = \|M\|_2 = \max_{\|x\|_2=1} \frac{\|Mx\|_2}{\|x\|_2}.$$

Lemma 2.4.1. *Let $M \in \mathcal{M}_m(\mathbb{R})$, the condition number of M is the ratio of the biggest and the smallest singular value*

$$\kappa(M) = \frac{\sigma_1}{\sigma_m}$$

This result follows from the SVD decomposition of M and the orthogonality of U and V. In fact, since $M = U\Sigma V^T$, with $\|\Sigma\| = \max \sigma_i = \sigma_1$, and $\|\Sigma^{-1}\| = \max \sigma_i^{-1} = \sigma_q^{-1}$ then,

$$\kappa(M) = \|U\Sigma V^T\| \cdot \|(U\Sigma V^T)^{-1}\| = \frac{\sigma_1}{\sigma_m}.$$

The condition number of the sensitivity matrix S is a measure for the estimability of the parameter vector p. It can be defined as the condition number of the non-singular part of matrix Σ, which results from the SVD decomposition of S. The computation of the condition number is theoretically more satisfactory, but computationally expensive since it requires the calculation of the singular values [53]. A more advantageous method using QR decomposition have therefore been developed to solve the problem of parameters estimability.

Theorem 2.4.2. *(QR decomposition)*

Let $S \in \mathcal{M}_{Nq}(\mathbb{R})$, with $N \leq q$, as the product of an $N \times N$ unitary matrix Q and an $N \times q$ upper triangular matrix R. As the bottom $(N - q)$ rows of an $N \times q$ upper triangular matrix consist entirely of zeros, it is often useful to partition R, or both R and Q:

$$S = QR = Q \begin{bmatrix} R_1 \\ 0 \end{bmatrix} = \begin{bmatrix} Q_1, Q_2 \end{bmatrix} \begin{bmatrix} R_1 \\ 0 \end{bmatrix} = Q_1 R_1,$$

where $R_1 \in \mathcal{M}_q(\mathbb{R})$ upper triangular matrix, $Q_1 \in \mathcal{M}_N(\mathbb{R})$, $Q_2 \in \mathcal{M}_{N(N-q)}(\mathbb{R})$, and Q_1 and Q_2 both have orthogonal columns. For the sake of simplicity, let us set $R_1 = R$ and $Q_1 = Q$.

Using a suitable transformation, a column permutation strategy (cf. [53]) with a permutation matrix Π, the diagonal elements of the matrix R can be arranged such that $|r_{11}| \geq \cdots \geq |r_{qq}|$ and

$$S\Pi = QR$$

Let ε denotes some reasonable input accuracy, then a numerical rank q may be defined by the maximum index such that

$$\varepsilon |r_{11}| < |r_{qq}|.$$

the so-called sub-condition number

$$sc(S) := \frac{r_{11}}{r_{qq}}$$

can be conveniently computed (see [53]). It has been proved in [55] that $sc(S) \leq \kappa(S)$. The sub-condition depends on the number of parameters that must be identified and on the number of components and measure time points.

2.5 Parameter identification from Cameroon's data

In this section, we present the numerical estimation of the most sensitive parameters of model (2.2) using Gauss-Newton iterations. Parameter identification have been computed using the software POEM/BioParkin. The program NLSCON included in this software, is a global unconstrained Gauss- Newton method with error oriented convergence criterion and adaptive trust region strategies (cf. [53]) used to solve least-square problems. Since some specific parameter values such as demographic data from Cameroon are well-known from the literature, we have estimated unknown data in order to keep the model more realistic.

Least-squares problem

Let us considered a set of experimental measurement data $(\tau_j, z_j),\ j = 1, \cdots, M$ where τ_j are different time point and z_j are state variables of the model equatio. (2.2). The goal consists of adjusting the parameters of a model function to best fit the data set. The model function has the form $f(t, y, p)$ as defined at (2.6), where the m adjustable parameters are held in the vector p. The least-squares method finds its optimum by minimizing the sum of squared residuals

$$g(p) = \frac{1}{M} \sum_{j=1}^{M} \parallel D_j^{-1}(y(\tau_j, p) - z_j) \parallel_2^2 \tag{2.15}$$

with diagonal weighting

$$D_j := diag((\delta z_j)_1, \ldots, (\delta z_j)_n) \in \mathcal{M}_n(\mathbb{R}), \qquad j = 1, \cdots, M, \tag{2.16}$$

where δz_j additionally denotes the statistical tolerance of the j^{th} measurement or the standard deviation of z_j. Data points may consist of more than one independent variable. Note that z_j are available for a specific measurement time point τ_j, the missing data in the least squares formulation is simply replaced by the computable model value, therefore effectively neglecting the corresponding contribution in the sum (2.15) [55]. The minimization problem (2.15) can be written in an equivalent least squares minimization problem defined by

$$g(p) := F(p)^T \cdot F(p) \to \min_p \tag{2.17}$$

where $F(p) = (F_1(p), \ldots, F_M(p))$ is a vector of length M with entries defined by

$$F(p) = \begin{bmatrix} D_1^{-1} \cdot (y(\tau_1, p) - z_1) \\ \vdots \\ D_M^{-1} \cdot (y(\tau_M, p) - z_M) \end{bmatrix}. \tag{2.18}$$

$F : \mathbb{R}^q \longrightarrow \mathbb{R}^N$ for $N = n_y M$ is a non-linear mapping and structured as a stacked vector. If not all components of a measurement z_j are given, the number q is accordingly made smaller $q < nM$. The goal is to minimize the relative deviation between data and the model (2.2) at the measurement time points τ_j.

2.5.1 Gauss-Newton method

The minimization problem such as problem (2.17) is usually non-linear in the unknown parameter vector p and can be solved by affine covariant Gauss-Newton iterations [55, 53]. The iterative Gauss-Newton procedure indeed converges to a solution vector $p^* \in \mathbb{R}^m$. The linearized model, taken at the solution points, readily enables a posteriori analysis. Sufficient conditions for a local minimum p^* where

$$g(p^*) = \min_p g(p)$$

are $g'(p^*) = 0$ and $g''(p^*) \in \mathcal{M}_q(\mathbb{R})$ positive definite.

Since

$$g'(p) = 2F(p)^T \cdot F(p)$$

holds, the problem can be formulated as finding the solution of the following system of M non-linear equations

$$G(p) := F'(p) \cdot F(p) = 0. \tag{2.19}$$

The Newton iteration scheme for this system of equations is

$$G'(p^k)\Delta p^k = -G(x^k), \quad k = 0, 1, 2, \cdots \tag{2.20}$$

where the Jacobian matrix $G'(p)$ is defined by

$$G'(p) = F'(p)^T \cdot F'(p) + F''(p)^T \cdot F(p)$$

is positive definite, so invertible in the neighbourhood of p^*. When the model and data fully agree at p^*, one has

$$F(p^*) = 0, \text{ and } G'(p^*) = F'(p^*)^T \cdot F'(p^*).$$

These are exactly the normal equations of the linear least-squares problem

$$\| F'(p^j) \cdot p^j + F(p^j) \|_2^2 = \min, \quad p^{j+1} = p^j + \lambda_j \Delta p_j, \quad j = 0, 1, 2, \ldots$$

for an initial guess p^0. A closer look of the expression of $F'(p)$ reveals that

$$\frac{d}{dp}F(p) = \left(\frac{1}{\delta z_j}\right)\mathcal{S}$$

where

$$\mathcal{S} = (S(t_1), \cdots, S(t_k))$$

where S_{ij}^* is defined in equation (2.10). Every row of the Jacobian $(M \times m)$-matrix $F'(p)$ represent the sensitivity analysis of the solution y with respect to the parameter p at the time point measurements. Estimable parameters are those with larger sensitivity. Some of the parameters might be linearly dependent, which leads to nearly identical columns in $F'(p)$. $F'(p)$ will be singular or, from a numerical point of view, nearly singular.

2.5.2 Numerical results

In this subsection, we present numerical results from the Gauss-Newton method for parameter identification. Some important parameters of the TB model are well-known because of their specificity to each population. We fixed these parameters and estimated those which are unknown.

POEM/BioParkin

In the software POEM/BioParkin, the ODE systems are solved numerically with LIMEX, a linearly implicit Euler method with extrapolation [54, 53]. To test the suitability of the model equation (2.2) in order to effectively enable the assessment

of targeted public health education strategies and chemoprophylaxis against TB spread in a population, the model is fitted using data of Cameroon [131]. The main difficulty is not to simulate the system, i.e. to solve the differential equations, but to identify the unknown parameters. We will briefly describe the mathematical techniques using for parameter identification in the software POEM/BioParkin. Let us considered the entry D_j as defined in equation(2.15) for $1 \leq j \leq m$. If a component of given error tolerance, δz_j, or even the whole vector, is set to zero, this contribution to the sum (2.15) is also taken out, and considered as a (non-linear) equality constraint to the least squares formulation instead. In NLSCON included in the software POEM/BioParkin, the measurement tolerances are computed as

$$(\delta z_j) = \max\{\max_i(z_i)_k, tresh(z_j)_k\},$$

with some user specified threshold mapping, $tresh(\cdot)$. The solution for the k-th step results then in

$$\begin{aligned} \Delta p^k &= F'(p^k)^+ \cdot F(p^k), \\ p^{k+1} &= p^k + \Delta p^k; \end{aligned} \tag{2.21}$$

where $F'(p^k)^+$ denotes the pseudo-inverse of $F'(p^k)$. In the global case it would be

$$p^{k+1} = p^k + \lambda_k \Delta p^k; 0 < \lambda_k \leq 1.$$

The step length $0 < \lambda_k < 1$, can be computed successively in each iteration. By a suitable permutation of the matrix columns of $J(p)$, the diagonal elements of the upper triangular matrix R can be ordered in the form $r_{11} \geq r_{22} \geq \cdots \geq r_{qq}$.

The sub-condition of parameter p_j is given by

$$sc_j = \frac{r_{11}}{r_{jj}}.$$

Using the QR decomposition of the matrix $J(p) \simeq F'(p)$, equation

$$F'(p^k) \cdot \Delta p^k = F(p^k)$$

is solved.

Thus, the permutation of matrix columns corresponds to a new ordering of parameters according to increasing sub-condition. The sub-condition indicates whether a parameter can be estimated from the given data or not. Only those parameters can be estimated for which

$$sc_j \leq 1/\varepsilon$$

where ε is the relative precision of the Jacobian $J(p)$ [61]. The above described method for solving a non-linear least squares problem were implemented in the software packages NLSCON [61, 122]. A renewed matlab-based version of this software, named POEM 2.0, which is especially adapted to parameter identification in ordinary differential equation models, has been used throughout the study.

Parameters	Symbol	Estimate	Source
Recruitment rate of susceptible	Λ	679685/yr	Fixed, [125]
Transmission rate	β_1, β_2	$1, 4$	Fixed [27]
Transmission rate	β_3	$6.05681 \cdot 10^{-06}$	Estimated
Fast route to infectious class	p_1	$9.36432 \cdot 10^{-04}$	Estimated
Fast route to diagnosed infectious class	p_2	$2.43736 \cdot 10^{-02}$/yr	Estimated
Reinfection parameter of latently infected individuals	σ_1	$2.38390 \cdot 10^{-04}$	Estimated
Reinfection parameter of recovered individuals	σ_2	$0.7 * (p_1 + p_2)$	Fixed, [10]
Slow route to active TB	k	$3.31390 \cdot 10^{-04}$/yr	Estimated
Natural mortality	μ	1/53.6/yr	Fixed, [27, 125]
TB mortality of diagnosed infectious	d_1	0.139/yr	Fixed,[27]
TB mortality of undiagnosed infectious	d_2	0.413/yr	Estimated
TB mortality of lost sight	d_3	0.20/yr	Estimated
Chemoprophylaxis of latently infected individuals	r_1	0/yr	Fixed, [123]
Detection rate of active TB	h	0.828248/yr	Estimated
Recovery rate of diagnosed infectious	r_2	0.758821/yr	Fixed, [123]
Recovery rate of lost sight	ω	0.5/yr	Estimated
Recovery rate of undiagnosed infectious	ρ	0.131140/yr	[27]
Relapse of recovered individuals	γ	$8.51257 \cdot 10^{-02}$/yr	[27]
Diagnosed infectious route to the lost sight class	α	0.216682/yr	Estimated
Lost sight route to the diagnosed infectious class	δ	0.39/yr	Estimated
Diagnosed rate	θ	0.495896/yr	Estimated

Table 2.2: Estimated numerical values of the TB model parameters

Parameters values of the model

Numerical values of all parameters are given in Table 2.2.

We subdivided the data by type and present the well-known and specific data of Cameroon. Using the method above, we fixed some parameters valued and estimated other using the software POEM. Table 2.2 below comprises the parameter values. As denoted in the last column some parameters have fixed values national institute of statistic of Cameroon, (NIS), [27, 10] and some were estimated using the software POEM/BioParkin.

Figure 2.3 shows the column norm of the sensitivity matrix with respect to the the parameter values. Obviously, parameters with the largest column norm are γ,

p_2 and ρ respectively. Parameters β_1, β_2 and σ_2 have the largest column norm. Identifiable parameters are those with smallest column norm with respect to the biggest column norm.

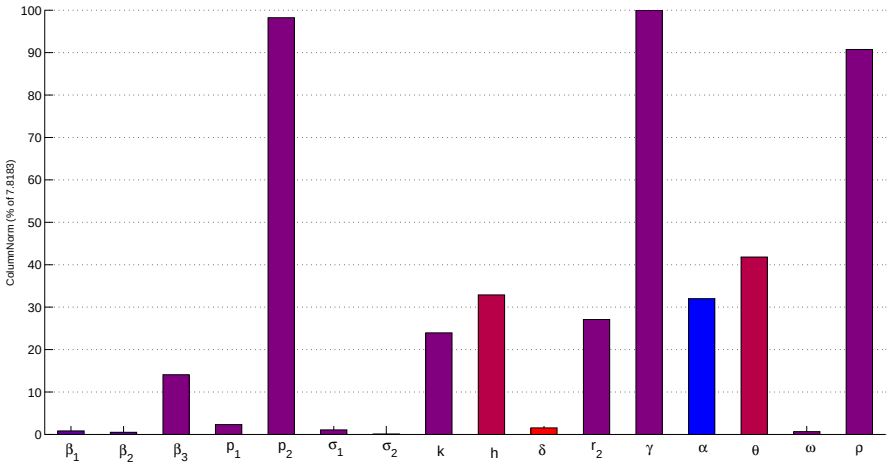

Figure 2.3: Column norm of all parameters of model 2.2.

Figure 2.4 shows the sub-condition of the sensitivity matrix with respect to the parameter values. One can see that parameters with largest sub-conditions are σ_1, σ_2, ω, p_1, β_1 and β_2 respectively. All other parameters have smaller sub-conditions. Figure 2.4 shows the sub-condition of the estimated parameters.

The sensitivity analysis reveals that 9 of 16 parameters are estimable. Since all parameters was not estimable simultaneously, we proceed by steps, using estimated values to identify others.

Demographic parameters

Most demographic parameters are well-known for a given population. In the following, we will give some of them and their values from Cameroon's data.

The natural mortality μ: The natural mortality is postulated to be equal to the inverse of the life expectancy at birth, which is now about 54.1 years in Cameroon [8, 125, 1, 126], i.e., $\mu = 1/53.6$ per year.

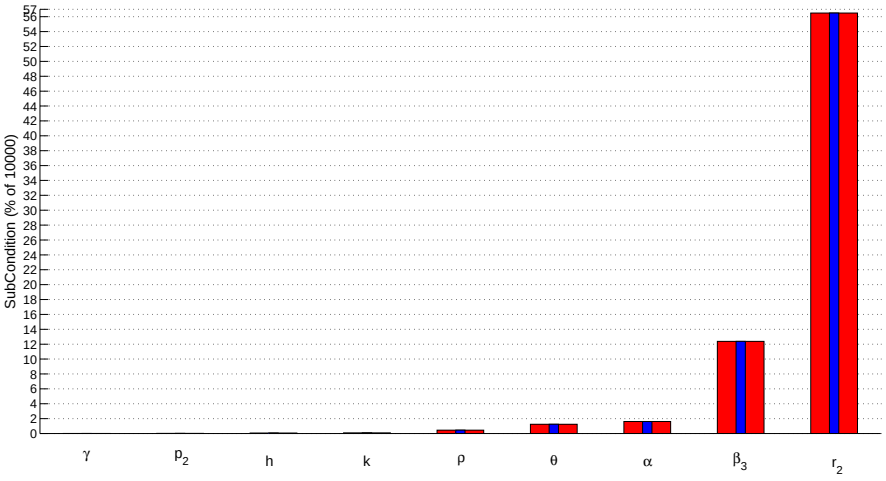

Figure 2.4: Sub-condition of all parameters of model (2.2).

The recruitment Λ : The recruitment parameter Λ is estimated taking into account the world population and migration and can be chosen to attain the total population. According to the Cameroonian national institute of statistics (NIS) [125, 126], the average recruitment in the Cameroonian population during the last fifteen year is an $\Lambda = 679685$ per year.

TB mortality d_1, d_2 *and* d_3 *of undiagnosed infectious and lost sight*: Per capita TB-induced mortality rate varies from country to country. It is 0.193 per year in developed countries, but could be as high as 0.45 per year in some African countries [26]. An intermediate value of 0.193 per year can be applied to most developed and developing countries [26]. We set the TB-induced mortality rates $d_1 = 0.193$, $d_2 = 0.413$ and $d_3 = 0.20$ per year for undiagnosed infectious and lost sight, respectively.

Progression rate to active TB parameters

M. tuberculosis transmission rate β_i, $\quad i = 1, 2, 3$. Estimating parameters β_i is the most difficult task. Usually, this parameter can be estimated using a known value of the basic reproduction ratio $\mathcal{R}_0$. Blower et al. (cf. [26]) estimated the contact rate $\beta_i \in (1, 4)$ in the case of a frequency dependent force of infection. In our case, we chose $\beta_1 = 1$, $\beta_2 = 4$ according to data of Blower et al. and we estimated $\beta_3 = 6.05681 \cdot 10^{-06}$ using the software POEM/BioParkin.

Parameters p_1, p_2 and k modelling the progression to active TB. The progression rate to active TB is a decreasing function of the time since infection. For HIV negative TB people, Bacaer et al. (cf. [10, 44]) estimated that people in a South Africa township have 11% annual risk of developing primary TB disease during five years following the first MTB infection and a 0.03% annual risk of reactivation after five years. For HIV positive people, the numbers were 30% and 22.5% per year. In Cameroon, the estimated average TB prevalence all forms in HIV positive is about 431 per 100,000 per year. Hence, we estimated that $p_1 = 9.36432 \cdot 10^{-04}$, $p_2 = 2.43736 \times 10^{-02}$ and $k = 3.31390 \cdot 10^{-04}$ per year.

Factors σ_1 and σ_2 are reducing risk of infection as a result of acquired immunity to a previous infection of latently infected and recovered individuals. Sutherland et al. [152] estimated that a previous MTB infection reduced the risk of disease after reinfection by 63% for HIV negative males and by 80% for HIV negative females. Vynnycky and Fine [160] found a reduction of the risk by 16% among HIV negative adolescents and by 41% among HIV negative adults. We estimate that $\sigma_1 = 2.38390 \cdot 10^{-04}$ and we use the data from [10] $\sigma_2 = 0.7 * (p_1 + p_2)$.

Detection rate h. The average percentage of new diagnosed smear positive cases that have been latently infected and which go immediately to the hospital after developing the disease is in the interval $50 - 90\%$ per year according to WHO data. Using POEM, it have been estimated to $h = 8.28248 \cdot 10^{-01}$ per year.

Other parameters

Rate θ at which undiagnosed infectious go to the hospital: Parameter θ is unknown due to the number of undiagnosed infectious TB cases. WHO estimated $\theta \in (0.30, 0.60)$ per years. The result giving by POEM shows that the model is largely sensitive to θ.

Proportions r_1 and r_2 of successful treatments of latently infected individuals and diagnosed infectious. The proportion of successful treatment of diagnosed infectious is about 74.72% per year. This Figure is insufficient compared with the WHO target for developing countries like Cameroon, which is at least 85% successful cure rate. Since the chemoprophylaxis is not practiced in Cameroon, we take $r_1 = 0$ per year.

Rate α at which diagnosed infectious become lost sight: The average percent of diagnosed infectious that begun their treatment and have not completed their sputum examination and check up is is also not well known. It have been estimated using POEM.

Rate δ at which lost sight return to the hospital: According to the data of TB in Cameroon, the average percent of lost sight who return to the hospital with disease after that they disappeared in the hospital is $\delta = 39\%$ per year.

Recovery rate ρ of undetected infectious: We assume that the rate at undiagnosed infectious who recover naturally or who have drugs by self-medication or traditional medicine, become latently infected correspond to the natural recovery rate of infectious. In [10], the authors estimated that the natural recovery for HIV negative TB and HIV positive TB cases are respectively, 0.139 and 0.24 per year. Herein, we take the average of these values and get $\rho = 0.245$ per year.

Recovery rate ω of lost sight: Since lost sight can take traditional medicine and self-medication in Cameroon, or we assume that the recovery rates of lost sight and undiagnosed infectious is the double of the natural recovery rate of infectious, that is, $\omega = 0.5$ per year.

Relapse rate of recovered individuals: The average relapse rate of recovered individuals is $\gamma = 0.01$ per year.

TB mortality d_1 of diagnosed infectious: According to data of TB in Cameroon, the average death of diagnosed infectious is $d = 0.0575$ per year.

2.6 Comparison to measurement data

In order to illustrate the theoretical results of the foregoing analysis, numerical simulations of model system (2.2) are carried out using a fourth order Runge-Kutta scheme in the software Matlab, version R2009. The comparison to measurement data allows to test the suitability of the model (2.2) to effectively enable the assessment of targeted public health education and chemoprophylaxis strategies against TB spread in a population. The model is fitted using data from Cameroon as follows. Parameters are giving in Table 2.2. The total population of Cameroon, as of 1994, is given by $N = 13240337$ [126]. The initial conditions used were set as in the following Table. Using the aforementioned data, the model (2.2) gives a very good fit of the Cameroonian data for the period 1994-2010 [132], as depicted in Figure 2.5. Hence, model (2.2) can be used to gain realistic insight into tuberculosis transmission dynamics at least for a relatively period.

Symbol	Initial value	Source
S	5576135	Estimated
E	8357382	Estimated
I	3092	WHO
J	1037	Estimated
L	251	Estimated
R	2140	Estimated
N	13240337	[126]

Table 2.3: Initial values of state variables of the TB model.

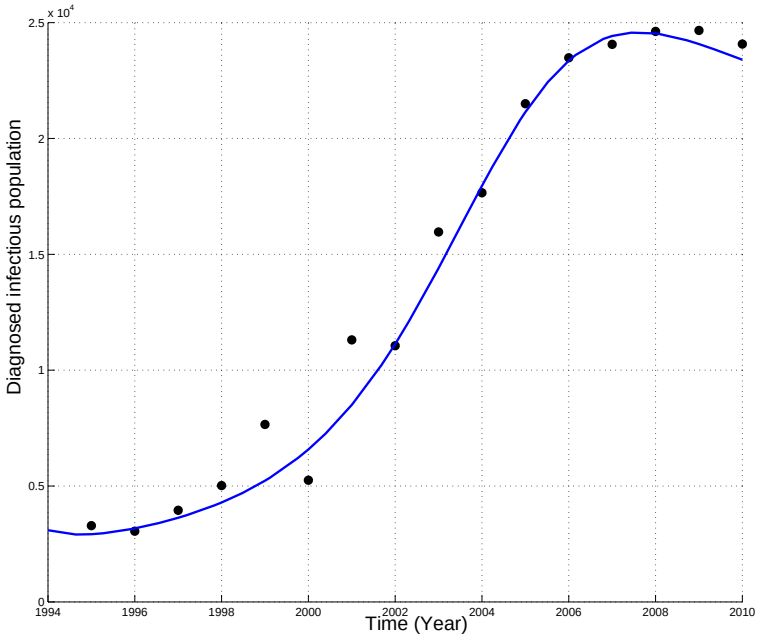

(a)

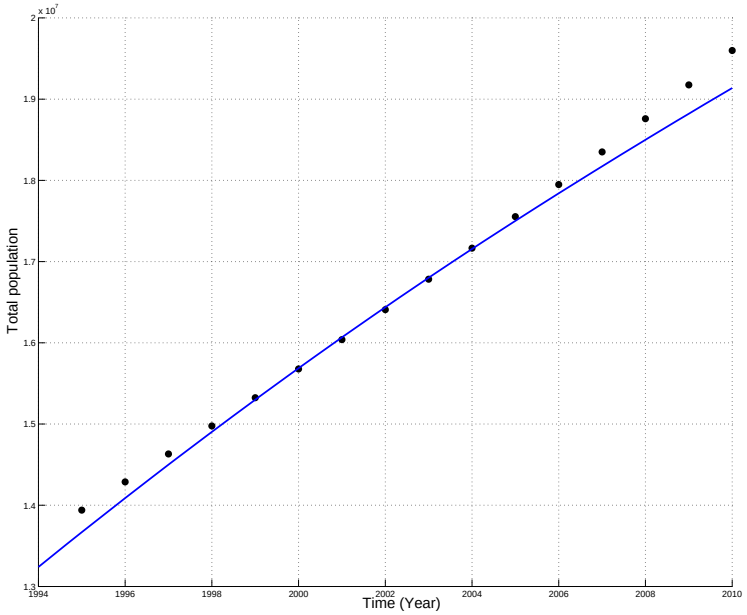

(b)

In Figure 2.5, (I) and (N) show the comparison between the data and the estimated trajectories; there are no obvious discrepancies (note that data are available only on I and N).

In Figure 2.6 we look more closely at how well the fitted model captures the variation in disease incidence, by re-plotting the data using the Runge-Kutta fourth other scheme and comparing this with model solutions and an increase of step size. Fig. 2.6 (S), (E), (L) and (R) show the time evolution of the estimated trajectories of model (2.2) at each time point. Here, while the agreement is not perfect, there are no evident consistent patterns in the discrepancy. The estimated trend in the number of susceptible population (top panel of Fig. 2.6 (S)), is due to the estimated linear trend $\beta_i, \quad i = 1, 2, 3$, in the transmission parameter. The rate of change is about 1% per year (1% per year decrease in S, 1% per year increase in the mean of β_i). However, there is very high uncertainty regarding the trend in β_i (e.g., a tenfold smaller trend is within two standard errors of the point estimate), so we cannot be confident that the estimated trends in S and β_i are real, even if those values remain in the right intervals. Forward solutions of the deterministic model follow fairly well the observed TB pattern of incidence. With the estimated transmission parameters, the deterministic model appears to capture all of the qualitative properties of the observed pattern.

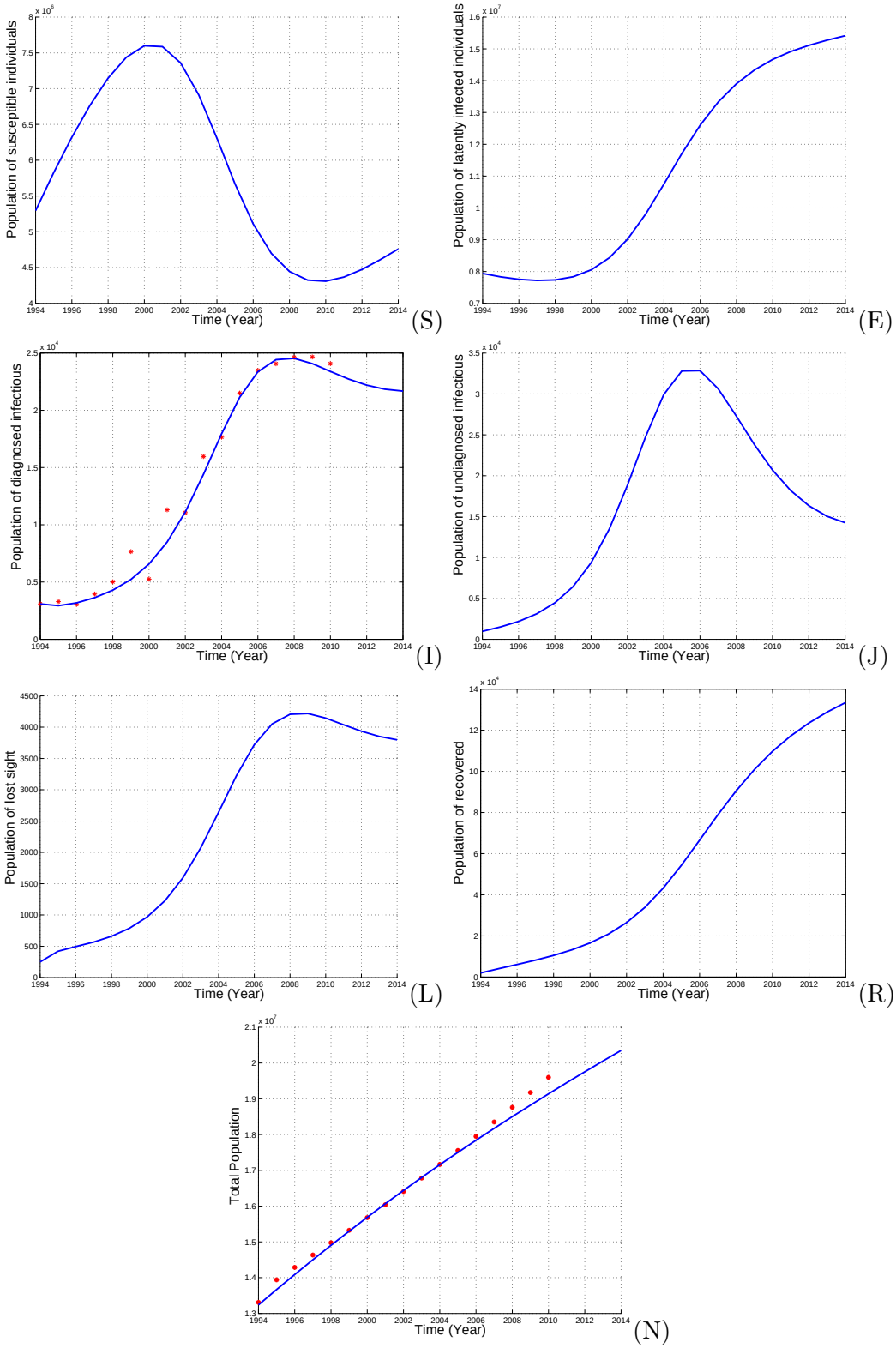

Figure 2.6: Time series of model (2.2) showing the estimated state trajectories of susceptible, latently infected, diagnosed infectious, undiagnosed infectious, lost sight, recovered and total population classes. The dot plots represent the year-by-year trend and variability in yearly case reports over the period 1994-2010. Parameter values are defined in Table 2.2 and initial values are presented in Table 2.3.

2.7 Effects of increased access to treatment

Herein, we investigate the impact of the variation of some specific parameters on the dynamics of model (2.2) by doing simulations of the model using parameters in Table 2.2, initial values in Table 2.3, and estimated states as artificial data for POEM. These results were reduced by 20% and 60% for classes of lost sight (L), diagnosed infectious, and undiagnosed infectious to find artificial data. Some model parameters have been considered as time dependent variable to reflect their possible change within time. However, the variation is assumed to be slow over the time. These parameters are assumed to be control functions for the dynamics of TB. Thus, the model (2.2) becomes a non-autonomous controlled system.

Effects of increase the access to TB treatment as a result of infrastructures and education are explored in Figure 2.7 by taking into account following expression of models parameters.

$$\begin{aligned}
\theta(t) &= \theta + \frac{(1-\theta)t}{\theta_\delta + t},\\
\delta(t) &= \delta + \frac{(1-\delta)t}{\delta_\delta + t},\\
p_1(t) &= p_1 + \frac{p_2 t}{p_\delta + t},\\
p_2(t) &= p_2 - \frac{p_2 t}{p_\delta + t}.
\end{aligned} \tag{2.22}$$

Herein, θ_δ, δ_δ and p_δ are positive constant to be estimated.

The increase (or decrease) in these parameters can be interpreted as the result of change on treatment access, diagnosed campaign or large scale education via social networks, TV, radio etc. Then, we estimated parameter values of θ_δ, δ_δ and p_δ using POEM as previously. The results presented in Figure 2.7 show that tuberculosis can be reduced by 20 % in five years if some efforts are make to increase the treatment access for rural population. We also observe that the number of diagnosed infectious increases at the beginning, but decreases after few years prior to the beginning of the controls strategies which allows increasing the treatment access.

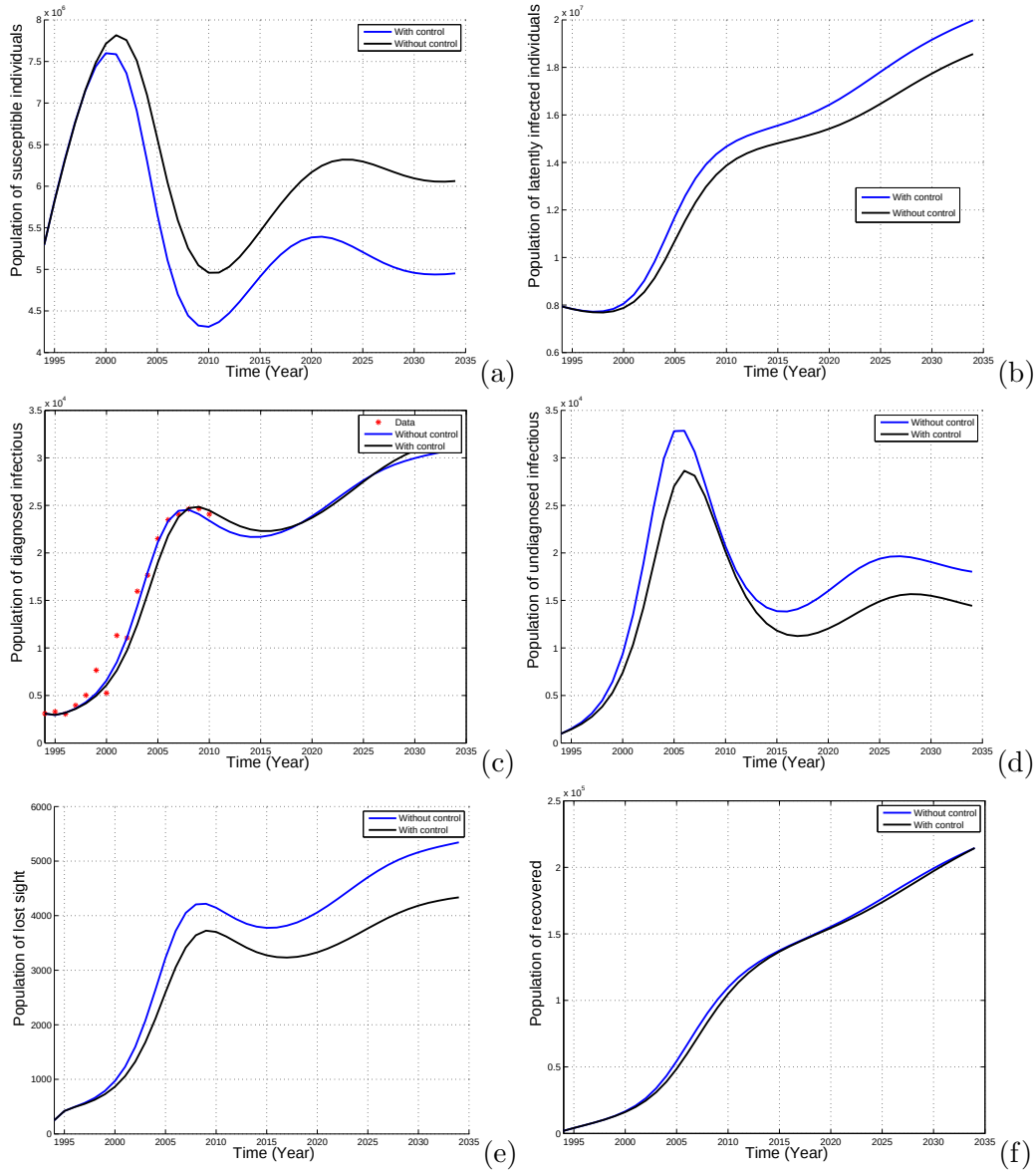

Figure 2.7: Time series of model (2.2) showing the impact of a slow change on parameter values θ, δ, p_1 and p_2 with respect to time in order to reduce the TB burden by 20% in 5 years. Blue lines present the model predictions for TB dynamics using parameter values of Table 2.2 and the black lines present the estimated trajectories for parameters θ, δ, p_1 and p_2 set as in equation 2.22. Simulation with POEM gave $p_\delta = 8.56660e+07$, $\theta_\delta = 37.1301e+03$, $\delta_\delta = 37.1301$ from artificial data reduced by 20% with respect to model predictions. All other parameters are defined as in Table (2.2).

Using artificial data reduced by 20% from the predicted states of model (2.2), with respect to parameters in Table 2.2, parameter identification with POEM gave $p_\delta = 8.56660e + 07$, $\theta_\delta = 37.1301e + 03$, $\delta_\delta = 37.1301$. In Figure 2.7, time series of model (2.2) showing the impact of a slow changed on parameter values θ, δ, p_1 and p_2 with respect to time on the dynamics of TB. Blue lines present the model predictions for TB dynamics using parameter values of Table 2.2 and the black lines present the estimated trajectories for parameters $\theta(t)$, $\delta(t)$, $p_1(t)$ and $p_2(t)$ set as in equation (2.22). All other parameters are kept as in Table 2.2.

The numerical results in Figures 2.7 illustrate that a small increase of the access to TB treatment could generally result in an increase in the number of TB diagnosed infectious, a decrease in the number of lost sight, latently infected and undiagnosed infectious individuals. The Figure shows also a positive change in the access to treatment will significantly affect the long term progression of the disease, through classes of susceptible and recovered.

Using again POEM 2.0 to estimate parameters θ_δ, δ_δ and p_δ, it follows that TB undiagnosed infectious and lost sight can be reduced by 60 % in fifteen years if some large and continuous efforts are made to increase the treatment access for rural population, and TB prevention for fast and immuno-compromised people. Using POEM 2.0, parameter values $p_\delta = 85.6660$, $\theta_\delta = 81.3256$, $\delta_\delta = 37.1301$ have been estimated in other to see the evolution of $\theta(t)$, $\delta(t)$, $p_1(t)$ and $p_2(t)$ which are necessary for the objective of 60% reduction in 15 years for undiagnosed and lost sight infectious.

Figure 2.8 shows for $p_\delta = 85.6660$, $\theta_\delta = 81.3256$, $\delta_\delta = 37.1301$ the dynamic of Tb inside the population in the presence (black curves) and absence (blue curves) of continuous effort to diagnose the population.

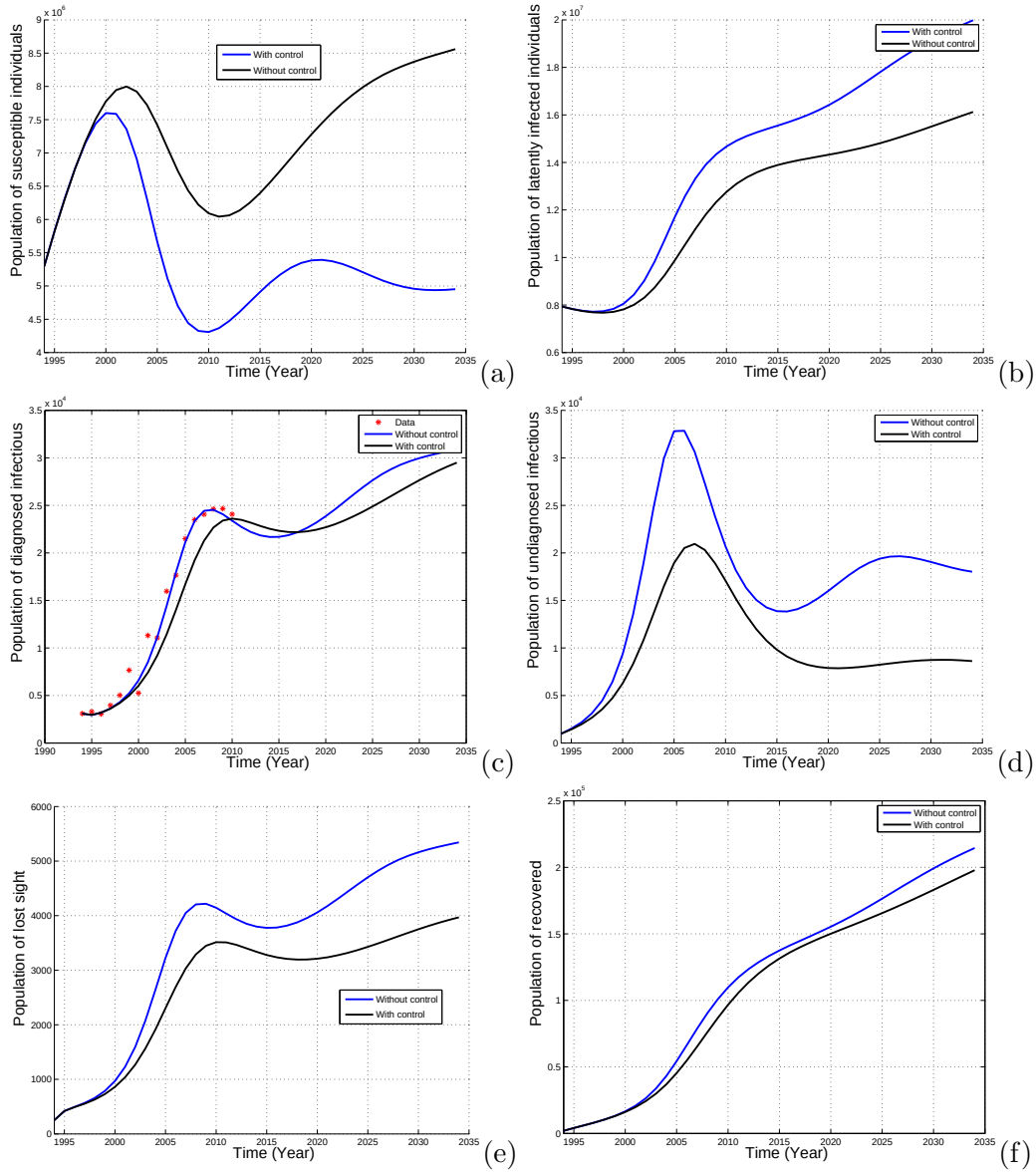

Figure 2.8: Time series of model (2.2) showing the impact of a slow change on parameter values θ, δ, p_1 and p_2 with respect to time in order to reduce the TB burden by 60% in 5 years. Blue lines present the model predictions for TB dynamics using parameter values of Table 2.2 and the black lines present the estimated trajectories for parameters θ, δ, p_1 and p_2 set as in equation (2.22). Simulation with POEM gave $p_\delta = 85.6660$, $\theta_\delta = 81.3256$, $\delta_\delta = 37.1301$ from artificial data reduced by 60% with respect to model predictions. All other parameters are defined as in Table (2.2).

The numerical results in Figure. 2.8 illustrate that a relative small increase of the access to TB treatment in general and education about TB for immune-compromised people will result in an increase in the number of susceptible, a decrease in a number of infectious, lost sight, latently infected and undiagnosed infectious individuals by 60% in fifteen years. The Figure shows also that a positive change in the access to treatment will significantly affect the long term progression of the disease even if it would not died out.

Chapter 3

Mathematical Analysis of the TB Model

For many epidemiological models, a threshold condition that indicates whether an infection introduced into a population will be eliminated or become endemic have been defined [35]. The basic reproduction number $\mathcal{R}_0$ is defined as the average number of secondary infections produced by an infected individual in a completely susceptible population [86]. In models with only two steady states and a transcritical bifurcation, $\mathcal{R}_0 > 1$ implies that the endemic state is stable (e.g. the infection persists), and $\mathcal{R}_0 \leq 1$ implies that the uninfected state is stable (e.g. the infection will die out). The co-existence of disease-free equilibrium and endemic equilibria when the basic reproduction number ($\mathcal{R}_0$) is less than unity is typically associated with the backward or subcritical bifurcation. This phenomenon has been found in many epidemiological settings (see for instance, [68, 81, 104, 151] and references therein). The epidemiological implication of is that the classical requirement of having the associated reproduction number less than unity, while necessary is not a sufficient condition for disease control. Results show that a threshold level of reinfection exists in all cases of the model. Beyond this threshold, the dynamics of the model are described by a backward bifurcation. However, uncertainty analysis of the parameters shows that this threshold is too high to be attained in a realistic epidemic [151]. In particular, when reinfection is present the basic reproductive number, $\mathcal{R}_0$, does not accurately describe the severity of an epidemic. In this chapter, we determine the basic reproduction ratio, and discuss the existence and the stability of the endemic equilibrium and the disease free equilibrium (DFE). The TB persistence condition will therefore been deduced.

3.1 Basic reproduction number

The global behavior of the TB model crucially depends on the basic reproduction number, i.e., an average number of secondary cases produced by a single infective individual, who is introduced into an entirely susceptible population. Model system (2.3) has an evident equilibrium $Q_0 = (x_0, 0)$ with $x_0 = \Lambda/\mu$ when there is no disease in the population. This equilibrium point is the disease-free equilibrium, obtained by setting the right hand sides of equations in model system (2.3) to zero. We calculate the basic reproduction number $\mathcal{R}_0$, using the next generation method developed in [157]. For that purpose, let us write system (2.3) in the form

$$\begin{cases} \dot{x} &= \varphi(x) - \nu(I,J,L)(t)x, \\ \dot{y} &= \mathcal{F}(x,y) - \mathcal{V}(x,y), \end{cases} \tag{3.1}$$

where

$$\mathcal{F}(x,y) = \nu(I,J,L)B_1 x \quad \text{and} \quad \mathcal{V}(x,y) = \nu(I,J,L)[B_2\langle e_1 \mid y\rangle + B_3\langle e_5 \mid y\rangle] + A\,y \tag{3.2}$$

Then, one has

$$F = \frac{\partial \mathcal{F}}{\partial y}(Q_0) \quad \text{and} \quad V = \frac{\partial \mathcal{V}}{\partial y}(Q_0)$$

where $\mathcal{F}(x,y)$ and $\mathcal{V}(x,y)$ are Jacobian matrices at the DFE. Using the same notations as in [157], the matrices F and V, for the new infection terms and the remaining transfer terms respectively, the basic reproduction number, which is the spectral radius of FV^{-1} is giving by

$$\mathcal{R}_0 = \rho(FV^{-1}). \tag{3.3}$$

For model (3.1), one has

$$F = B_1\left(e_1 + \frac{\Lambda}{\mu}e_2\right) \text{ and } V = -A.$$

Then, using the matrix transformation of [98, 92, 93, 94], the basic reproduction ratio is given by

$$\mathcal{R}_0 = \left\langle e_1 + \frac{\Lambda}{\mu}e_2 \mid (-A^{-1})B_1 \right\rangle. \tag{3.4}$$

We use the expression $(-A^{-1})$ to emphasize that $(-A^{-1}) \geq 0$ because the matrix A is Metzler stable.

The following result is established (from Theorem 1.3.1):

Lemma 3.1.1. *: The disease-free equilibrium Q_0 of model system (2.3) is locally asymptotically stable whenever $\mathcal{R}_0 < 1$, and instable if $\mathcal{R}_0 > 1$.*

From a biological point of view, Lemma 3.1.1 implies that TB can be eliminated from the community (when $\mathcal{R}_0 \leq 1$) if the initial sizes of the population are in the basin of attraction of Q_0. But if $\mathcal{R}_0 > 1$ the infection will be able to spread in a population. Generally, the larger the value of $\mathcal{R}_0$, the harder it is to control the epidemic.

3.2 Bifurcation analysis

Herein, the number of equilibrium solutions of model (2.3) is investigated. Let $Q^* = (x^*, y^*)$ be any arbitrary equilibrium of model system (2.3). To find existence conditions for an endemic equilibrium of tuberculosis in the population (steady state with y^* non zero), the equations in model equation (2.3) are set at zero, i.e.,

$$\begin{cases} \varphi(x^*) - x^*\nu^* \rangle = 0, \\ \\ \nu^*[x^*B_1 + \langle e_3 \mid y^* \rangle B_2 + \langle e_4 \mid y^* \rangle B_3] + A\, y^* = 0, \end{cases} \tag{3.5}$$

with

$$\nu^* = \frac{\langle e_1 \mid y^* \rangle}{N^*} + \langle e_2 \mid y^* \rangle, \tag{3.6}$$

is the force of infection at the steady state. For the sake of simplicity, we sets $\nu^* = \nu^*$ throughout this Section.

Multiplying the second equation of equation (3.5) by $-A^{-1}$, one obtains

$$y^* = \nu^*[x^*(-A^{-1})B_1 + \langle e_3 \mid y^* \rangle(-A^{-1})B_2 + \langle e_4 \mid y^* \rangle(-A^{-1})B_3]. \tag{3.7}$$

Then, one can deduce that

$$\begin{aligned} \langle e_1 \mid y^* \rangle &= \nu^*[x^*R_{01} + a_1\langle e_3 \mid y^* \rangle + a_2\langle e_4 \mid y^* \rangle], \\ \langle e_2 \mid y^* \rangle &= \nu^*[x^*R_{02} + a_3\langle e_3 \mid y^* \rangle + a_4\langle e_4 \mid y^* \rangle], \\ \langle e_3 \mid y^* \rangle &= \nu^*[x^*a_5 + a_6\langle e_3 \mid y^* \rangle + a_7\langle e_4 \mid y^* \rangle], \\ \langle e_4 \mid y^* \rangle &= \nu^*[x^*a_8 + a_9\langle e_3 \mid y^* \rangle + a_{10}\langle e_4 \mid y^* \rangle], \end{aligned} \tag{3.8}$$

where

$$R_{01} = \langle e_1 \mid (-A^{-1})B_1\rangle,\ \ R_{02} = \langle e_2 \mid (-A^{-1})B_1\rangle,\ \ a_1 = \langle e_1 \mid (-A^{-1})B_2\rangle,$$

$$a_2 = \langle e_1 \mid (-A^{-1})B_3\rangle,\ \ a_3 = \langle e_2 \mid (-A^{-1})B_2\rangle,\ \ a_4 = \langle e_2 \mid (-A^{-1})B_3\rangle,$$

$$a_5 = \langle e_3 \mid (-A^{-1})B_1\rangle,\ \ a_6 = \langle e_3 \mid (-A^{-1})B_2\rangle,\ \ a_7 = \langle e_3 \mid (-A^{-1})B_3\rangle,$$

$$a_8 = \langle e_4 \mid (-A^{-1})B_1\rangle,\ \ a_9 = \langle e_4 \mid (-A^{-1})B_2\rangle \text{ and } a_{10} = \langle e_4 \mid (-A^{-1})B_3\rangle.$$

Using the two last equation of equation (3.8), one can deduce that

$$\begin{aligned} \langle e_3 \mid y^*\rangle &= \frac{\nu^* x^*[a_5 + (a_7a_8 - a_5a_{10})\nu^*]}{-a_7a_9(\nu^*)^2 + (1 - a_6\nu(I,J,L)^*)(1 - a_{10}\nu^*)}, \\ \langle e_4 \mid y^*\rangle &= \frac{\nu^* x^*[a_8 + (a_5a_9 - a_6a_8)\nu^*]}{-a_7a_9(\nu^*)^2 + (1 - a_6\nu^*)(1 - a_{10}\nu^*)}. \end{aligned} \tag{3.9}$$

From the first equation of equation (3.5), one obtains

$$x^* = \frac{\Lambda}{\mu + \nu^*} \tag{3.10}$$

Combining equations (3.6), (3.8), (3.9) and (3.10), one can deduce that the total population size at the steady state is defined by

$$N^* = \frac{\Lambda\left(F_2(\nu^*)^2 + F_1\nu^* + R_{01}\right)}{H_3(\nu^*)^3 - (\mu H_3 - \Lambda C_2 - (a_6 + a_{10}))(\nu^*)^2 + (1 - \mu(a_6 + a_{10}) - \Lambda C_1)\nu^* + \mu - \mu R_{02}}, \tag{3.11}$$

where

$$\begin{aligned} F_2 &= R_{01}(a_{10}a_6 - a_7a_9) + a_1(a_7a_8 - a_5a_{10}) + a_2(a_5a_9 - a_8a_6), \\ F_1 &= -R_{01}(a_6 + a_{10}) + a_1a_5 + a_2a_8, \\ C_2 &= R_{02}(a_{10}a_6 - a_7a_9) + a_3(a_7a_8 - a_5a_{10}) + a_4(a_5a_9 - a_8a_6), \\ C_1 &= R_{02}(a_6 + a_{10}) + a_3a_5 + a_4a_8, \\ H_3 &= (a_6a_{10} - a_7a_9). \end{aligned}$$

Let $w_1 = (0,1,0,0,0)^T$, $w_2 = (0,0,1,0,0)^T$ and $w_3 = (0,0,0,1,0)^T$. Then, from

equation (3.7), one can deduce that

$$\begin{aligned} I^* = \langle w_1 \mid y^* \rangle &= \nu^*[x^* \langle w_1 \mid (-A^{-1})B_1 \rangle + \langle w_1 \mid (-A^{-1})B_2 \rangle \langle e_3 \mid y^* \rangle \\ &+ \langle w_1 \mid (-A^{-1})B_3 \rangle \langle e_4 \mid y^* \rangle], \\ J^* = \langle w_2 \mid y^* \rangle &= \nu^*[x^* \langle w_2 \mid (-A^{-1})B_1 \rangle + \langle w_2 \mid (-A^{-1})B_2 \rangle \langle e_3 \mid y^* \rangle \\ &+ \langle w_2 \mid (-A^{-1})B_3 \rangle \langle e_4 \mid y^* \rangle], \\ L^* = \langle w_3 \mid y^* \rangle &= \nu^*[x^* \langle w_3 \mid (-A^{-1})B_1 \rangle + \langle w_3 \mid (-A^{-1})B_2 \rangle \langle e_3 \mid y^* \rangle \\ &+ \langle w_3 \mid (-A^{-1})B_3 \rangle \langle e_4 \mid y^* \rangle]. \end{aligned} \tag{3.12}$$

Now, using equation (2.4) at the steady state, one has

$$N^* = \frac{\Lambda}{\mu} - \frac{d_1}{\mu} I^* - \frac{d_2}{\mu} J^* - \frac{d_3}{\mu} L^*. \tag{3.13}$$

Combining equations (3.9), (3.12) and (3.13) gives

$$N^* = \frac{\Lambda}{\mu} \frac{(\nu^*)^3(H_3 - D_2) + (\nu^*)^2(\mu H_3 - D_1 - (a_6 + a_{10})) + \nu^*(1 - \mu(a_6 + a_{10}) - g_0) + \mu}{H_3(\nu^*)^3 + (H_3\mu - (a_6 + a_{10}))(\nu^*)^2 + (1 - \mu(a_6 + a_{10}))\nu^* + \mu}, \tag{3.14}$$

where

$$\begin{aligned} g_0 &= d_1 \langle w_1 \mid (-A^{-1})B_1 \rangle + d_2 \langle w_2 \mid (-A^{-1})B_1 \rangle + d_3 \langle w_3 \mid (-A^{-1})B_1 \rangle, \\ g_1 &= d_1 \langle w_1 \mid (-A^{-1})B_2 \rangle + d_2 \langle w_2 \mid (-A^{-1})B_2 \rangle + d_3 \langle w_3 \mid (-A^{-1})B_2 \rangle, \\ g_2 &= d_1 \langle w_1 \mid (-A^{-1})B_3 \rangle + d_2 \langle w_2 \mid (-A^{-1})B_3 \rangle + d_3 \langle w_3 \mid (-A^{-1})B_3 \rangle, \\ D_1 &= -g_0(a_6 + a_{10}) + a_5 g_1 + a_8 g_2, \\ D_2 &= g_2(a_9 a_5 - a_6 a_8) + g_1(a_7 a_8 - a_5 a_{10}) + g_0(a_6 a_{10} - a_7 a_9). \end{aligned}$$

Equaling equations (3.11) and (3.14), it can be shown that the non-zero equilibria of model system (2.3) satisfies the following equation in term of ν^*:

$$E_6(\nu^*)^6 + E_5(\nu^*)^5 + E_4(\nu^*)^4 + E_3(\nu^*)^3 + E_2(\nu^*)^2 + E_1(\nu^*) + E_0 = 0, \tag{3.15}$$

where

$$
\begin{aligned}
E_6 &= H_3(H_3 - D_2),\\
E_5 &= H_3(\mu H_3 - D_1 - (a_6 + a_{10})) + (H_3 - D_2)(\mu H_3 - (a_6 + a_{10}) - \Lambda C_2) - \mu F_2 H_3,\\
E_4 &= H_3(1 - \mu(a_6 + a_{10}) - g_0) + (\mu H_3 - (a_6 + a_{10}) - \Lambda C_2)(\mu H_3 - (a_6 + a_{10}) - D_1)\\
&+ (H_3 - D_2)(1 - (a_6 + a_{10}) - \Lambda C_1) - \mu F_2(\mu H_3 - (a_6 + a_{10}) - \Lambda C_2) - \mu F_1 H_3,\\
E_3 &= \mu H_3 + (1 - \mu(a_6 + a_{10}) - g_0)(\mu H_3 - (a_6 + a_{10}) - \Lambda C_2) + (H_3 - D_2)(\mu - \Lambda R_{02})\\
&- \mu F_2(1 - \mu(a_6 + a_{10}) - \Lambda C_1) - \mu F_1(\mu H_3 - (a_6 + a_{10}) - \Lambda C_2),\\
E_2 &= (1 - (a_6 + a_{10}) - \Lambda C_1)(1 - \mu(a_6 + a_{10}) - g_0) + (\mu - \Lambda R_{02})(\mu H_3 - (a_6 + a_{10}) - D_1)\\
&- \mu^2 F_2 + \mu(\mu H_3 - (a_6 + a_{10}) - \Lambda C_2) - \mu F_1(1 - (a_6 + a_{10}) - \Lambda C_1)\\
&- \mu R_{01}(\mu H_3 - (a_6 + a_{10}) - \Lambda C_2),\\
E_1 &= \mu(1 - (a_6 + a_{10}) - \Lambda C_1) + (\mu - \Lambda R_{02})(1 - \mu(a_6 + a_{10}) - g_0) - \mu^2 F_2\\
&- (1 - (a_6 + a_{10}) - \Lambda C_1)\mu R_{01},\\
E_0 &= \mu^2(1 - \mathcal{R}_0).
\end{aligned}
$$

The positive endemic equilibria Q^* are obtained by finding ν^* from the polynomial equation (3.15) and substituting the numerical results (positive values of ν^*) into the expressions of the state variables at the steady state. Clearly, the coefficient E_0 of equation (3.15) is positive or negative whenever $\mathcal{R}_0$ is less or greater than unity, respectively. Thus, the number of possible real roots of the polynomial equation (3.15) depends on the signs of E_6, E_5, E_4, E_3, E_2, E_1 and E_0. This can be analyzed using the Descartes Rule of Signs on the function $f(\nu^*) = E_6(\nu^*)^6 + E_5(\nu(I, J, L)^*)^5 + E_4(\nu(I, J, L)^*)^4 + E_3(\nu(I, J, L)^*)^3 + E_2(\nu(I, J, L)^*)^2 + E_1(\nu^*) + E_0$ given in equation (3.15). We claim the following result.

Lemma 3.2.1. *The TB model (2.2)*

(i) *could have a unique endemic equilibrium wherever* $\mathcal{R}_0 > 1$*;*

(ii) *could have more than one endemic equilibrium wherever* $\mathcal{R}_0 > 1$*;*

(iii) *could have a unique endemic equilibrium wherever* $\mathcal{R}_0 < 1$*;*

(iv) *could have one or more endemic equilibria wherever* $\mathcal{R}_0 < 1$.

The existence of multiple endemic equilibria when $\mathcal{R}_0 < 1$ suggests the possibility of a backward bifurcation (see, [34, 9, 68] and references therein), where a stable disease-free equilibrium co-exists with a stable endemic equilibrium when the basic reproduction number is less than unity. This is explored below via numerical simulations. The function `roots` of Matlab is used to find the root of the polynomial 3.15.

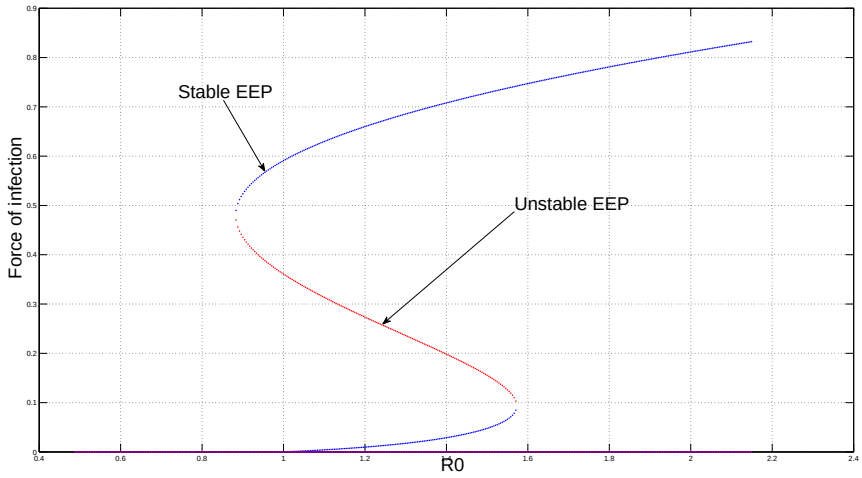

Figure 3.1: Bifurcation diagram for model system (2.2). The diagram shows the values of the force of the infection generating forward bifurcation as well as multiple supercritical endemic equilibria for $\sigma_1 = 0.015$ plotted for the parameters in Table 2.2 (except for β_3, which vary) and the value of the disease reinfection rate (σ_1). For the parameter values in Table 2.2, there are three equilibrium points in ω_ρ: a locally asymptotically stable disease-free equilibrium point on the boundary of the positive orthant of $\mathbb{R}^6$, and two endemic equilibrium points inside the positive orthant. Linear stability analysis shows that the "larger" endemic equilibrium point is locally asymptotically stable, while the "smaller" point is unstable. Further linear analysis with an increased value of β_3, (with $\mathcal{R}_0 > 1.155$) shows that the DFE is unstable, and there is one locally asymptotically stable endemic equilibrium point. The notation EE stands for endemic equilibrium point.

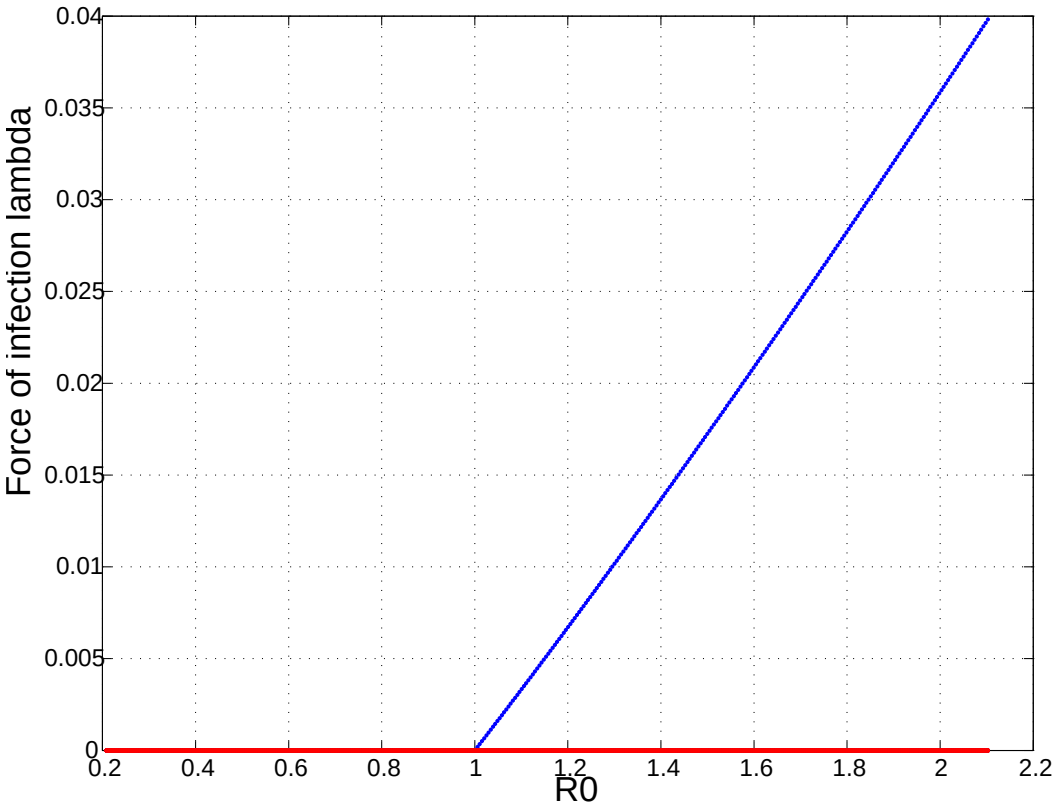

Figure 3.2: Bifurcation diagram for model system (2.2) showing the values of the force of the infection generating a transcritical bifurcation for $\sigma_1 = 2.38390E-04$.

The backward bifurcation phenomenon is illustrated by simulating model system (2.2) with the parameters of Table 2.2, and different values of β_3. The associated backward bifurcation diagram is depicted in Figure 3.1. compute $Q^*(j)$. Else, $\nu(I, J, L)^*(j) = 0$

The epidemiological significance of the phenomenon of backward bifurcation is that the classical requirement of $\mathcal{R}_0 < 1$ is, although necessary, no longer sufficient for disease eradication. In such a scenario, disease elimination would depend on the initial sizes of the population (state variables) of the model. The presence of backward bifurcation in TB transmission model (2.2) suggests that the feasibility of controlling TB when $\mathcal{R}_0 < 1$ could be dependent on the initial sizes of the population. Further, as a consequence, it is instructive to try to determine the "cause" of the backward bifurcation phenomenon in model system (2.2). The role of reinfection on backward bifurcation will be investigated.

3.3 Role of exogenous reinfections

Let us consider the case where there is no exogenous reinfection in the population. Then, $\sigma_1 = \sigma_2 = 0$, $B_2 = B_3 = 0$ and model system (2.3) means

$$\begin{cases} \dot{x} &= \varphi(x) - \nu(I,J,L)(t)x, \\ \dot{y} &= \nu(I,J,L)(t)B_1 x + A\,y, \end{cases} \tag{3.16}$$

where $\varphi(x)$, B_1, $\nu(I,J,L)$ and A are defined as in equation (2.3).

Non-existence of endemic equilibria for $\mathcal{R}_0 \leq 1$

The above model has the same disease-free equilibrium Q_0. Apart this equilibrium state, the model can also have a unique positive endemic equilibrium state. In the absence of exogenous reinfection $\sigma_1 = \sigma_2 = 0$ (i.e, $B_2 = B_3 = 0$), the coefficients E_0, E_1, E_2, E_3, E_4, E_5 and E_5 in equation (3.15) reduce to

$E_6 = E_5 = E_4 = E_3 = 0$, $\quad E_2 = 1 - g_0$, $\quad E_1 = \mu + (\mu(1 - R_{01}) - \Lambda R_{02})(1 - g_0)$, $E_0 = \mu^2(1 - \mathcal{R}_0)$.

In this case, the force of infection at the steady state satisfies the quadratic equation

$$E_2(\nu^*)^2 + E_1\nu^* + E_0 = 0. \tag{3.17}$$

It is worth noting that the coefficient E_0 is positive if $\mathcal{R}_0$ is less than unity, and negative if $\mathcal{R}_0$ is greater than unity. Thus, the number of possible real roots of equation (3.17) depends on the signs of E_2, E_1 and E_0. This can be analysed using again the Descartes Rule of Signs on the polynomial $g(\nu^*) = E_2(\nu^*)^2 + E_1\nu^* + E_0$.

From the equality $\nu(I,J,L) = \beta_1\dfrac{I}{N} + \beta_2\dfrac{L}{N} + \beta_3 J$, one can deduce that

$$0 \leq \nu^* \leq \left(\beta_1 + \beta_2 + \beta_3\frac{\Lambda}{\mu}\right).$$

On other side,

$g(0) = E_0 = \mu^2(1 - \mathcal{R}_0)$,

$g\left(\beta_1 + \beta_2 + \beta_3\frac{\Lambda}{\mu}\right) = \mu^2(1 - \mathcal{R}_0)$

$+ \left(\beta_1 + \beta_2 + \beta_3\frac{\Lambda}{\mu}\right)\left((1 - g_0)\left(\beta_1 + \beta_2 + \beta_3\frac{\Lambda}{\mu}\right) + \mu(1 - R_{01}) + (\mu - \Lambda R_{02})(1 - g_0)\right).$

A long but simple calculation proves that $1-g_0>0$, $\mu-\Lambda R_{02}>0$ and $1-R_{01}>0$ when $\mathcal{R}_0\leq 1$, and then $g\left(\beta_1+\beta_2+\beta_3\frac{\Lambda}{\mu}\right)>0$. It is straightforward to see that $g(0)<0$ when $\mathcal{R}_0>1$.

The existence of the endemic equilibrium follows from the intermediate value theorem. Since $g(\nu^*)$ is monotone increasing , then $g(\nu^*)=0$ has only one positive root in the interval $\left[0,\beta_1+\beta_2+\beta_3\frac{\Lambda}{\mu}\right]$. Hence, when $\sigma_1=\sigma_2=0$, no endemic equilibrium exists whenever $\mathcal{R}_0\leq 1$. It follows then that, owing to the absence of multiple endemic equilibria for model system (2.2) with $\sigma_1=\sigma_2=0$ and $\mathcal{R}_0\leq 1$, a backward bifurcation is unlikely model system (2.2) with $\sigma_1=\sigma_2=0$ and $\mathcal{R}_0\leq 1$. The absence of multiple endemic equilibria suggests that the disease-free equilibrium of model system (2.2) is globally asymptotically stable when $\mathcal{R}_0<1$.

Global stability of the disease-free equilibrium

We claim the following result about the global stability of the DFE of model (2.3) whenever $\sigma_1=\sigma_2=0$.

Theorem 3.3.1. *Consider model system (2.2) with $\sigma_1=\sigma_2=0$. Then, the DFE is globally asymptotically stable in Ω_ρ whenever $\mathcal{R}_0\leq 1$.*

Proof: The local stability of Q_0 is classic by the result of van den Driessche and Watmough [157]. Since we are interested in the global asymptotic behavior of model system (2.3), we will show that there exists $T>0$ such that, if $\mathcal{R}_0<1$, the solutions of model system (2.3) tend to the DFE $Q_0=(S_0,0,0,0,0)$ when $t\to\infty$, $\forall t>T$. Indeed, from the first equation of model system (2.3), one has

$$\dot{S}\leq\Lambda-\mu S. \tag{3.18}$$

This suggests the linear comparison system:

$$\dot{S}=\Lambda-\mu S. \tag{3.19}$$

The linear comparison system (3.19) has a unique positive equilibrium S_0 which is globally asymptotically stable. By the comparison theorem for cooperative systems, one has that

$$\limsup_{t\to\infty} S(t)\leq\lim_{t\to\infty} S(t)=S_0. \tag{3.20}$$

Thus, for any $\sigma>0$, there exists a sufficiently large $T>0$ such that $S(t)\leq S_0+\sigma$, for all $t>T$.

Since $\mathcal{R}_0$ depend of S_0, we set $F = F(S_0)$, $S_0^\sigma = S_0 + \sigma$ and $F_\sigma = F(S_0^\sigma) = F(S_0+\sigma) = [F_1 + (S_0+\sigma)F_2]B$. Since the spectral radius of $F_\sigma V^{-1}$ is a continuous function of σ, we can choose σ as small as possible such that if $\rho(FV^{-1}) < 1$, so $\rho(F_\sigma V^{-1}) < 1$.

Now, since $S(t) \leq S_0 + \sigma$ for all $t > T$ and $\dfrac{S(t)}{N(t)} \leq 1$, replacing $S(t)$ by $S_0 + \sigma$ in model system (2.3), we have the following comparison linear system in E, I, J, L and R :

$$\begin{cases} \dot{E} &= (1-p_1-p_2)(\beta_1 I + \beta_2 L + \beta_3 J(S_0+\sigma)) + \rho J - A_1 E, \\ \dot{I} &= p_1(\beta_1 I + \beta_2 L + \beta_3 J(S_0+\sigma)) + \delta L + \theta J + \gamma R + h(1-r_1)k - A_2 I, \\ \dot{J} &= p_2(\beta_1 I + \beta_2 L + \beta_3 J(S_0+\sigma)) + (1-h)(1-r_1)k - A_3 J, \\ \dot{L} &= \alpha I - A_4 L, \\ \dot{R} &= r_2 I + \omega L - A_5 R, \end{cases} \tag{3.21}$$

Model (3.21) can be written in the following compact form:

$$\dot{y} = (F_\sigma - V)\, y, \tag{3.22}$$

where y is defined as in equation (2.3). Note that $y = (0,0,0,0,0)$ is the unique equilibrium of the linear comparison system (3.22) which is globally asymptotically stable, since it is well known that if $s(F_\sigma - V)$ is the stability modulus of the matrix $(F_\sigma - V)$ defined as the maximal real part of the eigenvalues of $(F_\sigma - V)$, then from [157], $s(F_\sigma - V) < 0$ is equivalent to $\rho(F_\sigma V^{-1}) < 1$. Therefore, all solutions of the linear comparison system (3.22) converge to the trivial solution $y = (0,0,0,0,0)$ when $t \to \infty$, with $t > T$. It is obvious to see that $F_\sigma - V$ as the Jacobian of model system (3.22) is a M-matrix and irreducible. Thus, by the comparison theorem for monotone dynamical systems [21], we can conclude that the E, I, J, R components of model system (2.3) also converge to zero when $t \to \infty$, with $t > T$. Putting this last zero solution into the first equation of model system (2.3) gives the linear system (3.19) which admits a unique positive equilibrium S_0 which is globally asymptotically stable. Finally, by the asymptotically autonomous systems theory [43], we can conclude that the S-component of the solution of system (2.3) converges to S_0. This proves the global asymptotic stability of the DFE $Q_0 = (S_0, 0, 0, 0, 0, 0)$ when $\mathcal{R}_0 < 1$, and this completes the proof. □

Using various initial conditions and the parameter values as in Table 2.2 , we performed numerical simulations in order to analyze the stability of the endemic equilibrium. Figure 3.3 is showing the dynamics of (S) Susceptible population, (E) Latently infected population, (I) Diagnosed infectious population, (J) Undiagnosed

infectious population, (L) Lost Sight population and (R) Recovered population. Figure 3.3 shows simulation results converging to the disease free equilibrium of the model when $\mathcal{R}_0 \leq 1$. All other parameters are as in Table 2.2.

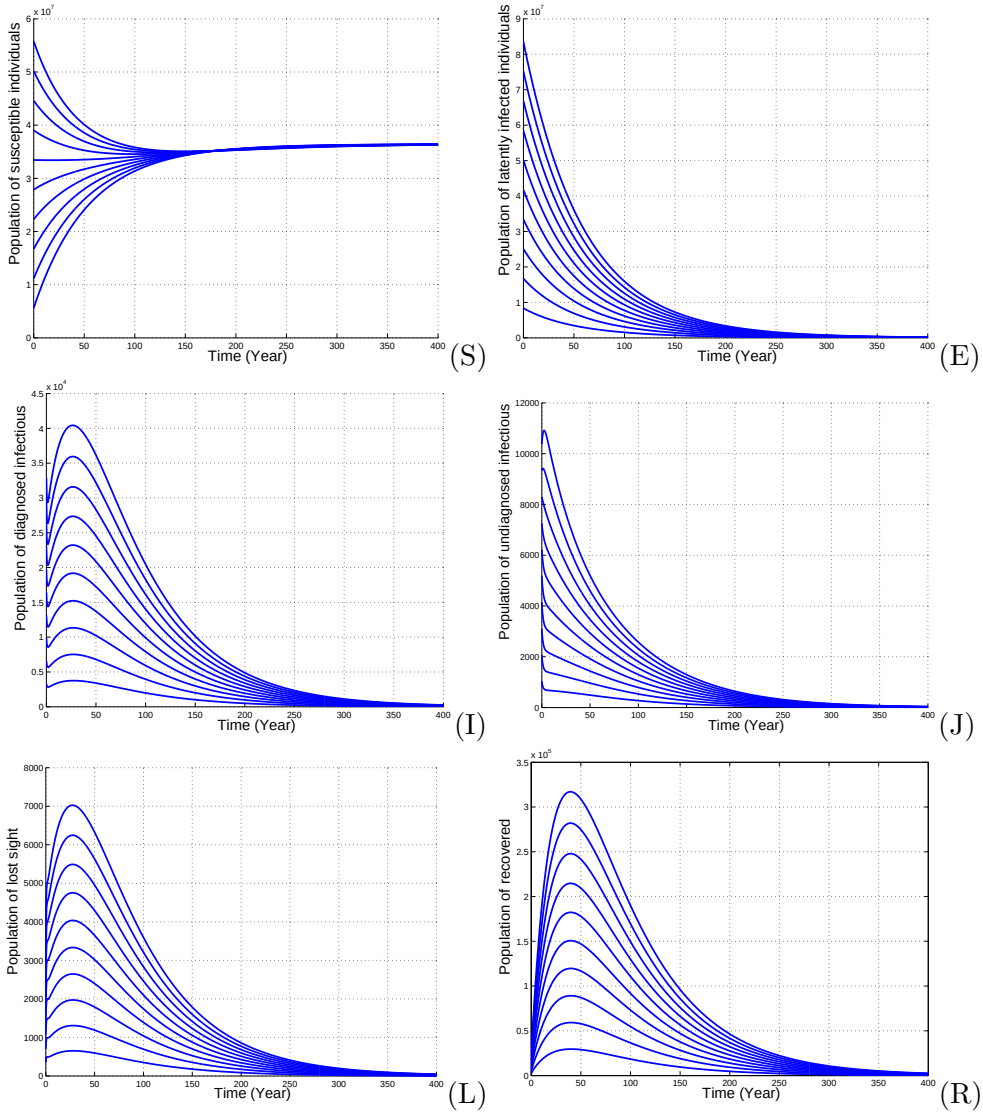

Figure 3.3: Simulation results of model system (2.2) showing the global asymptotic stability of the DFE when $\beta_3 = 0.2605681 \times 10^{-6}$ (so that $\mathcal{R}_0 = 0.4424$) using various initial conditions. One can see that after long time of decreasing, TB will die out in the absence of exogenous reinfection.

Local stability of the endemic equilibrium

In order to analyze the stability of the endemic equilibrium point, we make use of the Centre Manifold theory as described by Theorem 4.1 of Castillo-Chavez and Song [42], stated below (Theorem 3.3.2 for convenience), to establish the local asymptotic stability of the TB endemic equilibrium in the absence of reinfection.

Theorem 3.3.2. *[42]: Consider the following general system of ordinary differential equations with a parameter ϕ:*

$$\frac{dz}{dt} = f(z, \phi), \quad f : \mathbb{R}^n \times \mathbb{R} \to \mathbb{R} \ \text{ and } \ f \in C^2(\mathbb{R}^n, \mathbb{R}), \tag{3.23}$$

where 0 is an equilibrium point of the system (that is, $f(0, \phi) \equiv 0$ for all ϕ) and assume

1. *$A = D_z f(0,0) = \left(\dfrac{\partial f_i}{\partial z_j}(0,0)\right)$ is the linearization matrix of system (3.23) around the equilibrium 0 with ϕ evaluated at 0. Zero is a simple eigenvalue of A and other eigenvalues of A have negative real parts;*

2. *Matrix A has a right eigen-vector u and a left eigen-vector v (each corresponding to the zero eigenvalue).*

Let f_k be the k^{th} component of f and

$$a = \sum_{k,i,j=1}^{n} v_k u_i u_j \frac{\partial^2 f_k}{\partial z_i \partial z_j}(0,0),$$

$$b = \sum_{k,i=1}^{n} v_k u_i \frac{\partial^2 f_k}{\partial z_i \partial \phi}(0,0),$$

then, the local dynamics of the system around the equilibrium point 0 is totally determined by the signs of a and b.

1. *$a > 0$, $b > 0$. When $\phi < 0$ with $|\phi| \ll 1$, 0 is locally asymptotically stable and there exists a positive unstable equilibrium; when $0 < \phi \ll 0$, 0 is unstable and there exists a negative, locally asymptotically stable equilibrium;*

2. *$a < 0$, $b < 0$. When $\phi < 0$ with $|\phi| \ll 1$, 0 is unstable; when $0 < \phi \ll 1$, 0 is locally asymptotically stable equilibrium, and there exists a positive unstable equilibrium;*

3. $a > 0$, $b < 0$. *When* $\phi < 0$ *with* $|\phi| \ll 1$, 0 *is unstable, and there exists a locally asymptotically stable negative equilibrium; when* $0 < \phi \ll 1$, 0 *is stable, and a positive unstable equilibrium appears;*

4. $a < 0$, $b > 0$. *When* ϕ *changes from negative to positive, 0 changes its stability from stable to unstable. Correspondingly a negative unstable equilibrium becomes positive and locally asymptotically stable.*

Particularly, if $a > 0$ *and* $b > 0$, *then a backward bifurcation occurs at* $\phi = 0$.

Let us first make the following simplification and change of variables. Let $x_1 = S$, $x_2 = E$, $x_3 = I$, $x_4 = J$, $x_5 = L$ and $x_6 = R$ so that $N = x_1+x_2+x_3+x_4+x_5+x_6$. Further, by using vector notation $x = (x_1, x_2, x_3, x_4, x_5, x_6)^T$, the TB model (2.2) can be written in the form $\dot{x} = f(x)$, with $f = (f_1, f_2, f_3, f_4, f_5, f_6)^T$, as follows:

$$\begin{cases} x_1' &= f_1 = \Lambda - (\mu + \nu(I,J,L))x_1, \\ x_2' &= f_2 = (1-p_1-p_2)\nu(I,J,L)x_1 + \rho J - A_1 x_2, \\ x_3' &= f_3 = p_1\nu(I,J,L)x_1 + h(1-r_1)kx_2 + \delta x_5 + \gamma x_6 - A_2 x_3, \\ x_4' &= f_4 = p_2\nu(I,J,L)x_1 + (1-h)(1-r_1)kx_2 - A_3 x_4, \\ x_5' &= f_5 = \alpha x_3 - A_4 x_5, \\ x_6' &= r_2 x_3 + \omega x_5 - A_5 x_6, \end{cases} \tag{3.24}$$

where $\nu(I,J,L) = \dfrac{\beta_1 x_3 + \beta_2 x_5}{x_1+x_2+x_3+x_4+x_5+x_6} + \beta_3 x_4$, with A_1, A_2, A_3, A_4 and A_5 defined as in equation (2.2).

The Jacobian of the system (2.2), at the DFE Q_0, for all β_3^* is given by

$$J_{\beta_3^*}(Q_0) = \begin{pmatrix} -\mu & 0 & -\beta_1 & -\tilde{\beta}_3 & -\beta_2 & 0 \\ 0 & -A_1 & \beta_1(1-p_1-p_2) & (1-p_1-p_2)\tilde{\beta}_3 + \rho & (1-p_1-p_2)\beta_2 & 0 \\ 0 & hk(1-r_1) & p_1\beta_1 - A_2 & p_1\tilde{\beta}_3 + \theta & \beta_2 p_1 + \delta & \gamma \\ 0 & (1-h)k(1-r_1) & p_2\beta_1 & p_2\tilde{\beta}_3 - A_3 & \beta_2 p_2 & 0 \\ 0 & 0 & \alpha & 0 & -A_4 & 0 \\ 0 & 0 & r_2 & 0 & \omega & -A_5 \end{pmatrix}.$$

with $\tilde{\beta}_3 = \beta_3 N_0$.

The reproduction number of the transformed (linearized) model system (3.24) is the same as that of the original model given by (3.4). Therefore, choosing β_3 as

a bifurcation parameter and solving equation in β_3 when $\mathcal{R}_0 = 1$, we obtain

$$\beta_3 = \beta_3^* = \frac{1 - \langle e_1 \mid (-A^{-1})B_1 \rangle}{\langle N_0 e_2' \mid (-A^{-1})B_1 \rangle}.$$

where $e_2' = (0, 0, 0, 1, 0)$. It follows that the Jacobian $J(Q_0)$ of system (3.24) at the DFE Q_0, with $\beta_3 = \beta_3^*$, denoted by $J_{\beta_3^*}$ has a simple zero eigenvalue (with all other eigenvalues having negative real parts). Hence, the Centre Manifold theory [38] can be used to analyse the dynamics of the model (3.24). Now, the theorem 3.3.2 (cf. [42], can be used to show that the unique endemic equilibrium of the model (3.24) (or, equivalently, (2.2)) is locally asymptotically stable for $\mathcal{R}_0$ near 1.

Eigenvectors of $J_{\beta_3^*}$: For the case when $\mathcal{R}_0 = 1$, it can be shown that the Jacobian of system (3.24) at $\beta_3 = \beta_3^*$ (denoted by $J_{\beta_3^*}$) has a right eigenvector (corresponding to the zero eigenvalue), given by $U = (u_1, u_2, u_3, u_4, u_5, u_6)^T$, where,

$$\begin{aligned}
&u_1 = -\frac{1}{\mu}\left(\left(\beta_1 + \beta_2\frac{B_4}{C_4}\right)u_3 + \tilde{\beta}_3 u_4\right) < 0,\\
&u_2 = \frac{1}{A_1}\left((1-p_1-p_2)\left(\beta_1 + \frac{\beta_2\alpha}{A_4}\right) + (\tilde{\beta}_3(1-p_1-p_2)+\rho)\frac{B_4}{C_4}\right)u_3 > 0, \quad u_3 = u_3 > 0,\\
&u_4 = \frac{B_4}{C_4}u_3 > 0, \quad u_5 = \frac{\alpha}{A_4}u_3 > 0, \quad \text{and} \quad u_6 = \frac{r_2 A_4 + \omega\alpha}{A_4 A_5}u_3 > 0\\
&\text{with } B_4 = \left[p_2 + (1-p_1-p_2)\frac{(1-h)k(1-r_1)}{A_1}\right]\left(\beta_1 + \frac{\beta_2\alpha}{A_4}\right)\\
&\text{and } C_4 = A_3 - \left(\tilde{\beta}_3 p_2 + \frac{\tilde{\beta}_3(1-p_1-p_2)+\rho}{A_1}(1-h)(1-r_1)k\right).
\end{aligned} \tag{3.25}$$

Similarly, the components of the left eigenvectors of J_{β^*} (corresponding to the

zero eigenvalue), denoted by $V = (v_1, v_2, v_3, v_4, v_5, v_6)^T$, are given by,

$$
\begin{aligned}
&v_1 = 0, \quad v_2 = \frac{h(1-r_1)k}{A_1}v_3 + \frac{(1-h)(1-r_1)k}{A_1}v_4, \quad v_3 = v_3 > 0,\\
&v_4 = \frac{(\theta + \tilde{\beta}_3 p_1)A_1 + h(1-r_1)k(\rho + \tilde{\beta}_3(1-p_1-p_2))}{\tilde{\beta}_3((1-h)(1-r_1)k((1-p_1-p_2)+\rho) + p_2 A_1) + A_1 A_3}v_3 > 0,\\
&v_5 = \left((1-p_1-p_2)\frac{\beta_2}{A_4}\frac{h(1-r_1)k}{A_1} + \frac{\beta_2 p_1 N_0 + \delta}{A_4}\right)v_3 \\
&+ \left(\frac{\beta_2(1-p_1-p_2)}{A_4}\frac{(1-h)(1-r_1)k}{A_1} + \frac{\beta_2 p_2}{A_4}\right)v_4 > 0,\\
&\text{and} \quad v_6 = \frac{\gamma}{A_5}v_3 > 0
\end{aligned}
\tag{3.26}
$$

Computation of b: For the sign of b, it can be shown that the associated non-vanishing partial derivatives of f are

$$\frac{\partial^2 f_1}{\partial x_4 \partial \beta_3^*} = -N_0, \ \ \frac{\partial^2 f_2}{\partial x_4 \partial \beta_3^*} = (1-p_1-p_2)N_0, \ \ \frac{\partial^2 f_3}{\partial x_4 \partial \beta_3^*} = p_1 N_0, \ \ \frac{\partial^2 f_3}{\partial x_4 \partial \beta_3^*} = p_2 N_0$$

Substituting the respective partial derivatives into the expression

$$b = v_2 \sum_{i=1}^{6} u_i \frac{\partial^2 f_2}{\partial x_i \beta^*} + v_3 \sum_{i=1}^{6} u_i \frac{\partial^2 f_3}{\partial x_i \beta^*} + v_4 \sum_{i=1}^{6} u_i \frac{\partial^2 f_4}{\partial x_i \beta^*},$$

gives

$$b = u_4 N_0(v_2(1-p_1-p_2) + v_3 p_1 + v_4 p_2) > 0. \tag{3.27}$$

Computation of a: For the system (3.24), the associated non-zero partial derivatives of f (at the DFE Q_0) are given by

$$
\begin{aligned}
&\frac{\partial^2 f_1}{\partial x_3 \partial x_1} = -\frac{\beta_1}{N_0^2}, \ \ \frac{\partial^2 f_1}{\partial x_4 \partial x_1} = -\beta_3, \ \ \frac{\partial^2 f_1}{\partial x_5 \partial x_1} = -\frac{\beta_2}{N_0^2},\\
&\frac{\partial^2 f_2}{\partial x_3 \partial x_2} = -(1-p_1-p_2)\frac{\beta_1}{N_0}, \ \ \frac{\partial^2 f_2}{\partial x_5 \partial x_2} = -(1-p_1-p_2)\frac{\beta_2}{N_0},\\
&\frac{\partial^2 f_3}{\partial x_2 \partial x_3} = -p_1\frac{\beta_1}{N_0}, \ \ \frac{\partial^2 f_3}{\partial x_3^2} = -2p_1\frac{\beta_1}{N_0^2}, \ \ \frac{\partial^2 f_3}{\partial x_4 \partial x_3} = -p_1\frac{\beta_1}{N_0}, \ \ \frac{\partial^2 f_3}{\partial x_5 \partial x_3} = -(\beta_1+\beta_2)\frac{p_1}{N_0},\\
&\frac{\partial^2 f_3}{\partial x_6 \partial x_3} = -p_1\frac{\beta_1}{N_0}, \quad \frac{\partial^2 f_4}{\partial x_1 \partial x_4} = \beta_3 p_2, \ \ \frac{\partial^2 f_4}{\partial x_3 \partial x_4} = -\beta_1 p_2\frac{1}{N_0}, \ \ \frac{\partial^2 f_4}{\partial x_5 \partial x_4} = -\beta_2 p_2\frac{1}{N_0}
\end{aligned}
$$

Then, it follows that

$$\begin{aligned} a &= -2\left(v_2u_2(1-p_1-p_2)\frac{1}{N_0}(u_3\beta_1+u_5\beta_2)\right) \\ &- 2\left(v_3u_3p_1\frac{1}{N_0}\left[(u_2+\frac{u_3}{N_0}+u_4+u_5+u_6)\beta_1+\beta_2u_5\right]\right) \\ &- 2v_4u_4p_2\left[-u_1\beta_3+\beta_1u_3+\beta_2u_5\right]; \end{aligned}$$

so that the bifurcation coefficient $a < 0$ since $u_1 < 0$. Thus, we have $a < 0$ and $b > 0$. All conditions of Theorem 3.3.2 are satisfied and it should be noted that we use β_3^* as the bifurcation parameter, in place of ϕ in Theorem 3.3.2). Thus, it follows that the endemic equilibrium is locally asymptotically stable.

Figure 3.4 shows time series of (S) susceptible individuals, (E) latently infected individuals, (I) diagnosed infectious, (J) undiagnosed infectious, (L) lost sight and (R) recovered individuals using various initial values when all parameters are defined as in Table 2.2 and $\beta_3 = 1.2633563E^{-06}$ (so that $\mathcal{R}_0 = 1.6079$). In figure 3.4, we used various initial states to see numerically the impact of varying initial values on the stability of the endemic equilibrium. The results obtained illustrate the local stability of the endemic equilibrium as presented in Theorem 3.3.2. The backward bifurcation appears when there is coexistence of a disease free equilibrium and an endemic equilibrium when $\mathcal{R}_0$ is less than unity. Analysis of the backward bifurcation shows that with data from Cameroon, as estimated in the previous chapter, there is not backward bifurcation. Through numerical analysis, we have also observed that reach a disease free equilibrium, will take more decades than meet the endemic equilibrium point, because some latently infected individuals might not develop the disease over their life time.

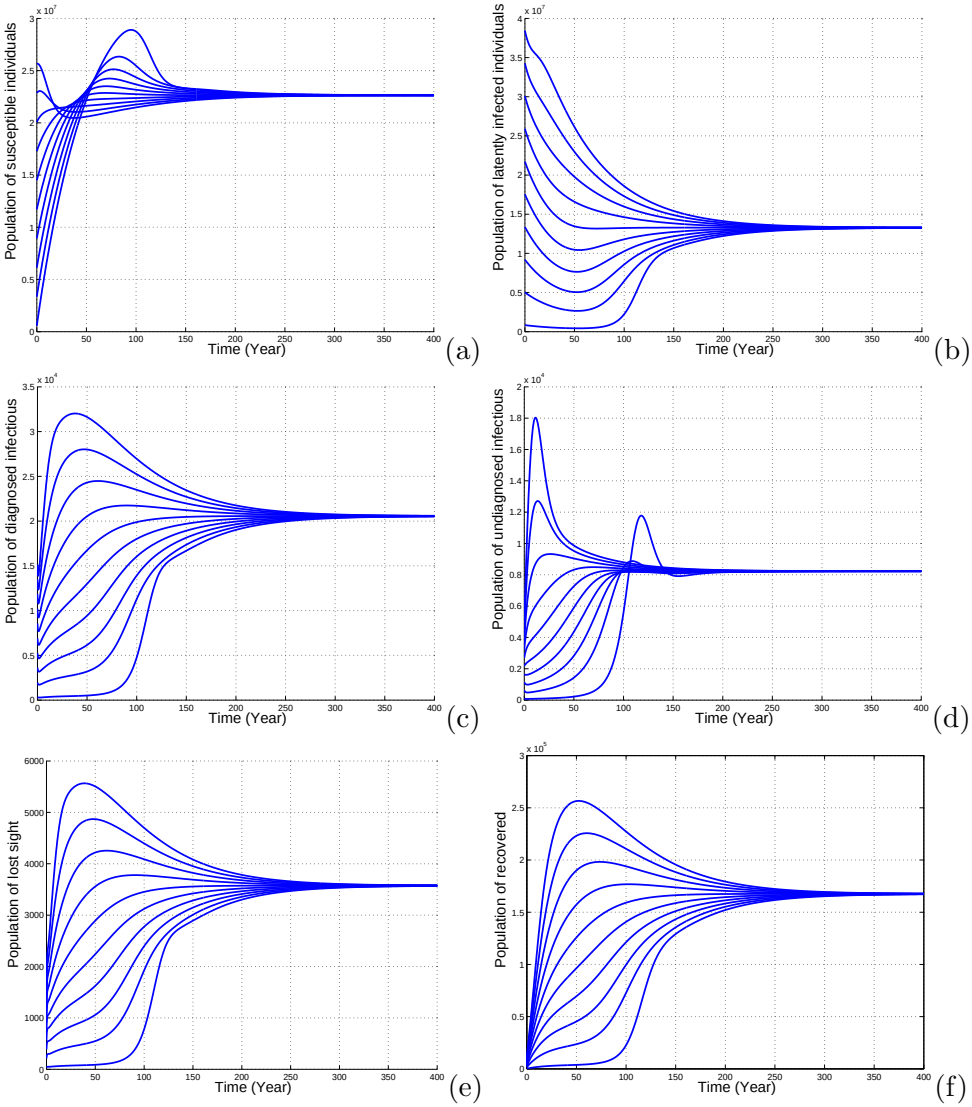

Figure 3.4: Time series of model system (2.2) presenting the local stability of the endemic equilibrium for various initial conditions when $\beta_3 = 1.2633563 \times 10^{-06}$, $\sigma_1 = \sigma_2 = 0$ (so that $\mathcal{R}_0 = 1.6079$).

Chapter 4

Impact of Education

Despite the development of many effective treatments over the past half century, TB remains one of the most destructive diseases. Identifying strategies of fighting TB abides a global task which involves all levels of government and public health officials around the world.

Mathematical analysis can provide valuable information about how to control infectious disease outbreaks best. One issue of really practical concern, for which mathematical modelling may provide promising insights, is in determining the best distribution of limited resources during an outbreak. Commonly, in preparation for an outbreak, a fixed amount of vaccine and other drugs are stockpiled, besides the allocation of a certain amount of funds for other control measures such as isolation, quarantine or education. Once the epidemic starts, the goal is then to optimally administer these resources given that their supply is limited.

Some past models of TB have discussed control of the disease by looking at the role of disease transmission parameters for time dependent control strategies. The time dependent control strategies have been applied for the studies of HIV models [74, 102], two strain tuberculosis models (see [96]), a TB model with lost sight class to reduce the rate by what people become lost sight [69], and SARS model with quarantine (cf. [172]). Some authors (see [83, 128]) discussed the optimal control on a model with reinfection. A tuberculosis model which incorporates treatment of infectives and chemoprophylaxis is considered together with time dependent optimal controls on treatment, chemoprophylaxis and disease relapses are incorporated to reduce the latently infected and actively infected individual populations (cf. [2]). In their recent article, Silva and Torres [150] studied the time optimal way to fight TB in Angola. Approaches of studying control strategies produce valuable theoretical results which suggest or design epidemic control programs. Depending on a chosen

goal, various objective criteria may be adopted.

As we studied in the previous chapters the key role of undiagnosed infectious and lost sight infectious populations on the disease transmission, our goal here is to minimize the number of people who are undiagnosed infectious, lost sight, thus also the number of people who die due to the infection. The number of TB new-cases, even if the success rate of treatment remains the same will decrease implicitly. In this chapter, we find out the optimal way to minimize the cost of TB on the model, calibrated with Cameroonian parameters. By cost of TB, one means the expenses needed by the government to fight TB compared to expenses of the government without strategy of fight TB when it remains a public health problem. Two control strategies will therefore be studied. The first one consists of education of the population about TB symptoms and large scale diagnosis campaigns. Through education, one can reduce the number of undiagnosed infectious people inside the population. Using the combined effect of education and free of charge treatment, one can first reduce the number of people infected in the population, make return people who have forsaken the treatment to the hospital and accelerate the detection of infected people who would stay to be treated naturally or through self-medication and traditional medicine. A proportion of them will die without good treatment. According to FAO, less than 73% of the Cameroonian population goes to the hospital after first disease symptoms. Because of the inaccessibility of certain regions of the country, access to health facilities is often difficult. Besides treatment facilities, some rural and even urban population prefer sometimes to use traditional medicine or self-medication for which the efficiency has not been established yet for TB. An increase in the treatment access should help to reduce the lost sight and undiagnosed classes. The immediate consequence will be a reduction in the number of infectious and then, on the number of diagnosed infectious.

The second TB control approach is the chemoprophylaxis treatment. According to the National Committee of Fight against TB (NCFT), the chemoprophylaxis is not practiced in Cameroon. The number of latently infected individuals that may develop an active TB will decrease if the chemoprophylaxis is practiced. We will see the impact of both strategies on the dynamics of TB. We intend to determine optimal control strategies that minimize not only undiagnosed infectious but also lost-sight and diagnosed infectious individuals which are the source of TB spread. We completely characterize the optimal controls and compute a numerical solution of the optimality system via analytic continuation.

4.1 Economic impact of tuberculosis

Adult mortality has a significant effect on national economies, through both the direct loss of productivity among those of working age and by altering fertility, incentives for risk-taking behavior, and investment in human and physical capital [110]. TB is the most important cause of adult death due to infectious disease after HIV/AIDS. TB has its greatest impact on adults between the ages of 15 and 59 [130]. So, the social and economic burden of TB is great because the most economically productive persons in society, parents on whom development and survival of children depend, are affected. TB places an extraordinary burden on those afflicted by the disease, their families, communities and on government budgets. In fact, the greatest burden of TB falls on productive adults who, once infected, are weakened and often unable to work. The burden of taking care of sick individuals usually falls to other family members and, besides putting them at greater risk of infection, can lower their productivity [110]. Diagnosed individuals with TB are often medically quarantined for a period of time, which can affect their financial well-being. The infected population have an economic impact on their families and in turn their countries' national economies through their inability to contribute financially, as they are often unable to be productive workers. Along with loss of productivity, the TB treatment charge can be significant. Average household spending on TB can account for as much as $8 - 20$ percent of annual household income, varying by region [66, 147].

Tuberculosis is most prevalent in developing nations and often coincides with malaria prevalence and HIV/AIDS. As an opportunistic disease, TB easily seats itself in carriers with weakened immune systems. These correlations of infection translate into weaker economic systems for those countries with a dense population of infected individuals. Taking into account some national characteristics Grimard and Harling [79] found that countries with a lower TB burden grew faster than those which were more heavily afflicted. Although tests of robustness suggest that some of this effect may be due to reverse causality, there remains a persistent effect of between 0.2 and 0.4 percent lower growth for every 10 percent higher incidence of tuberculosis. This corresponds to an annual loss of between US$ 1.4 and 2.8 billion in economic growth worldwide.

Few studies have looked at gender differentials in duration of incapacity from tuberculosis, quality of care given to TB patients, or the impact of tuberculosis on domestic work, social activities and personal life [90]. The economical influence of mortality of the population in their most productive age have been focused in some publication.

Yamano and Jayne (see [171]) found that an adult death and associated funeral expenses reduce purchases of agricultural inputs, such as farm animals and fertilizer,

and jeopardize agricultural production. Larson et al. [107] carried out a study of the effects of adult mortality on small farmers engaged in cotton and maize production in Zambia and found that an adult death resulted in a decline in crop output of roughly 15 percent. In addition, some other studies found that the effect of adult mortality is greatest on households that were relatively poor, in part because they are less able to cope with unanticipated events [11]. Besides these studies, some others have shown that adult mortality has a deterrent effect on the acquisition of human capital (cf. [97]). Individuals may be less willing to get a higher education or make investments that pay off in the longer term, especially those that cannot be transferred to future generations in the same way as financial investments, if there is a greater risk that they may not be around to enjoy the returns of that investment (see, [110]).

4.2 Modelling intervention methods

TB is spread through the air from an infectious person to a susceptible person. Two kinds of tests are used to determine if a person has been infected with TB bacteria: the tuberculin skin test and TB blood analysis. A positive TB skin test or TB blood test only tells that a person has been infected with TB bacteria and does not tell whether the person has latent TB infection or has progressed to TB disease [127]. Other tests, such as a chest X-ray and a sample of sputum, are needed to see whether the person has TB disease. Several TB treatment and prevention options are carried out in some rural and urban hospitals in Cameroon. Thus, the treatment of mild infections, classified as latent infections in our model, is not effective in Cameroon. On the other hand, infective individuals classed as infectious in our model, require a hard treatment of six months in the hospital. As preventive measures, population can be diagnosed, and latent TB infections can be treated to reduce the bacterial load in their body. This approach largely truncates the risk that TB infection will progress to TB disease. Certain groups are at very high risk of developing TB disease once infected. Every effort should be made to begin appropriate treatment and to ensure completion of the entire course of treatment for latent TB infection (cf. [127]). Controls are represented as functions of time and assigned reasonable upper and lower bounds. First, $u(t)$ represents the effort on education which allows people to go to the hospital, to be diagnosed fast and treated from the disease (to reduce the number of individuals that may be undiagnosed infectious). Second, $v(t)$ measures the rate of treatment of TB latent infections in each time period. The whole model flow diagram with control is shown in Figure 4.1.

The flow diagram Figure 4.1 yields the following differential equations: Using the same parameter and class names as in the model (2.2), we suggested the following

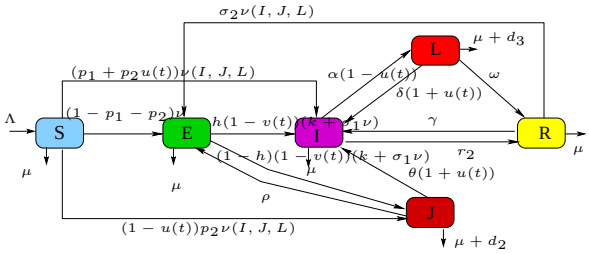

Figure 4.1: Transfer diagram for a transmission dynamics of tuberculosis.

ODEs system (4.1) describing the model with controls.

$$\begin{cases} \dot{S} &= \Lambda - \nu(I,J,L)S - \mu S, \\ \dot{E} &= (1-p_1-p_2)\nu(I,J,L)S + \rho J + \sigma_2\nu(I,J,L)R \\ &- \sigma_1(1-r_1-v(t))\nu(I,J,L)E - A_1E, \\ \dot{I} &= (p_1+p_2u(t))\nu(I,J,L)S + (1+u(t))\delta L + (1+u(t))\theta J + \gamma R \\ &+ h(1-r_1-v(t))(k+\sigma_1\lambda_T)E - A_2(t)I, \\ \dot{J} &= p_2(1-u(t))\nu(I,J,L)S + (1-h)(1-r_1-v(t))(k+\sigma_1\lambda_T)E - A_3J, \\ \dot{L} &= \alpha(1-u(t))I - A_4L, \\ \dot{R} &= r_2I + \omega L - \sigma_2\nu(I,J,L)R - A_5R, \end{cases} \tag{4.1}$$

where

$$A_1(t) = \mu + k(1-r_1-v(t)), \quad A_2 = \mu + d_1 + r_2 + \alpha(1-u(t)),$$

$$A_3(t) = \mu + d_2 + \theta(1+u(t)) + \rho, \quad A_4 = \mu + d_3 + \delta(1+u(t)) \text{ and } A_5 = \gamma + \mu.$$

subject to the initial conditions

$$S(0) = S_0, \quad E(0) = E_0, \quad I(0) = I_0, \quad J(0) = J_0, \quad L(0) = L_0 \quad R(0) = R_0. \tag{4.2}$$

The control functions $u(t)$ and $v(t)$ have to be bounded and *Lebesgue* integrable functions. $u(t)$ represents supplementary time dependent efforts of education campaigns, applied during a time interval $[0,T]$ to the whole population. The control function $v(t)$ measures the time dependent efforts on the preventive treatment of latently infected individuals to reduce the number of individuals that may be infectious. This control will have an impact on the output flow of people from the

latently infected class to infectious classes. The coefficient $1 - u(t)$ is a decreasing factor for fast route flow to undiagnosed as result of education. This factor aims to reduce the number of people becoming fast undiagnosed infectious and developing cavitation. The coefficient $v(t)$ represents the effort that prevents the inflow to the undiagnosed infectious classes to reduce the number of undiagnosed individuals developing cavitation. Our control problem involves the number of individuals with latent and active tuberculosis infections and the cost of applying chemoprophylaxis education and treatment controls $u(t)$ and $v(t)$ to be minimized subject to the differential Eqs. (4.1).

Note that in equation (4.1) the control $u(t)$ moves infectious individuals from classes J and L to class I and decreases the evolution to J and L classes. However, the control $v(t)$ reduces the progression rate from the latently infected class to the infectious classes. Since treatment effectively decreases the number of infectious individuals in the population, the control functions may provide a model of the impact of education and chemoprophylaxis in addition to medical treatments of TB.

4.3 Analysis of the optimal control problem

A successful TB mitigation strategy is one which reduces TB-related deaths with minimal cost. This performance specification involves the numbers of individuals with latent and active infections respectively, as well as the cost for applying education control (u) and chemoprophylaxis control (v) in individuals with tuberculosis. Thus, our goal is to solve the following problem: *given initial population sizes of all six classes, S_0, E_0, I_0, J_0, L_0 and R_0 find the best strategy in terms of efforts of education or chemoprophylaxis or both, that would minimize the number of people who die from the infection while at the same time minimizing the cost of the strategy.* There are various ways of expressing such a goal mathematically.

Formulation

In this work, for a fixed terminal time T, we consider the following objective. Thus, we seek to minimize the objective functional

Parameters	Value	Source
B_1	3000.00 USD per human death	[121]
B_2	563.00 USD per person treatment	[78]
C_1	200000 USD per proportion of effort to educated people	Assumed
C_2	200000 USD per logarithmic of the proportion of people to educate	Assumed
D_1	250000 USD per proportion of people treated by chemoprophylaxis	Assumed
D_2	250000 USD per logarithmic of level of chemoprophylaxis to implement	Assumed
D_3	5 per unity of distance between $y(T)$ and E_0	Assumed

Table 4.1: Numerical values for the cost functional parameters.

$$\begin{aligned} J(u,v) &= \int_0^T \{B_1(d_1 I(t) + d_2 J(t) + d_3 L(t)) + B_2 I(t) + C_1 u(t) + D_1 v(t) \\ &- C_2 \log(1-u(t)) - D_2 \log(1-v(t))\} dt + D_3 \|y_1(T) - y^*\|_2^2. \end{aligned} \tag{4.3}$$

The constants $B_1,\ B_2,\ C_1,\ C_2,\ D_1,\ D_2$ and D_3 have dual roles.On one hand, they are adjusting coefficients converting the dimension from population number into cost (in dollars) expended over a finite time period of T years. For the number of infectious individuals from the model (4.1) are more than hundreds, while u and v will necessarily lie between 0 and 1, in numerical simulations these constants are used to place stronger importance on the parameters involving the educational and chemoprophylaxis efforts. The first sum, multiplied by B_1 is the cost of a death due to TB. The expression multiplied by B_2 represents the treatment cost for diagnosed infectious. The expressions multiplied by C_1, C_2, D_1 and D_2 are the costs of implementation of both controls. In the objective functional, we intend to minimize also the distance between values at time T of infective classes and the DFE. D_3 is therefore a coefficient which aims to estimate the cost of this supplementary operation, and the norm is the distance between the steady state and the value of infective classes at time T. $y_1(t) = (I(t), J(t), L(t))$ is defined as in the general form (2.3) and $y^* = (0, 0, 0)$. All other final values are supposed to be unrestricted. Parameter values and description are inventoried in Table 4.1.

Parameters values C_1, C_2, D_1 and D_2 are cost to apply a strategy on the whole population. It has to be proportional to the total population when parameters B_1 and B_2 are only the cost for one person person.

The logarithmic expressions of the controls are included to model the poten-

tially non-linear costs at high educational and chemoprophylaxis levels. (See also [95, 96, 148, 121]). Education about TB, diagnosis campaigns and chemoprophylaxis are viewed as a nonlinear function since the implementation of any public health intervention does not have a linear cost, but rather there are increasing costs with reaching higher fractions of the population. The logarithm is a concave nonlinear function and therefore is used for education and chemoprophylaxis controls. Since the proportion of educated people will hardly achieve 1, the cost function is presumed to go to infinity when u and v are close to 1. While including the logarithmic expression, the upper-bound is more needed for the control functions. The remaining term in our objective functional seeks to increase the expenses of education when most of the population has already been educated or received chemoprophylaxis. The motivation of the logarithm is the fact that in a practical point of view, it is not possible to reach 100% of the population educated. The set of admissible controls is defined as follows.

$$\Gamma = \left\{u, v \in L^1(0,T) | (u(t), v(t)) \in [0, u_m] \times [0, v_m] \ \ \forall t \in [0,T]\right\} \tag{4.4}$$

Thus, we seek an optimal control pair (u^*, v^*) such that

$$J(u^*, v^*) = \min_{\Gamma} J(u, v). \tag{4.5}$$

4.3.1 Existence of an optimal control solution

Let us consider an optimal control problem having the form

$$J(u,v) \ = \ \int_0^T g(t, y(t), u(t), v(t))dt + \|y(T) - y^*\| \longrightarrow \min_{(u,v)} \tag{4.6}$$

subject to

$$\begin{cases} \dot{y} = f(t, y(t), u(t), v(t)), \\ y(t_0) = y_0. \end{cases}$$

where $y = (S, E, I, J, L, R)$ and f is the right hand side of system (4.1). We analyze sufficient conditions for the existence of a solution to the optimal control problem (4.6).

Theorem 4.3.1. *There exists an optimal control pair $(u^*(t), v^*(t))$, and corresponding solution S^*, E^*, I^*, J^*, L^*, R^* to the state initial value problem (2.2) that minimizes $J(u, v)$ over Γ.*

Proof : We refer to the conditions in Theorem III.4.1 and its corresponding corollary in [75]. The requirements there on the set of admissible controls and on the set of end conditions presented in Theorem 1.4.2 are clearly met here. The following nontrivial requirements from Fleming and Rishel's theorem are listed and verified below:

A- The set of all solutions to system (4.1) with corresponding control functions in Γ (as given in equation (4.4)) is nonempty.

B- The state system can be written as a linear function of the control variables with coefficients dependent on time and the state variables.

C- The integrand g in equation (4.6) is convex with respect to parameters u and v and additionally fulfills

$$g(t, S, E, I, J, L, R, u, v) \geq c_1 \mid (u, v) \mid^{\tau} - c_2,$$

where $c_1 > 0$ and $\tau > 1$.

In order to establish condition A, we refer to Theorem 3.1 by Picard-Lindelöf (cf. [50, 54]). If the solutions of the state equations are a priori bounded and if the state equations are continuous and Lipschitz-continuous in the state variables, then there is a unique solution corresponding to every admissible control pair in Γ.

With the bounds in equation (2.5), it follows that the state system is continuous and bounded. It is also straightforward to show the boundedness of the partial derivatives with respect to the state variables in the state system, which establishes that the system is Lipschitz-continuous with respect to the state variables (see [49], page 248). This completes the proof, thus condition A holds.

Condition B is verified by observing the linear dependence of the state equations on controls u and v as presented in theorem 1.4.2.

Finally, to verify condition C we note that the integrand g of the objective functional is clearly convex in the controls. To prove the bound on g we note that by the definition of u and v, we have $C_1 u^2 \leq C_1 u \leq C_1$, and thus, $C_1 u^2 - C_1 \leq C_1 u - C_1 \leq 0$; therefore,

$$\begin{aligned} g(t, S, E, I, J, L, R, u, v) &= B_1(d_1 I(t) + d_2 J(t) + d_3 L(t)) + B_2 I(t) + C_1 u(t) + D_1 v(t) \\ &- C_2 \log(1 - u(t)) - D_2 \log(1 - v(t)) \\ &\geq \min(C_1, D_1)(u + v) - C_1 \\ &\geq \min(C_1, D_1)(u^2 + v^2) - C_1 \end{aligned}$$

This completes the proof. □

4.3.2 Characterization of optimal controls

Let us consider an optimal control problem having the form

$$J(u,v) = \int_0^T g(t,y(t),u(t),v(t))dt + \|y(T)-y^*\| \longrightarrow \min_{(u,v)} \quad (4.7)$$

subject to

$$\begin{cases} \dot{y} = f(t,y(t),u(t),v(t)), \\ y(t_0) = y_0, \end{cases}$$

and constraints

$$u(t) \geq 0,$$
$$v(t) \geq 0.$$

We apply Pontryagin's Maximum Principle [135] which enables us utilizing costate functions to transform the optimization problem to the problem of determining the pointwise minimum relative to u^* and v^* of the Hamiltonian. First, we build the Hamiltonian from the cost functional (4.3) and the controlling dynamics (4.1) to derive the optimality conditions.

$$\begin{aligned} &H(t,S,E,I,J,L,R,u,v) = B_1(d_1I(t)+d_2L(t)+d_3J(t)) + B_2I(t) + C_1u(t) \\ &-C_2\log(1-u(t)) + D_1v(t) - D_2\log(1-v(t)) + \lambda_1\left(\Lambda - \nu(I,J,L)S - \mu S\right) \\ &+\lambda_2\left((1-p_1-p_2)\nu(I,J,L)S + \rho J + \sigma_2\nu(I,J,L)R - \sigma_1(1-r_1-v(t))\nu(I,J,L)E - A_1E\right) \\ &+\lambda_3\left((p_1+p_2u(t))\nu(I,J,L)S + (1+u(t))\delta L + (1+u(t))\theta J + \gamma R\right) \\ &+\lambda_3\left(h(1-r_1-v(t))(k+\sigma_1\lambda_T)E - A_2(t)I\right) \\ &+\lambda_4\left(p_2(1-u(t))\nu(I,J,L)S + (1-h)(1-r_1-v(t))(k+\sigma_1\lambda_T)E - A_3J,\right) \\ &+\lambda_5\left(\alpha(1-u(t))I - A_4L\right) + \lambda_6\left(r_2I + \omega L - \sigma_2\nu(I,J,L)R - A_5R\right) \end{aligned} \quad (4.8)$$

where the λ_i, $i = 1,\cdots,6$ are the associated adjoints for the states $S,\ E,\ I,\ J,\ L$ and R. The optimality system of equations is found by taking the appropriate partial derivatives of the Hamiltonian (4.8) with respect to the associated state variable.

The following theorem follows from the maximum principle.

Theorem 4.3.2. *Given an optimal control pair (u^*,v^*) and corresponding solutions to the state system S^*, E^*, I^*, J^*, L^*, R^*, that minimize the objective functional*

(4.3), there exist adjoint variables λ_1, λ_2, λ_3, λ_4, λ_5, *and* λ_6, *satisfying*

$$\begin{aligned}
\frac{d\lambda_1}{dt} &= \mu\lambda_1 - \left((\beta_1 I + \beta_2 L)\frac{N-S}{N^2} + \beta_3 J\right) \\
&\times (-\lambda_1 + (1-p_1-p_2)\lambda_2 + (p_1 + p_2 u(t))\lambda_3 + p_2(1-u(t))\lambda_4) \qquad (4.9)\\
&+ (\beta_1 I + \beta_2 L)\frac{1}{N^2}\left[\sigma_1(1-r_1-v(t))E\left(-\lambda_2 + h\lambda_3 + (1-h)\lambda_4\right) + \sigma_2 R\left(\lambda_2 - \lambda_6\right)\right]
\end{aligned}$$

$$\begin{aligned}
\frac{d\lambda_2}{dt} &= (\beta_1 I + \beta_2 L)\frac{S}{N^2}(-\lambda_1 + (1-p_1-p_2)\lambda_2 + (p_1 + p_2 u(t))\lambda_3 + p_2(1-u(t))\lambda_4) \\
&+ (\beta_1 I + \beta_2 L)\frac{R}{N^2}\sigma_2(\lambda_2 - \lambda_6) + \mu\lambda_2 \qquad (4.10)\\
&- (1-r_1-v(t))\left[\left((\beta_1 I + \beta_2 L)\frac{N-E}{N^2} + \beta_3 J\right)\sigma_1 + k\right](-\lambda_2 + h\lambda_3 + (1-h)\lambda_4)
\end{aligned}$$

$$\begin{aligned}
\frac{d\lambda_3}{dt} &= -\left(S\frac{\beta_1 N - (\beta_1 I + \beta_2 L)}{N^2}\right)(-\lambda_1 + (1-p_1-p_2)\lambda_2 + (p_1 + p_2 u(t))\lambda_3 + p_2(1-u(t))\lambda_4) \\
&- \left(\frac{\beta_1 N - (\beta_1 I + \beta_2 L)}{N^2}\right)\left[\sigma_1(1-r_1-v(t))E\left(-\lambda_2 + h\lambda_3 + (1-h)\lambda_4\right) + \sigma_2 R\left(\lambda_2 - \lambda_6\right)\right] \\
&+ (\mu + d_1)\lambda_3 - r_2(\lambda_6 - \lambda_3) - \alpha(1-u)(\lambda_5 - \lambda_3) - B_1 d_1 - B_2 \qquad (4.11)
\end{aligned}$$

$$\begin{aligned}
\frac{d\lambda_4}{dt} &= -B_1 d_2 - R\left(-\frac{\beta_1 I + \beta_2 L}{N^2} + \beta_3\right)\sigma_2(\lambda_2 - \lambda_6) \qquad (4.12)\\
&- S\left(-\frac{(\beta_1 I + \beta_2 L)}{N^2} + \beta_3\right)(-\lambda_1 + (1-p_1-p_2)\lambda_2 + (p_1 + p_2 u(t))\lambda_3 + p_2(1-u(t))\lambda_4) \\
&- \left(\frac{-(\beta_1 I + \beta_2 L)}{N^2} + \beta_3\right)E\sigma_1(1-r_1-v(t))(-\lambda_2 + h\lambda_3 + (1-h)\lambda_4) \\
&- \rho(\lambda_2 - \lambda_4) + (\mu + d_2)\lambda_4 - \theta(1+u(t))(\lambda_3 - \lambda_4)
\end{aligned}$$

$$\begin{aligned}
\frac{d\lambda_5}{dt} &= -\left(S\frac{\beta_2 N - (\beta_1 I + \beta_2 L)}{N^2}\right)(-\lambda_1 + (1-p_1-p_2)\lambda_2 + (p_1 + p_2 u(t))\lambda_3 + p_2(1-u(t))\lambda_4) \\
&- \left(\frac{\beta_2 N - (\beta_1 I + \beta_2 L)}{N^2}\right)\left[\sigma_1(1-r_1-v(t))E\left(-\lambda_2 + h\lambda_3 + (1-h)\lambda_4\right) + \sigma_2 R\left(\lambda_2 - \lambda_6\right)\right] \\
&+ (\mu + d_3)\lambda_5 - \delta(1+u(t))(\lambda_3 - \lambda_5) - \omega(\lambda_6 - \lambda_5) - B_1 d_3 \qquad (4.13)
\end{aligned}$$

$$\begin{aligned}
\frac{d\lambda_6}{dt} &= \frac{S(\beta_1 I + \beta_2 L)}{N^2}(-\lambda_1 + (1-p_1-p_2)\lambda_2 + (p_1 + p_2 u(t))\lambda_3 + p_2(1-u(t))\lambda_4) \\
&- \left((\beta_1 I + \beta_2 L)\frac{N-R}{N^2} + \beta_3 J\right)\sigma_2(\lambda_2 - \lambda_6) + \mu\lambda_6 - \gamma(\lambda_3 - \lambda_6) \qquad (4.14)\\
&+ \frac{E(\beta_1 I + \beta_2 L)}{N^2}\sigma_1(1-r_1-v(t))(-\lambda_2 + h\lambda_3 + (1-h)\lambda_4)
\end{aligned}$$

with terminal conditions

$$\begin{aligned}&\lambda_1(T)=0,\ \ \lambda_2(T)=0,\ \ \lambda_3(T)=2D_3(I(T)-I_0),\\&\lambda_4(T)=2D_3(J(T)-J_0),\ \ \lambda_5(T)=2D_3(L(T)-L_0),\ \lambda_6(T)=0.\end{aligned}\tag{4.15}$$

Furthermore, we may characterize the optimal pair by the piecewise continuous functions

$$\begin{aligned}u^* &= \max\left(0,1+\frac{C_2}{C_1+(\nu(I,J,L)Sp_2+\theta J)(\lambda_3-\lambda_4)+(\delta L+\alpha I)(\lambda_3-\lambda_5)}\right),\\ v^* &= \max\left(0,1+\frac{D_2}{D_1-(\sigma_1\nu(I,J,L)+k)E(-\lambda_2+h\lambda_3+(1-h)\lambda_4)}\right).\end{aligned}\tag{4.16}$$

Proof : The result follows from a direct application of a version of Pontryagin's Maximum Principle for bounded controls (cf. [111]). The differential equations governing the adjoint variables are obtained by differentiation of the Hamiltonian function (4.8), evaluated at the optimal control. Then the adjoint system can be written as dictated by the Maximum Principle, by the equations

$$\begin{aligned}\frac{d\lambda_1}{dt} &= -\frac{\partial H}{\partial S},\ \ \lambda_1(T)=0, \quad \frac{d\lambda_2}{dt}=-\frac{\partial H}{\partial E},\ \ \lambda_2(T)=0,\\ \frac{d\lambda_3}{dt} &= -\frac{\partial H}{\partial I},\ \ \lambda_3(T)=2D_3(I(T)-I_0),\\ \frac{d\lambda_4}{dt} &= -\frac{\partial H}{\partial J},\ \ \lambda_4(T)=2D_3(J(T)-J_0),\\ \frac{d\lambda_5}{dt} &= -\frac{\partial H}{\partial L},\ \ \lambda_5(T)=2D_3(L(T)-L_0),\\ \frac{d\lambda_6}{dt} &= -\frac{\partial H}{\partial R},\ \ \lambda_6(T)=0,\end{aligned}$$

evaluated at the optimal control pair (u^*, v^*) and corresponding states. This results in the stated adjoint system (4.9)-(4.14).

Finally, the optimality conditions dictate that,

$$\frac{\partial H}{\partial u}=\frac{\partial H}{\partial v}=0,\tag{4.17}$$

for the optimal pair (u^*, v^*), on the interior of the control set, and this condition is simplified in equations (4.16) with special attention on control arguments involving the bounds on the controls as defined with Γ in equation (4.4).

Note that as a result of the terminal condition, the optimal education and treatment will not necessarily be zero at the end time. □

One observes that by the characterization of the controls given in (4.16), the controls are not necessarily time C^1. The optimality system is defined as the combination of the state equations (4.1), the initial conditions, the adjoint equations (4.9-4.14), and the terminal conditions, with the optimality equations (4.16) substituted into the state and adjoint equations.

A restriction on the length of the interval may guarantee the uniqueness of the optimality system. Next, we will discuss the numerical solutions of the optimality system and the corresponding best control pairs, the parameter choices, and the interpretations for various cases.

4.4 Numerical simulation of optimal controls

In this section, we study numerically an optimal educational and chemoprophylaxis treatment strategies of our TB model. The optimal educational and chemoprophylaxis strategies are obtained by solving the optimality system, consisting of 12 ODEs from the state and adjoint equations above. An iterative method is used for solving the optimality system. We start solving the state equations with a guess for the controls over the simulated time using a forward Runge-Kutta scheme. The state system with an initial guess is solved forward in time and then the adjoint system is solved backward by a backward Runge-Kutta scheme, using the the transversality conditions (1.31). Note that, since the model is not stiff, a number of numerical scheme for ODEs in the literature may solve forward as well as backward the optimality problem. From model (4.1), we generated the state values of different epidemiological classes for the year 2015 using data in Tables 2.2 and 4.1. The initial values are thus defined as $S_0 = 4950585$, $E_0 = 15594821$, $I_0 = 21392$, $J_0 = 13009$, $L_0 = 3723$, $R_0 = 139455$ and $N_0 = 20722985$. These initial population sizes will be used throughout the rest of this chapter. Throughout the iterations, a lower bound $u = 0$ will be keep for the control through a projection of u and v on the interval $[0, u_m] \times [0, v_m]$ where $u_m = v_m = 1$.

Step size. A good ODE integrator as well as a good optimal control update should exert some adaptive control over its own progress, making frequent changes in its step-size. Usually the purpose of this adaptive step-size control is to achieve some predetermined accuracy in the solution with minimum computational effort. Implementation of adaptive step-size control requires that the stepping algorithm return information about its performance, most important, an estimate of its truncation error. Obviously, the calculation of this information will add to the computational overhead, but the investment will generally be repaid. In this work, an adaptive step-size implemented in the software `Dopri5` will be used to solve forward

the states equations and backward the adjoint equations. The control at the end of each iteration have been chosen to be updated through a convex combination $u^k = \frac{(u^{k-1}+u^*)}{2}$ of the previous control u^{k-1} and the value from the characterizations u^* in equation (4.16). The same type of convex combination is used for the second control function v update ($v^k = \frac{(v^{k-1}+v^*)}{2}$). This convex combination have been used several time in the literature to implement the FBSM [114, 111]. This choice does not make the program faster, but it have been made because the convergence to the optimal solution for this model, happened fast (after less than 2 minutes of computation). For the control update presented above, it is possible to include an adaptive step-size. However, for the sake of simplicity and and because the convergence of the FBSM is relatively fast, we chose a fixed control update. However, time points chosen by adaptive step-size control generally do not agree with discretization points of the controls. This problem make the accuracy very fragile. To solve, we use an integrator with dense output. It constructs an interpolation polynomial based on the available solution such that accuracy is not destroyed. `Dopri5` includes a dense output.

Stopping criteria. The optimal control iterations continue until convergence is achieved. Convergence is achieved when the relative errors between all of the state variables, the adjoint functions or the control functions are less than a defined value δ. One should have

$$\min_i \frac{\|x_i^k - x_i^{k-1}\|}{\|x_i^k\|} < \delta$$

where x_i is either a state variable, the adjoint function or the control. The value $\delta = 0.0001$ will be considered in this numerical simulation.

In the following Paragraph, the optimal educational schedule will be first determined, then the chemoprophylaxis only will be simulated, a numerical schedule for both strategies will be computed, and finally, the sensitivity of the optimal control will be analyzed with respect to some model and cost functional parameters. Parameter values are defined in Table 2.2 and data in Table 4.1 will be divided by 10000 in order to have good values for the adjoint Hamiltonian.

4.4.1 Optimal educational strategy

Let us first focus on the optimal educational strategy for the population of Cameroon. We performed numerical simulations using the FBSM, $D_1 = D_2 = 0$ without v.

Then, the optimal control problem is defined by

$$
\begin{aligned}
J(u,v) &= \int_0^T g(t,y(t),u(t))dt + \|y(T) - y^*\| \longrightarrow \min_u \qquad (4.18)\\
&\text{subject to}\\
&\begin{cases} \dot{y} = f(t,y(t),u(t)), \\ y(t_0) = y_0. \end{cases}
\end{aligned}
$$

where $y = (S, E, I, J, L, R)$,

$$g(t,y,u) = B_1(d_1 I(t) + d_2 J(t) + d_3 L(t)) + B_2 I(t) + C_1 u(t) - C_2 \log(1 - u(t))$$

and f the right hand side of system (4.1).

Graphs in Figure 4.2 show a time optimal educational schedule for $T = 10$ years. In that Figure (S), (E), (I), (J), and (R) stand for susceptible, latently infected, diagnosed infectious, undiagnosed infectious, lost sight and recovered population when (u) is the effort in educating the population. It appears that the disease burden will indeed decrease due to the influence of education u. A closer look on Figure 4.2 (J), (E) and (L) reveals that the number of undiagnosed infectious, latently infected and lost sight will plummet as soon as the education campaign will be applied. Obviously, education strategy only can help to reduce the the number of undiagnosed infectious (J), lost sight (L), and latently infected (E) in 10 years.

Figure 4.2 (I) reveals an increase of the number of diagnosed infectious (I) for one year as result of the campaign. After one year, the number of undiagnosed infectious will drop and be less than the expected number after 3 years for an effort of 95% in education. As a result of the decrease of the number of infectious, the susceptible population will increase and the recovered population will decrease (Figure 4.2 (S) and (R)) . The control function in Figure 4.2 (u) is continuous and decreasing with respect to time.

Figure 4.3 illustrates the convergence of the FBSM throughout the iterations when only education is applied in the population. From the Figure, one can see that at the end of the iterations, the norm of the Hamiltonian's gradient goes very close to 0.

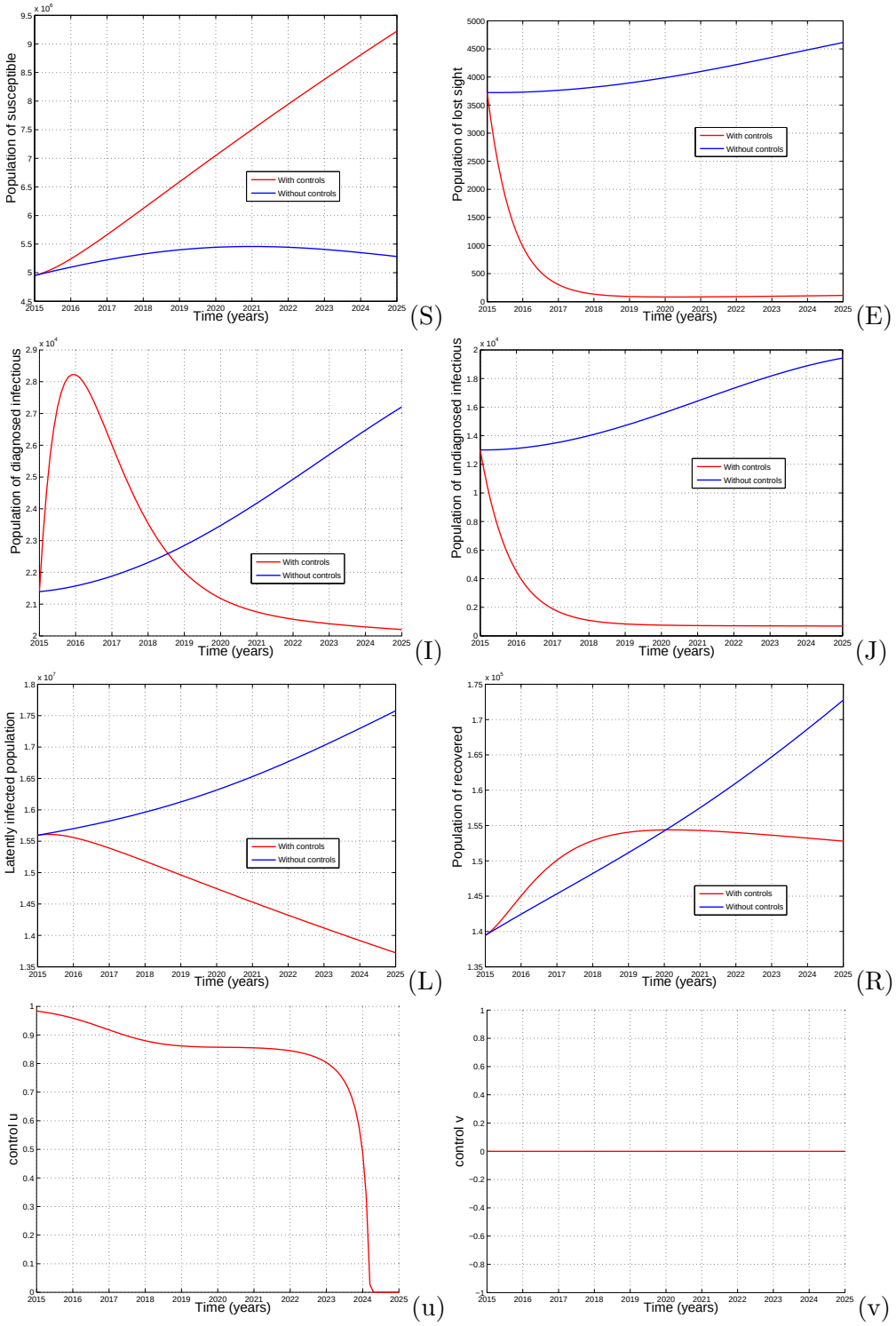

Figure 4.2: Simulations of the TB model (4.1) showing the effect of optimal educational and treatment rates against constant chemoprophylaxis and treatment rates on the infected population. In this Figure (S), (E), (I), (J), and (R) stand for susceptible, latently infected, diagnosed infectious, undiagnosed infectious, lost sight and recovered population when (u) is the effort in educating the population.

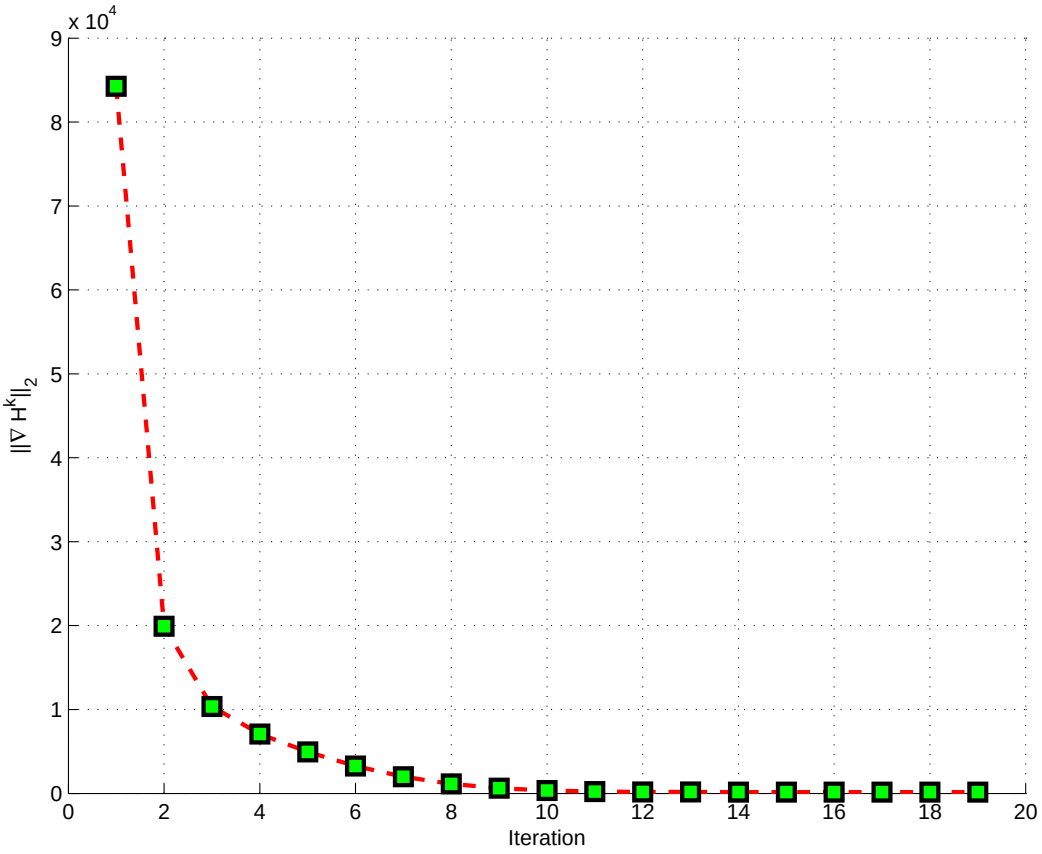

Figure 4.3: Evolution of the norm of the Hamiltonian's gradient throughout iterations corresponding to the educational only optimal strategy.

4.4.2 Optimal chemoprophylaxis strategy

In this Section, we consider the case where only chemoprophylaxis strategy is carried out on the population, without any educational strategy. Numerical simulations of the optimality problem have been performed to find the optimal chemoprophylaxis schedule when there is not upper-bound for control functions In fact, the upper-bound is regulated by the logarithm included in the objective functional. In Figure 4.2, model parameters are defined as in Table 2.2. We set $C_1 = C_2 = 0$ and we set $u = 0$ in system 4.1. The corresponding cost function is defined by

$$\begin{aligned} J_v(v) &= \int_0^T \{B_1(d_1 I(t) + d_2 J(t) + d_3 L(t)) + B_2 I(t) + D_1 v(t) - D_2 \log(1 - v(t))\} dt \\ &+ D_3 \|y(T) - y^*\|^2. \end{aligned} \tag{4.19}$$

Figure 4.4 presents the numerical results of a chemoprophylaxis optimal control on the dynamics of tuberculosis in $T = 10$ years.

Figure 4.4, reveals that the population of infectious will drop for five years, but then, increase again. The reverse effect will be observed for the susceptible population. It increases for five years, then decreases again. The results in Figure 4.4 reveal that chemoprophylaxis of latently infected population will delay the propagation of TB, but cannot eradicate the disease. The chemoprophylaxis strategy will downgrade the number of infected population by more than 30 percent during the 10 years of optimal control. The fact is that chemoprophylaxis does not refine the contact between infectious and susceptible population, but only minimizes the evolution to the disease for the latently infected population. In the presence of fast progression, this strategy obviously can not lead to a satisfactory way for reducing TB if applied without further efforts.

Similarly to Figure 4.3, an analysis of the Hamiltonian can reveal the convergence of the FBSM. This analysis can be performed in a similar way to Figure 4.3, to illustrate how the norm of the Hamiltonian's gradient goes to 0 with respect to iterations.

4.4.3 Optimal education and chemoprophylaxis

Let us find now the optimal schedule for both education and chemoprophylaxis on the population using data from Cameroon. In this case, we use parameter values of Table 4.1. For the Figures presented here, we assume that the weight factor C_1 associated with control u is smaller than D_1 which is associated with control v. This assumption is based on following facts: the cost associated with chemoprophylaxis v will include the cost of screening and treatment programs, and the cost associated with u including those of educating people about the TB diagnosis in the hospital or sending people to watch the patients to finish their treatment. Treating an infectious TB individual takes longer (by several months) than treating a latent TB individual [96]. In the subsequent, we used the objective functional

$$\begin{aligned} J_1(u,v) &= \int_0^T \{B_1(d_1 I(t) + d_2 J(t) + d_3 L(t)) + B_2 I(t)\}dt + D_3\|y(T) - y^*\|^2 \\ &+ \int_0^T C_1 u(t) - C_2 \log(1-u(t)) + D_1 v(t) - D_2 \log(1-v(t)). \end{aligned} \tag{4.20}$$

One can generate several educational and diagnosed schedules for various time periods. In Figure 4.5, we illustrate a case for a $T = 10$-years treatment schedule.

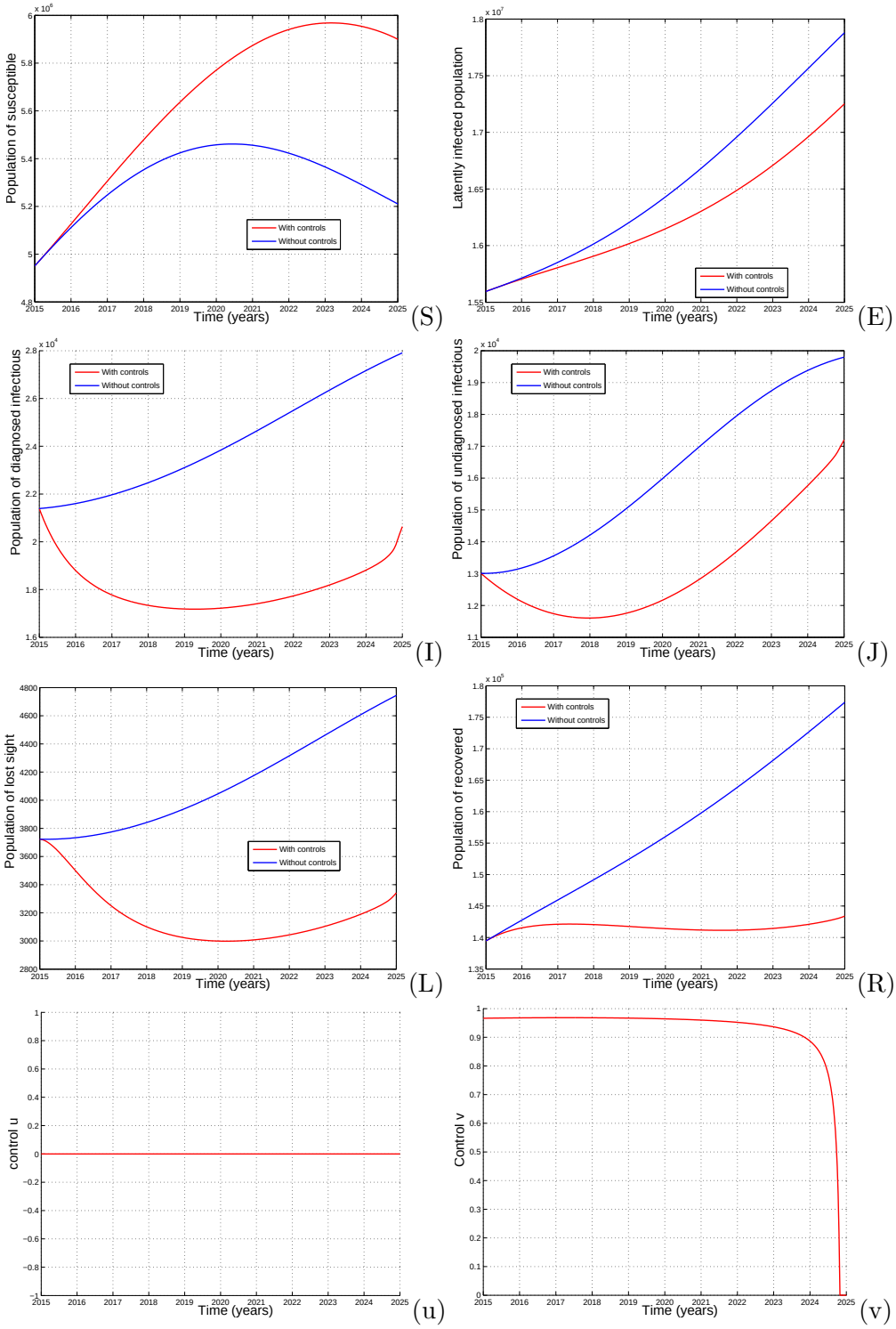

Figure 4.4: Simulations of the TB model (4.1) showing the effect of optimal chemoprophylaxis and treatment rates against constant education and treatment rates on the infected population. In this Figure (S), (E), (I), (J), and (R) stand for susceptible, latently infected, diagnosed infectious, undiagnosed infectious, lost sight and recovered population when (v) is the time dependent effort in chemoprophylaxis.

In this Figure (S), (E), (I), (J), and (R) stand for susceptible, latently infected, diagnosed infectious, undiagnosed infectious, lost sight and recovered population and (v) is the time dependent effort in chemoprophylaxis. To minimize the total number of TB induced death, the optimal control u decreases during the $T = 10$ years and v is also decreasing from the upper bound, while the steadily decreasing value for u is applied over the most of the simulated time, $T = 10$ years. The initial conditions used in this case are extracted from numerical simulations of the model corresponding to year 2015. We can also observe that the model controls are not differentiable in some points. Combining chemoprophylaxis and education, the burden of TB can obviously be reduced by 80% in 10 years

The convergence of the FBSM throughout the iterations when both control strategies are applied have been checked through the Hamiltonian gradient's norm. As in Figure 4.3, one have observed that at the end of the iterations, the norm of the Hamiltonian's gradient goes is closed to 0. The program stopped after 22 iterations when both control are applied.

4.4.4 Analysis of the optimal control

Impact of the objective functional parameters. The sensitivity of the optimal control with respect to constants such as C_1, C_2, D_1 and D_2 is a well known and recurrent question. In this Paragraph, we compute the optimal control solutions for several values of C_1, C_2, D_1, and D_2. Figures 4.6 and 4.6 illustrates how the optimal control strategies depend on the parameter C_1, C_2, D_1, and D_2, which are the coefficients of the logarithmic and the linear part of the objective functional defined in equation (4.20). Coefficients D_1, and D_2 show the influence of the logarithmic non-linear term on other control parameters. These parameters values may vary from place to place depending on many factors including living conditions, culture and amount of money available for the control. In Figure 4.8 the controls u and v are plotted as a function of time for the 6 different values of $C_1 = C_2 \in \{1, 21, 41, 61, 81, 101\}$ and $D_1 = D_2 \in \{1, 21, 41, 61, 81, 101\}$. Other parameters are presented in Tables 2.2 and 4.1. Figure 4.6 and 4.7 shows that the coefficients play a decreasing role on the control while states values remains almost the same as $C_1 = C_2 = D_1 = D_2$ increases. The values $C_1 = C_2$ and $D_1 = D_2$ have been chosen to express the particular case where the amount of money for educational and chemoprophylaxis campaigns are available in different proportion. Other situations may be computed in the same way.

Figure 4.8 illustrates the convergence of the FBSM throughout the iterations. One can see that at the end of the iterations, the norm of the Hamiltonian's gradient is very close to 0. It comes that that the Hamiltonian is close the minimum. From Figure 4.8 , it can also be seen that the number of iteration to reach the optimal

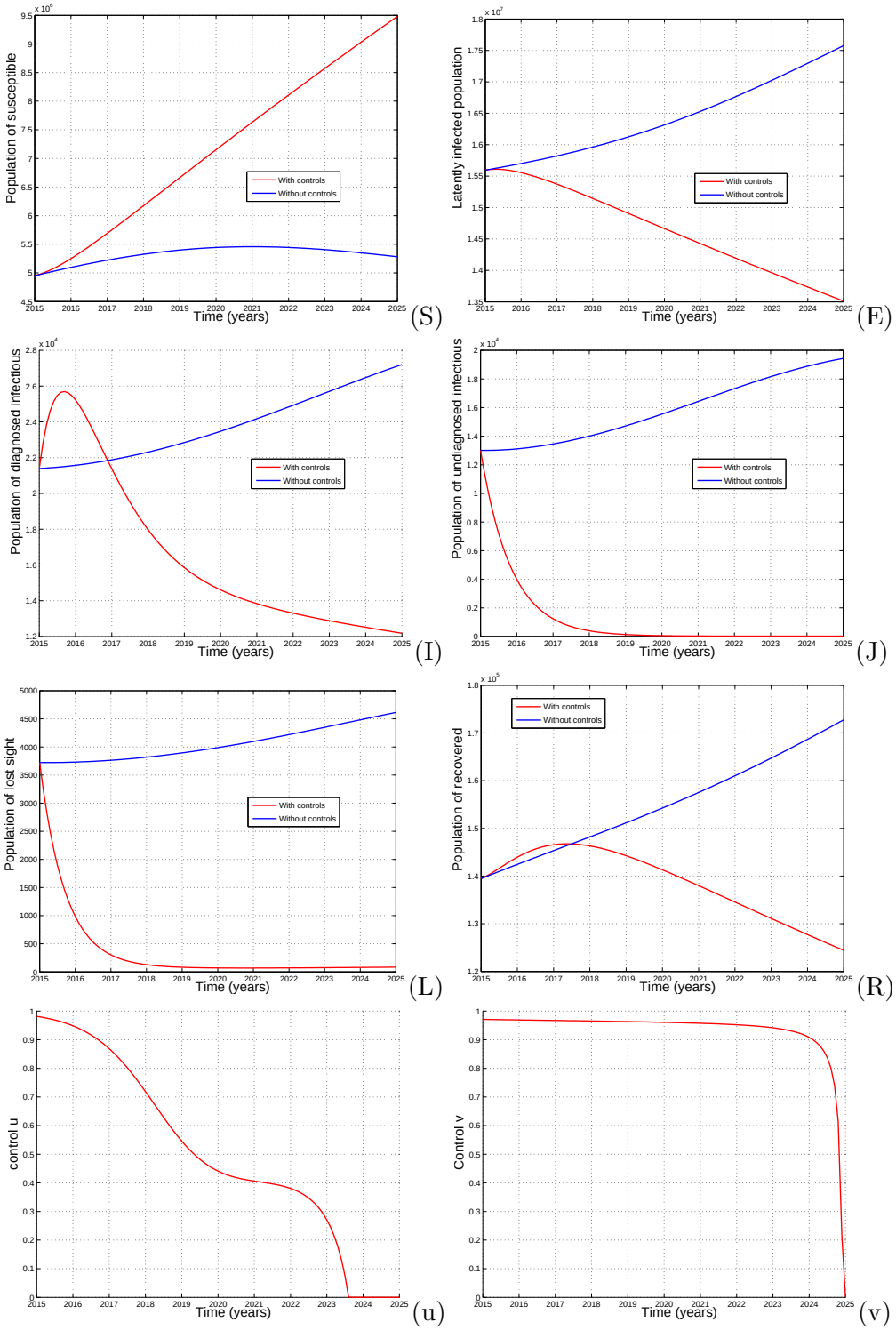

Figure 4.5: Time series of model (4.1) result from optimal education and chemoprophylaxis strategies, blue lines, compared with that of no education and chemoprophylaxis control strategies (red lines). Susceptible (S), latently infected (E), diagnosed infectives (I), undiagnosed infectives (J), lost sight (L) and recovered (R) are pictured. Without education and chemoprophylaxis, the number of infectious increases little and the number of susceptible decreases little. In the presence of education and chemoprophylaxis, the opposite effect is observed.

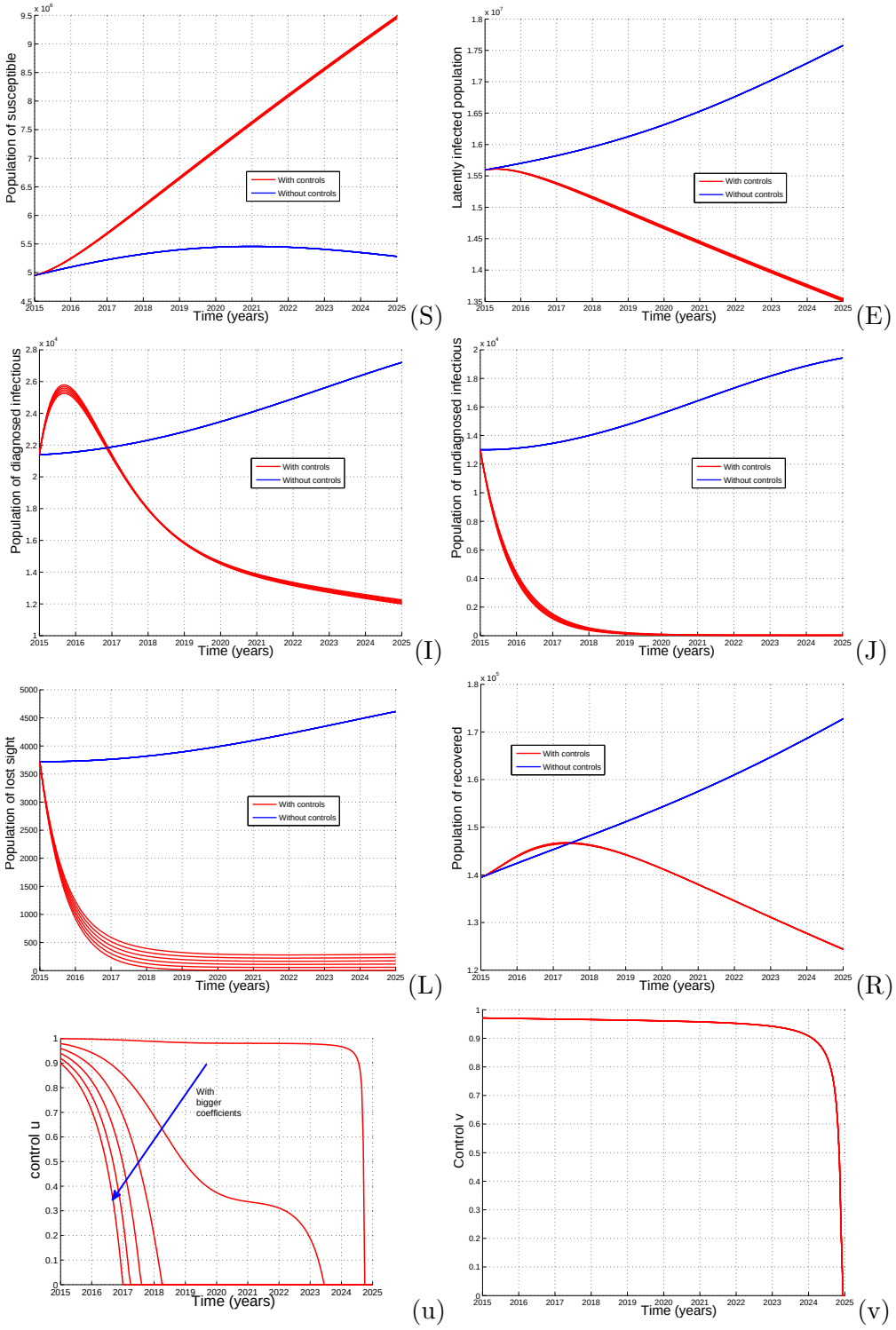

Figure 4.6: Evolution of model (4.1) result from optimal education and chemoprophylaxis strategies, blue lines, compared with that of no education and chemoprophylaxis control strategies (red lines). Susceptible (S), latently infected (E), diagnosed infectives (I), undiagnosed infectives (J), lost sight (L) and recovered (R) are pictured for $C_1 = C_2 \in \{1, 11, 21, 31, 41, 51, 61, 71, 81, 91\}$. Other parameters are presented in Tables 2.2 and 4.1. One observed a large change on v and v with the constants.

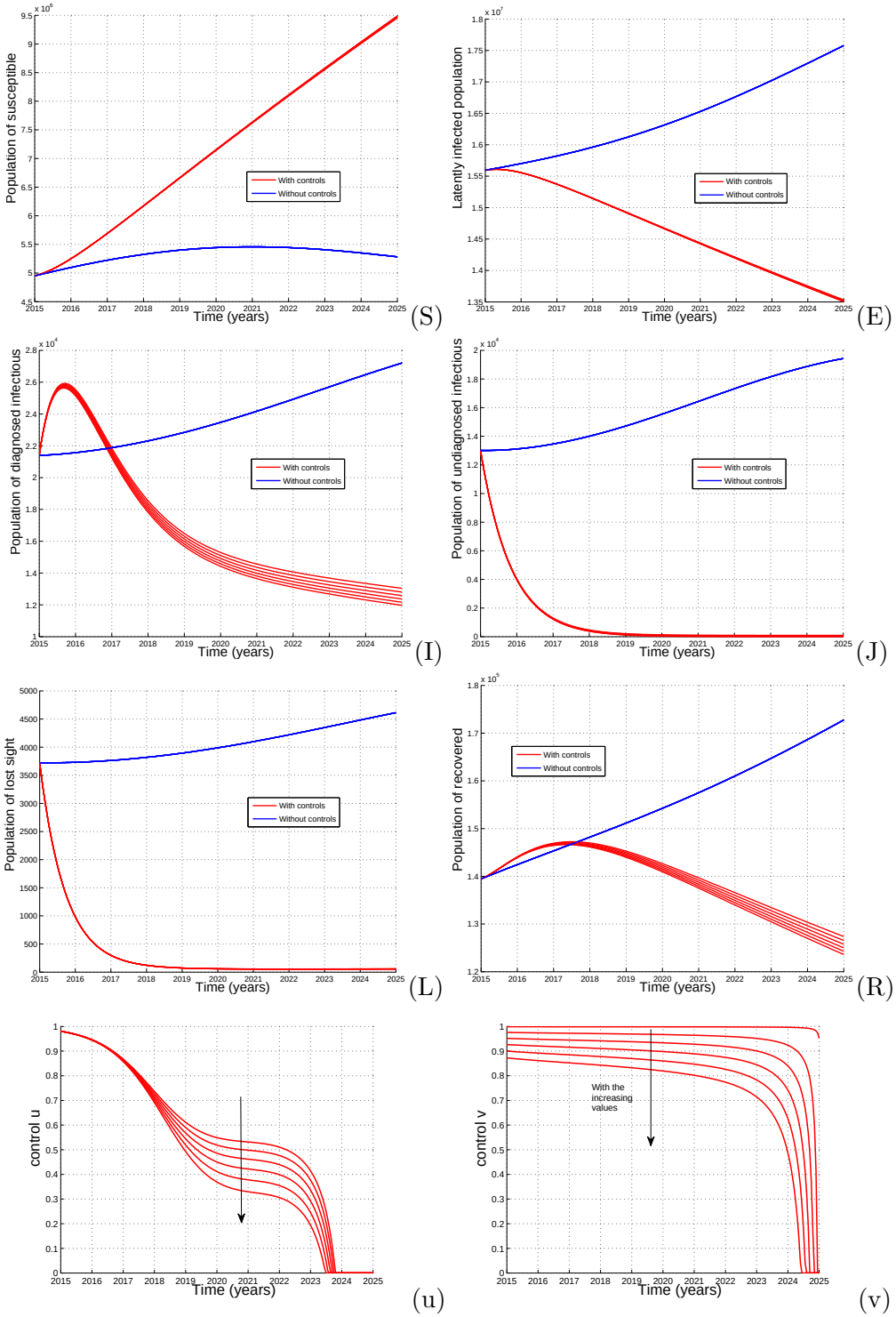

Figure 4.7: Evolution of model (4.1) result from optimal education and chemoprophylaxis strategies, blue lines, compared with that of no education and chemoprophylaxis control strategies (red lines). Susceptible (S), latently infected (E), diagnosed infectives (I), undiagnosed infectives (J), lost sight (L) and recovered (R) are pictured for $D_1 = D_2 \in \{1, 11, 21, 31, 41, 51, 61, 71, 81, 91\}$. Other parameters are presented in Tables 2.2 and 4.1. One observed a large change on v and v with the constants.

solution changes with the values of the constants.

Impact of the contact rate. In this paragraph, the sensitivity of the optimal control with respect to contact rate β_3 is analyzed numerically by computing the corresponding values of the control function for different values of β_3. In fact, β_3 can change resulting from change in ventilation or climate from one area to others. The purpose of the study is to analyze the impact of the change of β_3 on the optimal control solution. The optimal control solutions for several values of β_3 is presented in Figure 4.9 for $\beta_3 \in \{1.33563 \cdot 10^{-6}, 11.33563 \cdot 10^{-6}, 21.33563 \times 10^{-6}, 31.33563 \cdot 10^{-6}, 41.33563 \cdot 10^{-6}, 51.33563 \cdot 10^{-6}, 61.33563 \cdot 10^{-6}, 71.33563 \cdot 10^{-6}, 81.33563 \cdot 10^{-6}, 91.33563 \cdot 10^{-6}, 10.133563 \cdot 10^{-5}\}$. It appears that the educational control is highly sensitive to the model parameters for an optimal fight of TB in all cases. The chemoprophylaxis control increase slightly with increasing value of β_3.

The convergence of the FBSM throughout the iterations when both control strategies are applied can be checked through the Hamiltonian gradient's norm as in Figure 4.8. The change on β_3 does not influence the convergence of the FBSM.

Effect of the initial population size. We analyzed numerically in this Paragraph, the sensitivity of the optimal control with respect to total initial population sizes N_0 by computing the corresponding values of the control functions for different values of N_0.

The optimal control solutions for several values of N_0 are presented in Figure 4.10 for values of N_0 presented in 4.1 multiplied by $k \in \{0.5, 1, 1.5, 2, 2.5, 3\}$. It appears that the educational control is sensitive to the initial population. The chemoprophylaxis control increase slightly with increasing value of The initial population size. It appears that the educational optimal control last longer with an increasing population size. The chemoprophylaxis optimal control doe not change a lot with the population size.

The convergence of the FBSM throughout the iterations can be checked through the Hamiltonian gradient's norm as in Figure 4.8 for different population sizes. The change on N_0 has not influence on the convergence of the FBSM. The number of iterations to reach the optimal solution does not change with the values of N_0.

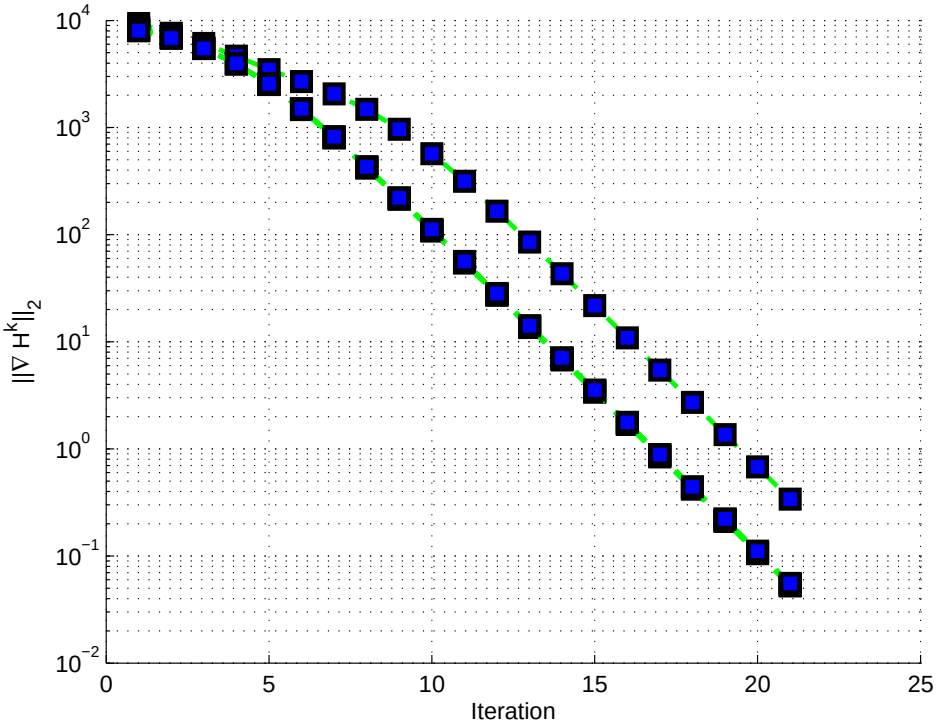

(a))

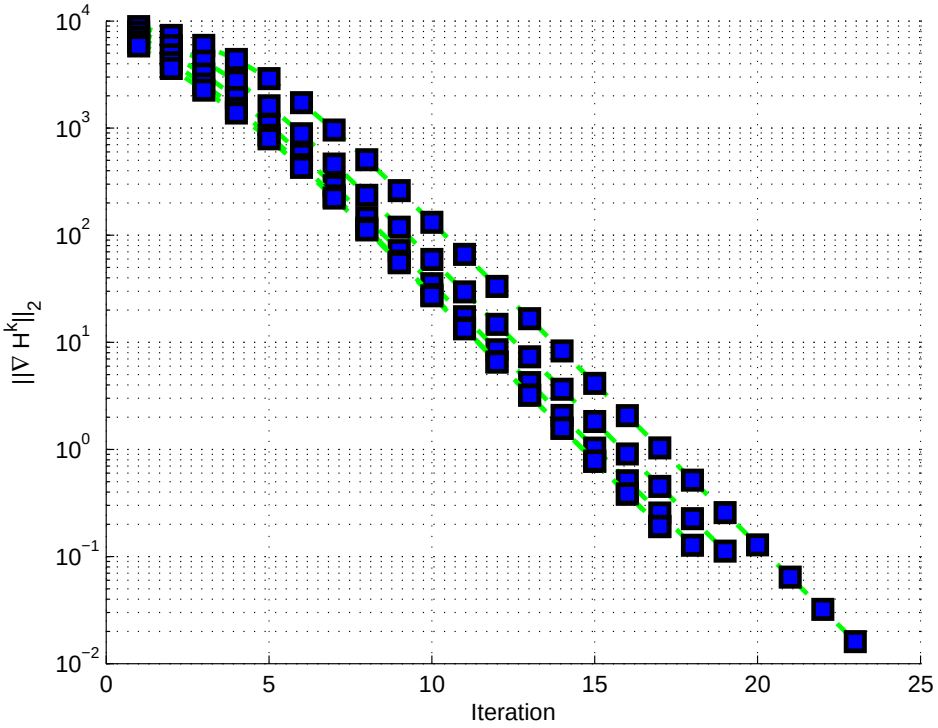

(b))

Figure 4.8: Evolution of the norm of the Hamiltonian's gradient with respect to iterations.

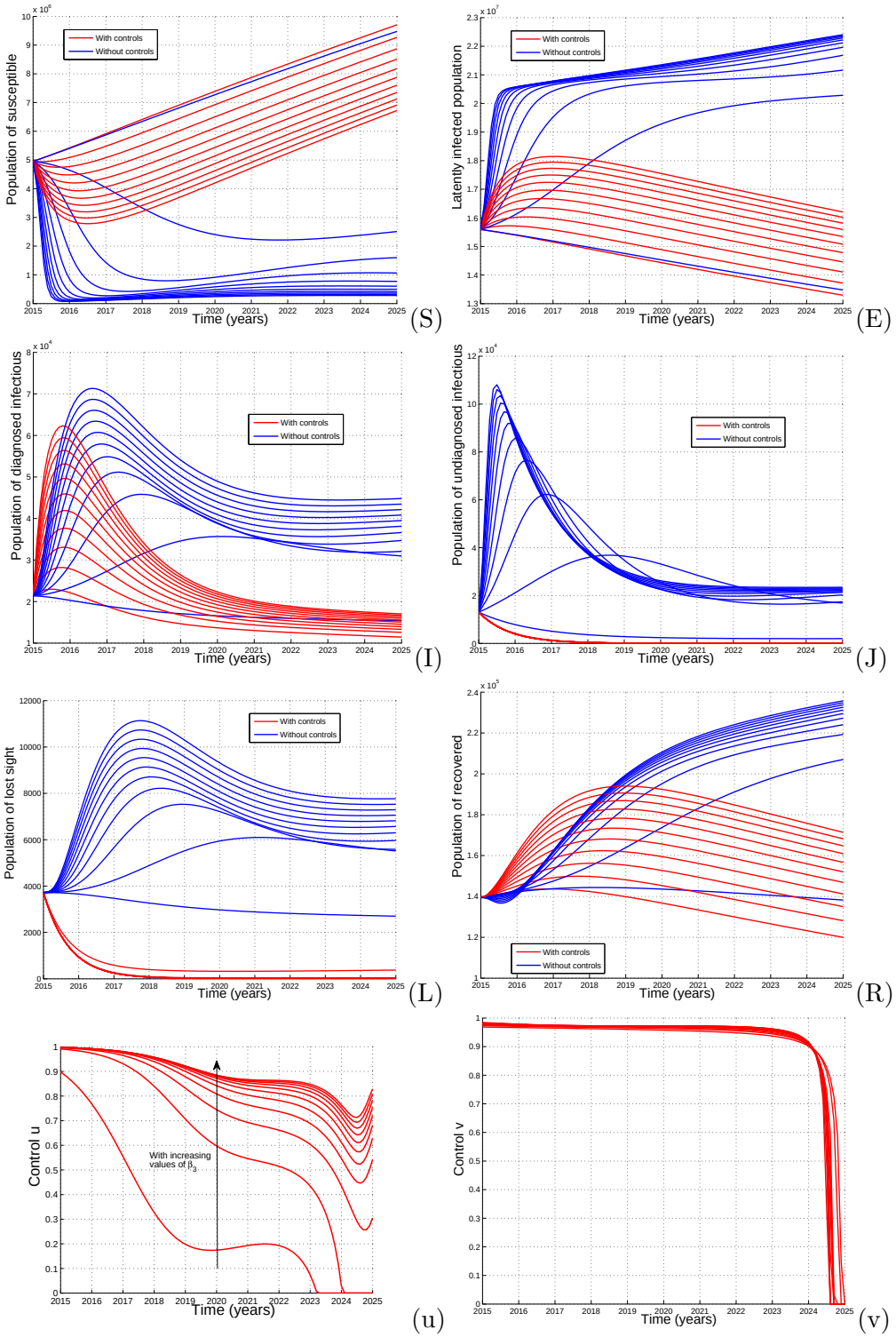

Figure 4.9: Evolution of model (4.1) result from optimal education and chemoprophylaxis strategies, blue lines, compared with that of no education and chemoprophylaxis control strategies (red lines). Susceptible (S), latently infected (E), diagnosed infectives (I), undiagnosed infectives (J), lost sight (L) and recovered (R) are pictured for $\beta_3 \in \{1.33563 \cdot 10^{-6}, 11.33563 \cdot 10^{-6}, 21.33563 \cdot 10^{-6}, 31.33563 \cdot 10^{-6}, 41.33563 \cdot 10^{-6}, 51.33563 \cdot 10^{-6}, 61.33563 \cdot 10^{-6}, 71.33563 \cdot 10^{-6}, 81.33563 \cdot 10^{-6}, 91.33563 \cdot 10^{-6}, 10.133563 \cdot 10^{-5}\}$. Other parameters are presented in Tables 2.2 and 4.1. One observed a large change on u and v with the constants.

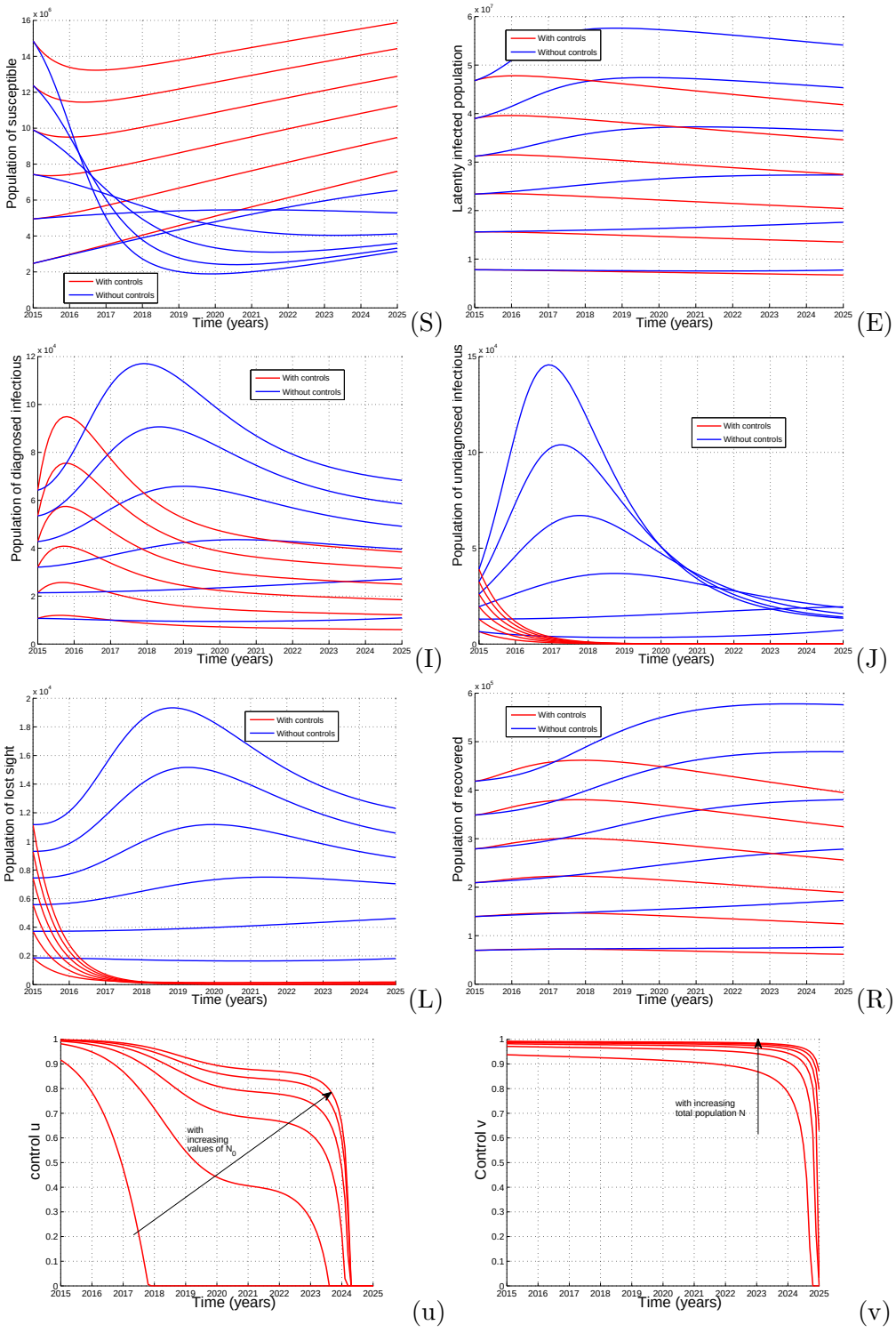

Figure 4.10: Time series of model (4.1) result from optimal education and chemoprophylaxis strategies, blue lines, compared with that of no education and chemoprophylaxis control strategies (red lines). Susceptible (S), latently infected (E), diagnosed infectives (I), undiagnosed infectives (J), lost sight (L) and recovered (R) are pictured for values of N_0 presented in 4.1 multiplied by $k \in \{0.5, 1, 1.5, 2, 2.5, 3\}$. Other parameters are presented in Tables 2.2 and 4.1.

Conclusion

This dissertation has presented mathematical and epidemiological insights about the control of TB in Sub-Saharan Africa countries, concentrating on data of Cameroon. The present study was designed to examine following questions:

- What is happening with the undiagnosed cases of active TB and lost sight?
- How do these people affect the dynamics of TB in Sub-Saharan Africa?
- Which conditions on the diagnosed rate can ensure the eradication of TB, or at least minimize its incidence?
- Are the undiagnosed TB-cases undermining the efforts of the DOTS strategy?
- What should be the impact of chemoprophylaxis of TB latently infected on TB dynamics in Sub-Saharan Africa?
- What is the mathematical and the numerical consequence of adding such classes?
- What is the optimal chemoprophylaxis and educational strategies to eradicate TB in Sub-Saharan Africa?

A deterministic mathematical model for the transmission dynamics of TB in the context of low- and middle-income countries has been built to answer these questions. Model parameters have been identified in Chapter 2 using the software POEM/BioParkin. The model has been rigorously analyzed to gain insight into its qualitative dynamics. Using data from WHO, parameters of the model have been identified and the model is shown to describe TB dynamic in Cameroon from 1994 to 2010. Many identified parameters of the model are close to values given in the literature [24, 10]. Using artificial data generated from the model, it is shown that the number of TB diagnosed, undiagnosed and lost sight dynamics can be reduced by 20% and 60% if a small but continuous effort to improve the diagnose rate and the detection of lost sight infectious is implemented. Optimal control strategies

based on education of population and chemoprophylaxis of latently infected have been studied. We have computed and compared two optimal control strategies for several scenarios. Control programs that follow these strategies can effectively reduce the number of TB-latent and TB-infectious cases. The optimal control simulations have shown that education and treatment of TB can plummet the disease incidence inside the population.

The results of this research support the idea that in sub-Saharan Africa people must be strongly encouraged to go for TB diagnosis, and the rate of successful treatment should be correlated with the population of diagnosed infectious. Then, the population of diagnosed infectious and the numbers of TB-related death-cases will decrease. The present study, however makes several contributions to TB control and the role of undiagnosed population and lost sight infectious on the public heath problem.

A number of caveats need to be noted regarding the present study. The model developed in this thesis may include in a better way the co-infection between TB and HIV, TB and malaria, TB and diabetes, impact of some behavior such as alcohol and tobacco abuse, and resistances to TB chemotherapy treatment. In fact, the impact of diseases such as HIV/AIDS and diabetes on TB have been model in the literature using a different class of co-infected individuals. This allows to study more precisely the impact of these diseases on the TB dynamics. A new aspect to improve the study in this thesis may be to develop and analyze a TB model including HIV/AIDS, diabetes, alcohol and/or tobacco abuse. The mathematical tools on the controllability and observability theory of non-linear models describing infectious diseases remain an actual problem, since models for infectious diseases includes non-linear ODEs. As biologists turn to mathematics to provide a framework for understanding more and more complicated phenomena, it is important to have as many modelling techniques as possible available for use. Exploring the mathematical tool behind seasonal behavior of the TB in most countries remains a challenge. One can also explore how short-term variations in climatic conditions and extreme weather events can exert direct effects on health response against MTB, HIV/AIDS and many other diseases (cf. [77]). These results can be used to develop targeted interventions aimed at disease eradication, source of poverty in many developing countries.

Bibliography

[1] Central Intelligence Agency. CIA–the world factbook, July 2012.

[2] F. B. Agusto. Optimal chemoprophylaxis and treatment control strategies of a tuberculosis transmission model. *World Journal of Modelling and Simulation*, 5(3):163–173, 2009.

[3] R. M. Anderson and R. May. *Population Biology of infectious diseases*. Springer-Verlag, 1982.

[4] R. M. Anderson and R. May. *Infectious Diseases of Humans: Dynamics and Control*. Oxford University Press, 1991.

[5] J. P. Aparicio, A. F. Capurro, and C. Castillo-Chavez. Transmission and dynamics of tuberculosis on generalised households. *J. Theor. Biol.*, 206:327–341, 2000.

[6] J. P. Aparicio, A. F. Capurro, and C. Castillo-Chavez. Markers of disease evolution: the case of tuberculosis. *J. Theo. Biol.*, 215:227–237, 2002.

[7] J. P. Aparicio and C. Castillo-Chavez. Mathematical modelling of tuberculosis epidemics. *Math Biosci Eng*, 6(2):209–37, April 2009.

[8] J. P. Aparicio and J.C. Hernandez. *Preventive Treatment of Tuberculosis through Contact Tracing. Mathematical Studies on Human Disease Dynamics: Emerging paradigms and Challenges*. AMS Contemporary Mathematics Series, 2006.

[9] J. Arino, C. C. McCluskey, and P. van den Driessche. Global result for an epidemic model with vaccination that exihibits backward bifurcation. *SIAM Journal on Applied Mathematics*, 64:260–276, 2003.

[10] N. Bacaër, R. Ouifki, C. Pretorius, R. Wood, and B. Williams. Modeling the joint epidemics of TB and HIV in a South African township. *J Math Biol*, 57(4):557–93, October 2008.

[11] K. Beegle. Labor effects of adult mortality in tanzanian households. *Economic Development and Cultural Change*, 53:655–83, 2005.

[12] M. Begon, M. Bennett, R. G. Bowers, N. P. French, S. M. Hazel, and J. Turner. A clarification of transmission terms in host-microparasite models : numbers, densities and areas. *Epidemiol. Infect.*, 129:147–153, 2002.

[13] R. Bellman. *On the Theory of Dynamic Programming.* Proceedings of the National Academy of Sciences, 1952.

[14] R. E. Bellman. *Dynamic Programming.* ISBN 0-486-42809-5. Princeton University Press, Princeton, NJ, Dover, 1957, Republished 2003.

[15] A. Berman and R. J. Plemmons. *Nonnegative matrices in the mathematical sciences.* SIAM, 1994.

[16] D. Bernoulli. Essai d'une nouvelle analyse de la mortalité causée par la petite vérole, et des avantages de l'inoculation pour la prévenir. *Histoire de l'Acad. Roy. Sci. (Paris) avec Mém. des Math. et Phys. and Mém.*, 00:1–45, 1760.

[17] C. Bhunu, W. Garira, Z. Mukandavire, and M. Zimba. Tuberculosis transmission model with chemoprophylaxis and treatment. *Bulletin of Mathematical Biology*, 70:1163–1191, 2008. 10.1007/s11538-008-9295-4.

[18] C. P. Bhunu, W. Garira, and Z. Mukandavire. Modeling HIV/AIDS and tuberculosis coinfection. *Bull. Math. Biol.*, 71(7):1745–80, October 2009.

[19] C. P. Bhunu, W. Garira, Z. Mukandavire, and G. Magombedze. Modelling the effects of pre-exposure and post-exposure vaccines in tuberculosis control. *J. Theor. Biol.*, 254(3):633–49, October 2008.

[20] C. P. Bhunu, W. Garira, Z. Mukandavire, and M. Zimba. Tuberculosis transmission model with chemoprophylaxis and treatment. *Bull. Math. Biol.*, 70(4):1163–91, May 2008.

[21] G. Birkhoff and G.-C. Rota. *Ordinary Differential Equations.* John Wiley and Sons new York, 3rd edition, 1978.

[22] K. W. Blayneh, A. B. Gumel, S. Lenhart, and T. Clayton. Backward bifurcation and optimal control in transmission dynamics of west nile virus. *Bull. Math. Biol.*, 72(4):1006–28, May 2010.

[23] S. M. Blower and C. L. Daley. Problems and solutions for the Stop TB partnership. *Lancet Infect Dis*, 2(6):374–6, June 2002.

[24] S. M. Blower, A. R. Mclean, T. C. Porco, P. M. Small, P. C. Hopewell, M. A. Sanchez, and A. R. Moss. The intrinsic transmission dynamics of tuberculosis epidemics. *Nat. Med.*, 1:44–56, 1995.

[25] S. M. Blower, A. R. McLean, T. C. Porco, P. M. Small, P. C. Hopewell, M. A. Sanchez, and A. R. Moss. The intrinsic transmission dynamics of tuberculosis epidemics. *Nat. Med.*, 1(8):815–21, August 1995.

[26] S. M. Blower, T. C. Porco, and T. M. Lietman. Tuberculosis: The evolution of antibiotic resistance and the design of epidemic control strategies. In M. A. Horn, G. Simonett, and G. F. Webb, editors, *Mathematical Models in Medical and Health Science*. Vanderbilt University Press and Nashville, 1998.

[27] S. M. Blower, P. Small, and P. Hopewell. Control strategies for tuberculosis epidemics: new method for old problem. *Science*, 273:497–500, 1996.

[28] S. M. Blower, P. M. Small, and P. C. Hopewell. Control strategies for tuberculosis epidemics: new models for old problems. *Science*, 273(5274):497–500, July 1996.

[29] S. Bowong. *Contribution à la stabilisation et stabilité des systèmes non-linéaires: Application à des systèmes épidémiologiques et mécaniques*. PhD thesis, Université de Metz, 2003.

[30] S. Bowong. Optimal control of the transmission dynamics of tuberculosis. *Nonlinear Dynamics*, 61(4):729–748, 2010.

[31] S. Bowong and J. Kurths. Modeling and parameter Estimation of tuberculosis with Application to Cameroon. *I. J. Bifurcation and Chaos*, 21(7):1999–2015, 2011.

[32] S. Bowong, D. P. Moualeu, J. J. Tewa, and M. A. Aziz-Alaoui. On the role of alcohol drinking on the dynamics transmission of hepatitis b. In *Understanding the dynamics of emerging and Re-emerging infectious diseases using mathematical model*, volume 2 of *Transworld Research Network 37/661*, pages 000–000. Springer Verlag, 2011.

[33] S. Bowong and J. J. Tewa. Mathematical analysis of a tuberculosis model with differential infectivity. *Com. Non. Sci. Num. Sim.*, 14:4010–4021, 2009.

[34] F. Brauer. Backward bifurcation in simple vaccination models. *Journal of Mathematical Analysis and Application*, 298:418–431, 2004.

[35] F. Brauer and C. Castillo-Chavez. *Mathematical Models in Population Biology and Epidemiology.* Springer-Verlag New York, Inc., 2001.

[36] E. Brooks-Pollock, T. Cohen, and M. Murray. The impact of realistic age structure in simple models of tuberculosis transmission. *PLoS ONE*, 5(1):e8479, 2010.

[37] V. Capasso. *Mathematical structures of epidemic systems.* Lecture notes in biomathematics, Berlin Springer, 1993.

[38] J. Carr. *Applications Centre Manifold theory.* Springer-Verlag New York, 1981.

[39] C. Castillo-Chavez, K . Cooke, W. Huang, and S. A. Levin. On the role of long incubation periods in the dynamics of acquired immunodeficiency syndrome (AIDS). Part 1: Single population models. *J Math Biol*, 27(4):373–98, 1989.

[40] C. Castillo-Chavez and Z. Feng. To treat or not to treat: the case of tuberculosis. *J. Math. Biol.*, 35:629–635, 1997.

[41] C. Castillo-Chavez and B. Song. Dynamical models of tuberculosis and their applications. *Math Biosci Eng*, 1(2):361–404, September 2004.

[42] C. Castillo-Chavez and B. Song. Dynamical models of tuberculosis and their applications. *Math. Biosci. Eng.*, 1:361–404, 2004.

[43] C. Castillo-Chavez and H. R. Thieme. Asymptotically autonomous epidemic models. In Arino et al, editor, *Mathematical Population Dynamics: Analysis of heterogeneity Theory of epidemics*, volume 1, pages 33–50. Wuerz, Winnipeg, 1995.

[44] C. P. Chaulk, M. Friedman, and R. Dunning. Modeling the epidemiology and economics of directly observed therapy in baltimore. *Int. J. Tuberc. Lung. Dis.*, 4:201–207, 2000.

[45] W. Cheney and D. Kincaid. *Numerical Mathematics and Computing.* Thomson Learning Inc, 2008.

[46] C. Y. Chiang and L. W. Riley. Exogenous reinfection in tuberculosis. *Lancet Infect. Dis.*, 5:629–636, 2005.

[47] C. Chintu and A. Mwinga. An african perspective of tuberculosis and hiv/aids. *Lancet*, 353:997–1005, 1999.

[48] K. M. De Cock and R. E. Chaisson. Will dots do it? a reappraisal of tuberculosis control in countries with high rates of hiv infection. *Int. J. Tuberc. Lung Dis.*, 3:457–465, 1999.

[49] E. A. Coddington. *An Introduction to Ordinary Differential Equations.* Prentice-Hall Inc, 1961.

[50] E. A. Coddington and N. Levinson. *Theory of Ordinary Di?erential Equations.* Mc-Graw Hill Co. Inc., 1955.

[51] T. Cohen, D. Wilson, K. Wallengren, E. Y. Samuel, and M. Murray. Mixed-strain Mycobacterium tuberculosis infections among patients dying in a hospital in KwaZulu-Natal, South Africa. *J. Clin. Microbiol.*, 49(1):385–8, January 2011.

[52] C. Colijn, T. Cohen, and M. Murray. Mathematical models of tuberculosis: accomplishments and future challenges. In *Proceedings of BIOMAT International Symposium on Mathematical and Computational Biology*. World Scientific Publisher, 2006.

[53] P. Deuflhard. *Newton Methods for Nonlinear Problems: Affne Invariance and Adaptive Algorithms*, volume 35. Springer Series in Computational Mathematics. Springer Verlag, Berlin, 2004.

[54] P. Deuflhard and F. Bornemann. *Scientific computing with ordinary differential equations.*, volume 42. Texts in Applied Mathematics, Springer, Berlin, 2002.

[55] P. Deuflhard and A. Hohmann. *Numerical Analysis in Modern Scientific Computing. An Introduction*. Springer, New York, second edition, 2003.

[56] R. P. Dickinson and R. J. Gelinas. Sensitivity analysis of ordinary differential equation systems-a direct method. *Journal of Computational Physics*, 21:123–143, 1976.

[57] R. P. Dickinson and R. J. Gelinas. Sensitivity analysis of ordinary differential equation systemsâa direct method. *Journal of Computational Physics*, 21(2):123 – 143, 1976.

[58] O. Diekmann and J. A. P. Heesterbeek. *Mathematical epidemiology of infectious diseases. Model building, analysis and interpretation*. Wiley Series in Mathematical and Computational Biology, John Wiley & Sons Ltd., Chichester, 2000.

[59] O. Diekmann, J. A. P. Heesterbeek, and J. A. J. Metz. On the definition and the computation of the basic reproduction ratio r0 in models for infectious diseases in heterogeneous populations. *J. Math. Biol*, 28:365–382, 1990.

[60] O. Diekmann, J. A. P. Heesterbeek, and M. G. Roberts. The construction of next-generation matrices for compartmental epidemic models. *J. R. Soc. Interface*, 7:873–885, 2010.

[61] T. Dierkes, M. Wade, U. Nowak, and S. Röblitz. Bioparkin- biology-related parameter identification in large kinetic networks. ZIB-Report, pp 11-15, December 2011.

[62] K. Dietz. Transmission and control of arboviruses. In D. Ludwig and K. L. Cooke, editors, *Epydemiology*, pages 104–121. SIAM, Philadephia, 1975.

[63] S. Dreyfus. Richard Bellman on the birth of dynamic programming. *Operations Research*, 50(1):48–51, 2002.

[64] J. Dushoff, W. Huang, and C. Castillo-Chavez. Backwards bifurcations and catastrophe in simple models of fatal diseases. *J. Math. Biol.*, 36(3):227–48, February 1998.

[65] C. Dye, G. P. Garnett, K. Sleeman, and B. G. Williams. Prospects for worldwide tuberculosis control under the who dots strategy. directly observed short-course therapy. *Lancet*, 352(9144):1886–1891, Dec. 1998.

[66] C. Dye, K. Lönnroth, E. Jaramillo, B. G. Williams, and M. Raviglione. Trends in tuberculosis incidence and their determinants in 134 countries. *Bull. World Health Organ.*, 87(9):683–91, September 2009.

[67] C. Dye, S. Schele, P. Dolin, V. Pathania, and M. Raviglione. For the WHO global surveillance and monitoring project. Global burden of tuberculosis estimated incidence and prevalence and mortality by country. *JAMA*, 282:677–686, 1999.

[68] E. H. Elbasha and A. B. Gumel. Theoretical assesssment of public health impact of imperfect prophylatics hiv-1 vaccines with therapeutic benefits. *Bulletin of Mathematical Biology*, 68:577–614, 2006.

[69] Y. Emvudu, R. Demasse, and D. Djeudeu. Optimal control of the lost to follow up in a tuberculosis model. *Comput. Math. Methods Med.*, 00:1–12, 2011.

[70] Z. Feng, C. Castillo-Chavez, and A. F. Capurro. A model for tuberculosis with exogenous reinfection. *Theor Popul Biol*, 57(3):235–47, May 2000.

[71] Z. Feng, W. Huang, and C. Castillo-Chavez. On the role of variable latent periods in mathematical models for tuberculosis. *Journal of Dynamics and Differential Equations*, 13(2):425–452, 2001.

[72] S. Ferebee. An epidemiological model of tuberculosis in the united states. *Bulletin of the National Tuberculosis Association*, 53:4, 1967.

[73] M. Fiedler. *Special Matrices and their Applications in Numerical Mathematics*. Martinus Nijhoff Publishers, Dordrecht, Boston, Lancaster., 1986.

[74] K. R. Fister, S. Lenhart, J. McNally, Vol. 1998, o. 32, pg. 1-12, and December 1998. Optimizing chemotherapy in an hiv. *Electronic Journal of Differential Equations*, 1998(32):1–12, December 1998.

[75] W. H. Fleming and R. W. Rishel. *Deterministic and Stochastic Optimal Control and Applications of Mathematics*. 1. Springer-Verlag, 1975.

[76] T. Frieden and R. C. Driver. Tuberculosis control: past 10 years and future progress. *Tuberculosis*, 83:82–85, 2003.

[77] C. B. Fries and J.Mayer. Climate change and infectious disease. *Interdisciplinary Perspectives on Infectious Diseases*, 00:2 pages, 2009. Article ID 976403.

[78] M. N. Gourevitch, P. Alcabes, W. C. Wasserman, and P. S. Arno. Cost-effectiveness of directly observed chemoprophylaxis of tuberculosis among drug users at high risk for tuberculosis. *Int J Tuberc Lung Dis.*, 2(7):531–40, July 1998.

[79] F. Grimard and G. Harling. The impact of tuberculosis on economic growth. Technical report, Department of Economics, McGill University, Montréal, 2004.

[80] J. Guckenheimer and P. Holmes. *Nonlinear Oscillations, Dynamical Systems, and Bifurcations of Vector Fields*. Applied Mathematical Sciences, Springer-Verlag, 2002.

[81] K. P. Hadeler and P. van den Driessche. Backward bifurcation in epidemic control. *Math. Biosci.*, 146:15–35, 1997.

[82] J. K. Hale and H. Kocak. *Dynamics and Bifucations*. Springer-Verlag New York, Inc., 1991.

[83] K. Hattaf, M. Rachik, S. Saadi, Y. Tabit, and N. Yousfi. Optimal control of tuberculosis with exogenous reinfection. *Applied Mathematical Sciences*, 3(5):231–240, 2009.

[84] J. A. P. Heesterbeek. A brief history of r0 and a recipe for its calculation. *Acta Biotheorica*, 50:189–204, 2002.

[85] H. W. Hethcote. Mathematical models for the spread of infectious diseases. In D. Ludwig and K. L. Cooke, editors, *Epidemiology*, pages 121–131. SIAM, Philadephia, 1975.

[86] Herbert W. Hethcote. The mathematics of infectious diseases. *SIAM Review*, 42:599–653, 2000.

[87] S. Hildebrandt, N. Bagheri, R. Gunawan, H. Mirsky, J. Shoemaker, S. Taylor, L. Petzold, and F. J. Doyle III. Chapter 10 - systems analysis for systems biology. pages 249 – 272, 2010.

[88] R. A. Horn and C. R. Johnson. *Topics in Matrix Analysis*. Cambridge University, Cambridge, 1991.

[89] P.-F. Hsieh and Y. Sibuya. *Basic Theory of Ordinary Differential Equations*. Springer-Verlag, New York Inc., 1999.

[90] P. Hudelson. Gender differentials in tuberculosis: The role of socio-economic and cultural factors. *Tubercle and Lung Disease*, 77(5):391 – 400, 1996.

[91] N. Hussaini. *Mathematical Modelling and Analysis of HIV Transmission Dynamics*. PhD thesis, Brunel University, West London, 2010.

[92] A. Iggidr, J. C. Kamgang, G. Sallet, and J. J. Tewa. Global analysis of new malaria intrahost models with a competitive exclusion principle. *SIAM J. App. Math.*, 1:260–278, 2007.

[93] A. Iggidr, J. Mbang, and G. Sallet. Stability analysis of within-host parasite models with delays. *Math. Biosci.*, 209:51–75, 2007.

[94] A. Iggidr, J. Mbang, G. Sallet, and J. J. Tewa. Multi-compartment models. *Discrete Contin. Dyn. Syst. Ser. B*, 1:506–519, 2007.

[95] H. R. Joshi. Optimal control of an hiv immunology model. *Optimal Control Applications & Methods*, 23:199–213, 2002.

[96] E. Jung, S. Lenhart, and Z. Feng. Optimal control of treatments in a two-strain tuberculosis. *Discrete and Continuous Dynamical Systems. Series B*, 164:183–201, 2002.

[97] S. Kalemli-Ozcan, H. Ryder, and D. N. Weil. Mortality decline, human capital investment and economic growth. *Journal of Development Economics*, 62:1–23, 2000.

[98] J. C. Kamgang and G. Sallet. Computation of threshold conditions for epidemiological models and global stability of the disease-free equilibrium (DFE). *Math Biosci*, 213(1):1–12, May 2008.

[99] J.C Kamgang. *Contribution à la stabilisation des modèles mécaniques and Contribution à l'étude de la stabilité des modeles épidémiologiques*. PhD thesis, Université de Metz, 2003.

[100] S. H. E. Kaufmann. Deadly combination. *Nature*, 453(15):295–6, May 2008.

[101] S. H. E. Kaufmann. Fact and fiction in tuberculosis vaccine research: 10 years later. *The Lancet Infectious Diseases*, 11(8):633 – 640, 2011.

[102] D. Kirschner, S. Lenhart, and S. Serbin. Optimal control of the chemotherapy of hiv. *Math. Biol.*, 35:775–792, 1997.

[103] Mark A. Kramer, Herschel Rabitz, and Joseph M. Calo. Sensitivity analysis of oscillatory systems. *Applied Mathematical Modelling*, 8(5):328 – 340, 1984.

[104] C. Kribs-Zaleta and J. Halesco-Hernandez. A simple vaccination model with multiple endemic states. *Math. Biosci.*, 164:183–201, 2000.

[105] V. Kumar, A. K. Abbas, N. Fausto, and R. N. Mitchell. *Basic Pathology (8th ed.)*, volume ISBN 978-1-4160-2973-1. Saunders Elsevier, 2007.

[106] V. Lakshmikantham, S. Leela, and A. A. Martynyuk. *Stability Analysis of Nonlinear Systems*, volume 164. Marcel Dekker, Inc. New York and Basel, 1989.

[107] B. Larson, P. Hamazakaza, C. Kapunda, C. Hamusimbi, and S. Rosen. *Morbidity, mortality and crop production: An empirical study of smallholder cotton growing households in the Central Province of Zambia.* Boston University, 2004.

[108] J.P. LaSalle. Stability theory for ordinary differential equations. stability theory for ordinary differential equations. *J. Differ. Equations*, 41:57–65, 1968.

[109] J.P. LaSalle. *The Stability of Dynamical Systems*, volume 25. SIAM, 1976.

[110] R. Laxminarayan, E. Klein, C. Dye, K. Floyd, S. Darley, and O. Adeyi. Economic benefit of tuberculosis control. In *Policy research Working paper WS 4295*, volume 1. The World Bank; Human Development Network; Health, Nutrition and Population Team, August 2007.

[111] S. L. Lenhart and J. T. Workman. *Optimal Control Applied to Biological Models*. Chapman Hall/CRC, 2007.

[112] A. Lotka. Contribution to the analysis of malaria epidemiology. *Am. J. Trop. Med. Hyg.*, 3:1–121, 1923.

[113] D. G. Luenberger. *Introduction to dynamic systems: theory, models, and applications*. John Wiley & Sons Ltd., 1979.

[114] M. McAsey, L. Mou, and W. Han. Convergence of the forward-backward sweep method in optimal control. *Computational Optimization and Applications*, 53(1):207–226, 2012.

[115] D.P. Moualeu, S. Bowong, and Y. Emvudu. Global properties of a tuberculosis model with n latents classes. *JAMI*, 29(5-6):1097–116, 2011.

[116] B. M. Murphy, B. H. Singer, and D. Kirschner. On the treatment of tuberculosis in hetergeneous populations. *J. Theor. Biol.*, 223:391–404, 2003.

[117] Brian M. Murphy, Benjamin H. Singer, Shoana Anderson, and Denise Kirschner. Comparing epidemic tuberculosis in demographically distinct heterogeneous populations. *Mathematical Biosciences*, 180(12):161–185, 2002.

[118] C. J. L. Murray, K. Styblo, and A. Rouillon. Tuberculosis in developing countries: burden, intervention, and cost. *Bull. Int. Union Tuberc. Lung Dis.*, 65:6–24, 1990.

[119] J. D. Murray. *Mathematical biology: I. an introduction*. Springer-Verlag, 2002.

[120] J. D. Murray. *Mathematical Biology II.* Springer-Verlag, 3rd edition, 2003.

[121] R. L. Miller Neilan, E. Schaefer, H. Gaff, K R. Fister, and S. Lenhart. Modelling optimal control strategies for cholera. *Bulletin of Mathematical Biology, Springer New York*, 72:2004–2018, 2010.

[122] U. Nowak and P. Deuflhard. Numerical identification of selected rate constants in large chemical reaction systems. *Appl. Numer. Math.*, 1(1):59–75, 1985.

[123] P. Nunn, B. G. Williams, K. Floyd, C. Dye, G. Elzinga, and M. C. Raviglione. Tuberculosis control in the era of hiv. *Nat. Rev. Immunol.*, 5:819–826, 2005.

[124] National Committee of Fight Against Tuberculosis. *Guide de Personnel de la Santé.* Ministère de la Santé Publique du Cameroun, 2001.

[125] National Institute of Statistics. *Evolution des systèmes statistiques nationaux*, 2007.

[126] National Institute of Statistics. Rapport sur la présentation des résultats définitifs. Technical report, Bureau Central des Recensements et des Etudes de Population, 2010.

[127] Division of Tuberculosis Elimination (DTBE). Fact sheets. Technical report, Centers for Disease Control and Prevention, 2011.

[128] D. Okuonghae and V. U. Aihie. Optimal control measures for tuberculosis mathematical models including immigration and isolation of infective. *Journal of Biological Systems*, 18(01):17–54, 2010.

[129] D. Okuonghae and A. Korobeinikov. Dynamics of tuberculosis: The effect of direct observation therapy strategy (dots) in nigeria. *Math. Mod. Nat. Phen.*, 2:101–113, 2007.

[130] World Health Organization. Global tuberculosis control: surveillance, planning, financing. Technical report, World Health Organization, Geneva, Switzerland, 2009.

[131] World Health Organization. Global tuberculosis control: surveillance, planning, financing. Technical report, World Health Organization, Geneva, Switzerland, 2012.

[132] World Health Organization. Tuberculosis: Who fact sheet. Technical Report 104, Stop TB Department, Geneva, Switzerland, 2012.

[133] C. Ozcaglar, A. Shabbeer, S. L. Vandenberg, B. Yener, and K. P. Bennett. Epidemiological models of mycobacterium tuberculosis complex infections. *Mathematical Biosciences*, 236(2):77 – 96, 2012.

[134] L. Perko. *Differential Equations and Dynamical Systems*. Springer-Verlag New York Inc., 2000.

[135] L. S. Pontryagin, V. G. Boltyanskii, R. V. Gamkrelize, and E. F. Mishchenko. *The Mathematical Theory of optimal processes*. Wiley, New York, 1962.

[136] T. C. Porco and S. M. Blower. Quantifying the intrinsic transmission dynamics of tuberculosis. *Theor. Popul. Biol.*, 54:117–132, 1998.

[137] H. Rabitz, M. Kramer, and D. Dacol. Sensitivity analysis in chemical kinetics. *Annual review of Physical Chemistry*, 34:419–461, 1983.

[138] M. C. Raviglione and Pio. Evolution of who, 1948-2001 policies for tuberculosis control. *Lancet*, 359:775–780, 2002.

[139] C. S. Revelle, W. R. Lynn, and F. Feldmann. Mathematical models for the economic allocation of tuberculosis control activities in developing nations. *Am. Rev. Respir. Dis.*, 96(5):893–909, November 1967.

[140] C. S. Revelle and J. Male. A mathematical model for determining case finding and treatment activities in tuberculosis control programs. *Am. Rev. Respir. Dis.*, 102(3):403–11, September 1970.

[141] M. G. Roberts and J. A. P. Heesterbeek. Mathematicals models in epidemiology. Encyclopedia of Life Support Systems (EOLSS), 2004.

[142] G. A. W. Rook, K. Dheda, and A. Zumla. Immune responses to tuberculosis in developing countries: implications for new vaccines. *Nature Reviews Immunology*, 5:661–667, August 2005.

[143] I. M. Ross. *A Primer on Pontryagin's Principle in Optimal Control*. Collegiate Publishers, 2009.

[144] R. Ross. *The prevention of malaria*. John Murray, 1911.

[145] R. Ross. An application of the theory of probabilities to the study of a priori pathometry. part ii. *Proc. R. Soc. Lond. A.*, 92:204–230, 1916.

[146] R. Ross and H. Hudson. An application of the theory of probabilities to the study of a priori pathometry. part ii. *Proc. R. Soc. Lond. A.*, 93:212–225, 1917.

[147] S. Russell. The economic burden of illness for households in developing countries: a review of studies focusing on malaria, tuberculosis, and human immunodeficiency virus/acquired immunodeficiency syndrome. *Am J Trop Med Hyg*, 71(2 suppl):147–55, 2004.

[148] S. P. Sethi. Quantitative guidelines for communicable disease control program: A complete synthesis. *Biometrics*, 30(4):681–691, 1974.

[149] S. P. Sethi and G. L. Thompson. *Optimal Control Theory: Applications to Management Science and Economics*. Kluwer, Boston, 2nd edition edition, 2000.

[150] C. J. Silva and D. F. M. Torres. Optimal control strategies for tuberculosis treatment: A case study in angola. *Numer. Algebra Control Optim.*, 2(3):601–617, September 2012.

[151] B. S. Singer and D. E. Kirchner. Influence of backward bifurcation on interpretation of r0 in a model of epidemic tuberculosis with reinfection. *Math. Biosc. and Engeneering*, 1(1):81–91, 2004.

[152] I. Sutherland, E. Svandova, and S. Radhakrishna. The development of clinical tuberculosis following infection with tubercle bacilli. *Tubercle*, 63:255–268, 1992.

[153] J. J. Tewa. *Analyse globale des modeles epidemiologiques multi-compartimentaux: Application à des modeles intra-hotes du paludisme et du VIH*. PhD thesis, Université de Metz, 2007.

[154] J. J. Tewa, J. L. Dimi, and S. Bowong. Lyapunov functions for a dengue disease transmission model. *Chaos, Solitons and Fractals*, 39:936–941, 2009.

[155] H. R. Thieme. *Mathematics in Population Biology*. Princeton University Press, Princeton, NJ, 2003.

[156] R. Tomovic and M. Vokobratovic. *General Sensitivity Theory*. Elsevier, New York, 1972.

[157] P. van den Driessche and J. Watmough. Reproduction numbers and subthreshold endemic equilibria for compartmental models of disease transmission. *Math. Biosc.*, 180:29–28, 2002.

[158] R. Varga. *Factorization and normalized iterative methods in Boundary problems in differential equations*. University of Wisconsin Press, 1960.

[159] E. Vynnycky and P. E. Fine. The annual risk of infection with Mycobacterium tuberculosis in England and Wales since 1901. *Int. J. Tuberc. Lung Dis.*, 1(5):389–96, October 1997.

[160] E. Vynnycky and P. E. M. Fine. The natural history of tuberculosis: the implications of age-dependent risks of disease and the role of reinfection. *Epidemio. Infect.*, 119:183–201, 1997.

[161] H. Waaler, A. Geser, and S. Andersen. The use of mathematical models in the study of the epidemiology of tuberculosis. *Am J Public Health Nations Health*, 52:1002–13, June 1962.

[162] H. T. Waaler. Cost-benefit analysis of BCG-vaccination under various epidemiological situations. *Bull Int Union Tuberc*, 41:42–52, December 1968.

[163] H. T. Waaler. The economics of tuberculosis control. *Tubercle*, 49:Suppl:2–4, March 1968.

[164] H. T. Waaler. Model simulation and decision-making in tuberculosis programmes. *Bull Int Union Tuberc*, 43:337–44, June 1970.

[165] H T Waaler. The definition of high risk groups. *Scand J Respir Dis Suppl*, 72:106–12, 1970.

[166] H. T. Waaler. [Evaluation of measures in tuberculosis control–theoretic principles (short communication)]. *Prax Pneumol*, 28 Suppl:861–2, December 1974.

[167] H. T. Waaler, G. D. Gothi, G. V. Baily, and S. S. Nair. Tuberculosis in rural South India. A study of possible trends and the potential impact of antituberculosis programmes. *Bull. World Health Organ.*, 51(3):263–71, 1974.

[168] H T Waaler and M A Piot. The use of an epidemiological model for estimating the effectiveness of tuberculosis control measures. Sensitivity of the effectiveness of tuberculosis control measures to the coverage of the population. *Bull. World Health Organ.*, 41(1):75–93, 1969.

[169] H. T. Waaler and M. A. Piot. Use of an epidemiological model for estimating the effectiveness of tuberculosis control measures. Sensitivity of the effectiveness of tuberculosis control measures to the social time preference. *Bull. World Health Organ.*, 43(1):1–16, 1970.

[170] H. T. Waaler and A. Rouillon. [BCG vaccination policies as a function of the epidemiological situation]. *Bull Int Union Tuberc*, 49(1):181–206, 1974.

[171] T. Yamano and T. S. Jayne. Measuring the impacts of working-age adult mortality on small-scale farm households in kenya. *World Development*, 32(1):91–119, 2004.

[172] X. Yan, Y. Zou, and J. Li. Optimal quarantine and isolation strategies in epidemics control. *World Journal of Modelling and Simulation*, 33:202–211, 2007.

[173] E. Ziv, C. L. Daley, and S. M. Blower. Early therapy for latent tuberculosis infection. *Am. J. Epidemiol.*, 153(4):381–5, February 2001.

Summary

This thesis firstly presents a nonlinear extended deterministic model for the transmission dynamics of tuberculosis, based on realistic assumptions and data collected from the WHO. This model enables a comprehensive qualitative analysis of various aspects in the outbreak and control of tuberculosis in Sub-Saharan Africa countries and successfully reproduces the epidemiology of tuberculosis in Cameroon for the past (from 1994-2010). Some particular properties of the model and its solution have been presented using the comparison theorem applied to the theory of differential equations. The existence and the stability of a disease free equilibrium has been discussed using the Perron-Frobenius theorem and Metzler stable matrices.

Furthermore, we computed the basic reproduction number, i.e. the number of cases that one case generates on average over the course of its infectious period. Rigorous qualitative analysis of the model reveals that, in contrast to the model without reinfections, the full model with reinfection exhibits the phenomenon of backward bifurcation, where a stable disease-free equilibrium coexists with a stable endemic equilibrium when a certain threshold quantity, known as the basic reproduction ratio ($\mathcal{R}_0$), is less than unity. The global stability of the disease-free equilibrium has been discussed using the concepts of Lyapunov stability and bifurcation theory.

For a theoretical bifurcation analysis, rather than numerical computations, we have analyzed some polynomials using the Descartes sign rule. All these theoretical tools were successfully used within the study of endemic equilibria also besides the center manifold theory. The models incorporate the critical roles of health care workers, transmission heterogeneity and super-spreading events.

With the help of a sensitivity analysis using data of Cameroon, we identified the relevant parameters which play a key role for the transmission and the control of the disease. This was possible applying sophisticated numerical methods (POEM) developed at ZIB. Using advanced approaches for optimal control considering the costs for chemoprophylaxis, treatment and educational campaigns should provide a framework for designing realistic cost effective strategies with different intervention methods. The forward-backward sweep method has been used to solve the numerical

optimal control problem. The numerical result of the optimal control problem reveals that combined effort in education and chemoprophylaxis may lead to a reduction of 80% in the number of infected people in 10 years. The mathematical and numerical approaches developed in this thesis could be similarly applied in many other Sub-Saharan countries where TB is a public health problem.

Zusammenfassung

In der vorliegendenen Arbeit wird ein nichtlineares deterministisches Modell für die Übertragungsdynamik der Tuberkulose basierend auf epidemiologischen Konzepten und Daten der Weltgesundheitsorganisation (WHO) entwickelt. Das Modell ermöglicht eine detaillierte qualitative Analyse des Ausbruchs, der Ausbreitung und der Kontrolle von Tuberkulose in subsaharischen afrikanischen Ländern und reproduziert den Verlauf der Tuberkulose-Epidemie in Kamerun von 1994 bis 2010.

Spezielle Eigenschaften des Modells und seiner Lösungen werden mithilfe von Vergleichssätzen für Differentialgleichungen abgeleitet; Existenz und Stabilität eines krankheitsfreien Gleichgewichts werden unter Verwendung des Satzes von Perron-Frobenius und den Eigenschaften von Metzler-Matrizen analysiert. Die globale Stabilität des krankheitsfreien Gleichgewichts wird mittels der Konzepte der Lyapunov-Stabilität und der Bifurkationstheorie diskutiert.

Die für das Studium des Verlaufs von Infektionsepidemien grundlegende Kennziffer ist die Basisreproduktionszahl, d.h. die Zahl von weiteren Infektionen, die im Mittel von einem Infizierten während seiner infektiösen Periode verursacht wird. Die Analyse des Modells zeigt, dass die Berücksichtigung von Reinfektionen zu einer rückwärtsgerichteten Bifurkation führt, d.h. ein stabiles krankheitsfreies Gleichgewicht koexistiert mit einem stabilen endemischen Gleichgewicht, in dem die Basisreproduktionszahl kleiner als eins ist.

Die theoretischen Methoden werden zur Untersuchung endemischer Gleichgewichtszustände verwendet, ebenso wie die Theorie der Zentrumsmannigfaltigkeiten. Die Modelle berücksichtigen auch die kritische Rolle des Gesundheitspersonals, die Übertragungsheterogenität und sogenannte âsuper-spreading Eventsâ.

Durch eine Sensitivitätsanalyse mit Hilfe von am ZIB entwickelter Verfahren (POEM/BioParkin) anhand realer Daten aus Kamerun lassen sich die Modellparameter identifizieren, die eine Schlüsselrolle für die Übertragung und Kontrolle der Tuberkulose innehaben.

Für die Entwicklung wirksamer und kosteneffektiver Strategien zur Bekämpfung der Tuberkulose werden Methoden des Optimalsteuerung verwendet. Hierbei werden Kosten für Chemoprophylaxe, Behandlung und Aufklärungskampagnen berücksichtigt. Zur Lösung der Optimalsteuerungsprobleme wird ein Forward-Backward-Sweep-Ansatz eingesetzt. Die numerischen Ergebnisse zeigen, dass eine kombinierte Strategie in Aufklärung und Chemoprophylaxe zu einer Reduktion der Zahl infizierter Personen um 80% in 10 Jahren führen könnte.

Die mathematischen und numerischen Ansätze, die im Rahmen dieser Arbeit entwickelt wurden, könnten auf viele andere subsaharische Länder übertragen werden, in denen Tuberkulose eines der gröÃten Gesundheitsproblem darstellt.

Acknowledgments

This thesis owes a great deal to the support and encouragement of many people. To thank exhaustively is a sweet utopia as the number of people who have helped and supported me during these PhD years is important. I will nevertheless try here to thank the key people without whom, to be sure, this work could not be done.

I would like to thank The Almighty God, who remains for me the source of all things. No words can describe His wonders in my life.

My supervisor Prof. Peter Deuflhard, who made me very welcome in Berlin, have been there for me, despite his multiple occupations and gave me an excellent environment to pursue and finish this work. I will always be grateful for his confidence in me and for his continued interest in my work, his support and encouragement.
I am specially thankful to my supervisor Dr. Samuel Bowong, for introducing me to the world of research in general, and also first made me love applied mathematics. His advises and recommendations helped attending my first conferences, workshops and some research visits. I will remain forever deeply indebted to him for his unwavering support and guidance.

I am deeply grateful to Dr. Rainald Ehrig who accompanied me during my stay at the ZIB. He accompanied me using available ZIB material, and also in all academical, mathematical, numerical and personal difficulties I faced during my stay at ZIB.
Many thanks to Dr. Susanna Röblitz who taught me sensibility analysis for ODEs and the Gauss-Newton method for the parameters identification, and for very useful suggestions and comments for the whole thesis. She has been for me a very good adversor.
I am thankful to Dr. Martin Weiser for frequent fruitful discussions which helped completing the optimal control problem, besides comments and suggestions when drafting the chapter.

I would like to acknowledge, with thanks, IMU Einstein Foundation, and Berliner

Mathematical School for funding partly this research. I am grateful to ZIB, who gave me every computational resources, books and publications necessary to further my comprehension of mathematical theories and numerical method including in this thesis. I would like to thank UMMISCO and the GRIMCAPE Project for the material provided during the research phase in Cameroon.

Many thanks also to my teachers of the Department of Mathematics of the University of Yaounde I and especially to Dr. Yves Emvudu for his support. Special thanks go to Dr. Marcus Weber, Sebastian Götschel, Lars Lukbol, Bodo Erdmann, Alexander Bujotzek, Vedat Durmaz, Olga Scharkroi, and Claudia Stötzel, Dr. Karsten Andrea, Dr. Julia Plöntzke and Masha Berg for their kind hospitality, help and support which kept me sane outside mathematical biology.

Finally, huge thanks go to my wife Agnès Flore, my parents Fréderic and Jeanne Ngangue and my brothers and sisters Joel, Olivier, Serge, Marie, Anne, Stève, Derick, Clarisse, Eric. I am indebted to them for their love and support throughout the period of my studies.